Refinement of the Southern Florida Reef Tract Benthic Habitat Map With Habitat Use Patterns of Reef Fish Species

Jerald S. Ault, Steven G. Smith, and Jiangang Luo

University of Miami
Rosenstiel School of Marine and Atmospheric Science
4600 Rickenbacker Causeway
Miami, FL 33149

In partnership with

Laura Jay Grove[1], Matthew W. Johnson[2], and Jeremiah Blondeau[3]

NOAA Fisheries
Southeast Fisheries Science Center
[1]75 Virginia Beach Dr., Miami, FL 33149
[2]4700 Avenue U, Galveston, TX 77551
[3]UVI, under contract to NOAA Fisheries,
#2 John Brewers Bay, St Thomas, USVI 00802

Funded by NOAA's Coral Reef Conservation Program (CRCP)
Project Number: 31242

1.0 Introduction

The benthic habitat map for the southern Florida coral reef ecosystem provides the critical infrastructure for: (i) large-scale baseline ecosystem monitoring surveys of fishes, corals, and macroinvertebrates and their habitats; (ii) ecological understanding of animal use of habitats and evaluation of the efficacy of spatial fishery management strategies (e.g., no-take marine reserves); and (iii) habitat-based fish abundance at length data for the entire reeffish community (exploited and non-targeted) with high spatial resolution for use in multi-species stock assessment models. Habitats are currently classified according to a qualitative, descriptive scheme—e.g., patch reefs, reef pavement, reef rubble, etc.—at a minimum resolution of 100 x 100 m map units (i.e., grid cells). At this scale, monitoring costs increase and usability is limited because the ability to discriminate among highly productive habitats is reduced. Recently, high-resolution remote-sensed mapping products for bathymetry have become available for the southern Florida coral reef tract. Concurrently, analytical methods utilizing these mapping products have been developed to derive quantitative metrics of benthic characteristics, e.g., reef complexity, etc., which enable more refined classification of reef habitats.

The project goal was to develop a refined benthic habitat map for the southern Florida reef tract based on quantitative habitat metrics at a spatial scale of 50 x 50 m map units. The project was a collaboration between scientists at the University of Miami Rosenstiel School of Marine and Atmospheric Science (Drs. Jerry Ault, Steve Smith, and Jiangang Luo) and NOAA's Southeast Fisheries Science Center (Drs. Jay Grove and Matt Johnson, and Mr. Jeremiah Blondeau).

2.0 Overview of Project Tasks

An overview of the specific tasks for this project is illustrated in **Fig. 2.1**. Numbers in parenthesis denote the associated report section for a given task.

3.0 Synthesis of High-Resolution Mapping Data

A major initial task was to obtain and synthesize high-resolution remotely-sensed mapping data for bathymetry and substrate hardness from aerial LIDAR and ship-based multibeam sonar surveys conducted in the southern Florida coral reef ecosystem (**Fig. 3.1**). Data were compiled from mapping surveys conducted by a variety of federal and state agencies, including NOAA, NPS, USGS, and the state of Florida. High-resolution (1-2 m) bathymetry was obtained for much of the Florida Reef Tract, with the exception of Hawk's Channel, the deeper forereef (>15 m) in the Florida Keys, and deeper reefs (>15 m) in Dry Tortugas National Park. High-resolution data for substrate hardness (backscatter from multibeam sonar) was only obtained for the Tortugas Bank region (**Fig. 3.2**). Various diagnostic checks were conducted to ensure that the various mapping data were of sufficient quality for developing a new 50 x 50 m survey sampling grid (e.g., **Fig. 3.3**).

Figure 2.1. Flow diagram of project tasks. Numbers in parentheses denote the associated report section for a given task.

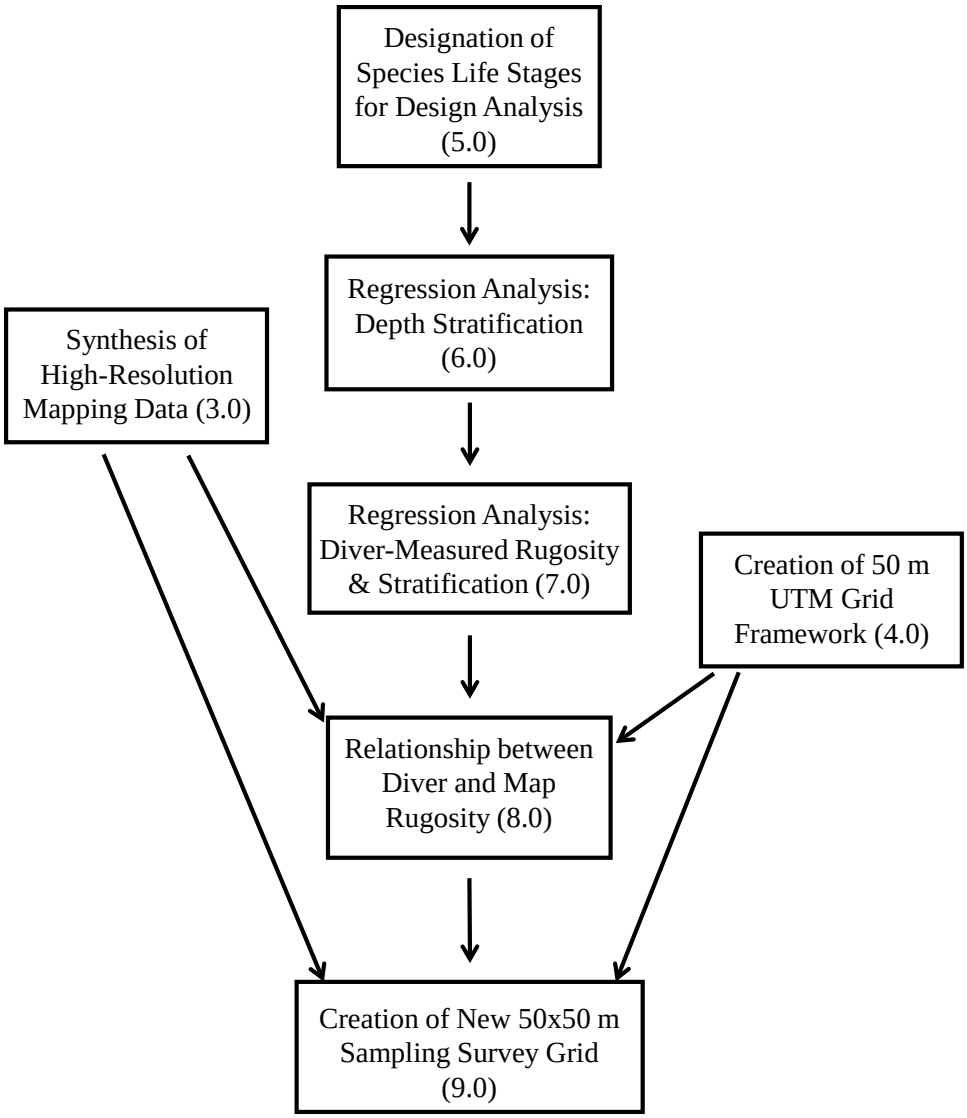

Figure 3.1. LIDAR and multibeam high-resolution bathymetry data coverage for southern Florida from Miami to Dry Tortugas (top panel). The inserts of lower panels are for the zoomed regions of Miami, Marquesas, and Dry Tortugas.

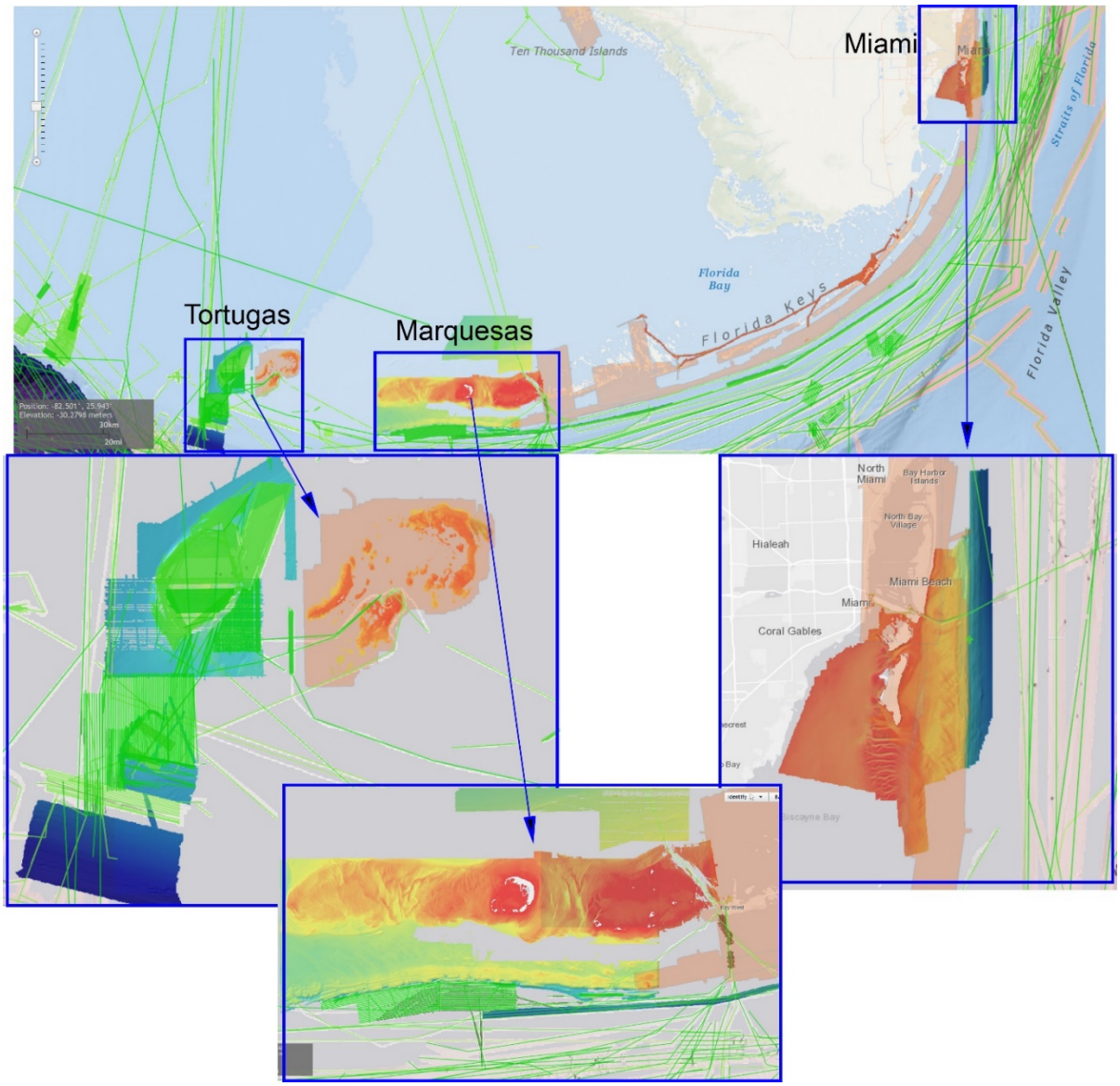

Figure 3.2. (a) Shaded relief of bathymetry and (b) backscatter of Tortugas Bank from multi-beam sonar surveys. Higher backscatter values denote higher substrate hardness.

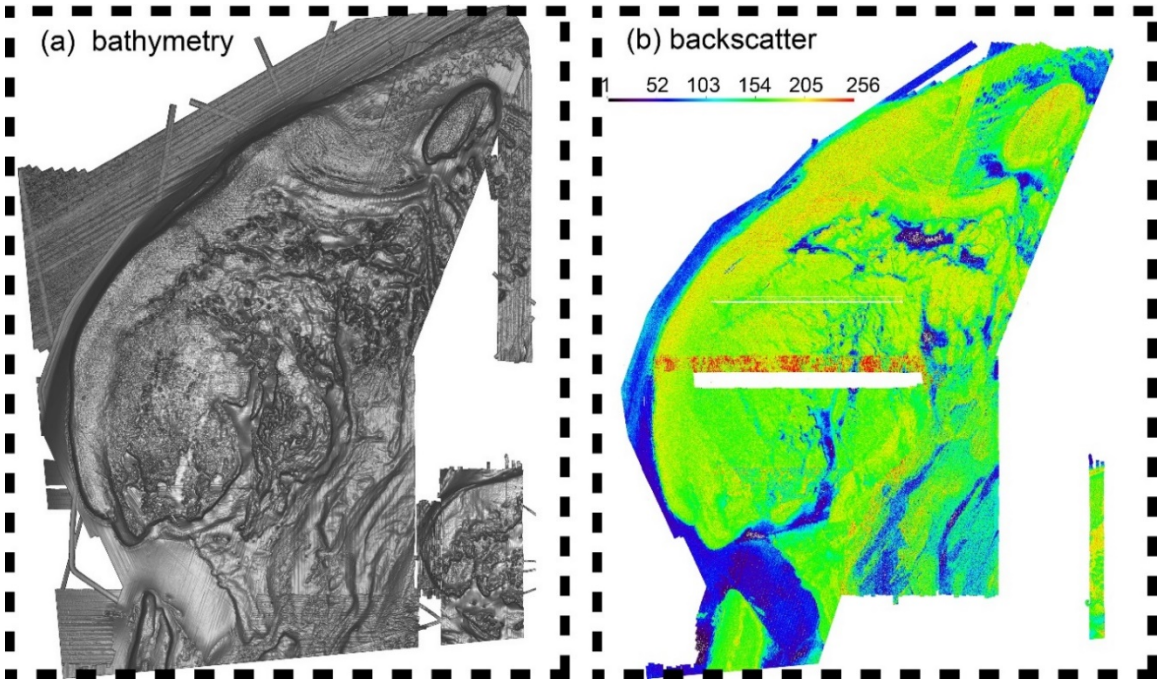

Figure 3.3. The values of backscatter vs depth from multi-beam sonar, indicating that backscatter values are independent of depth.

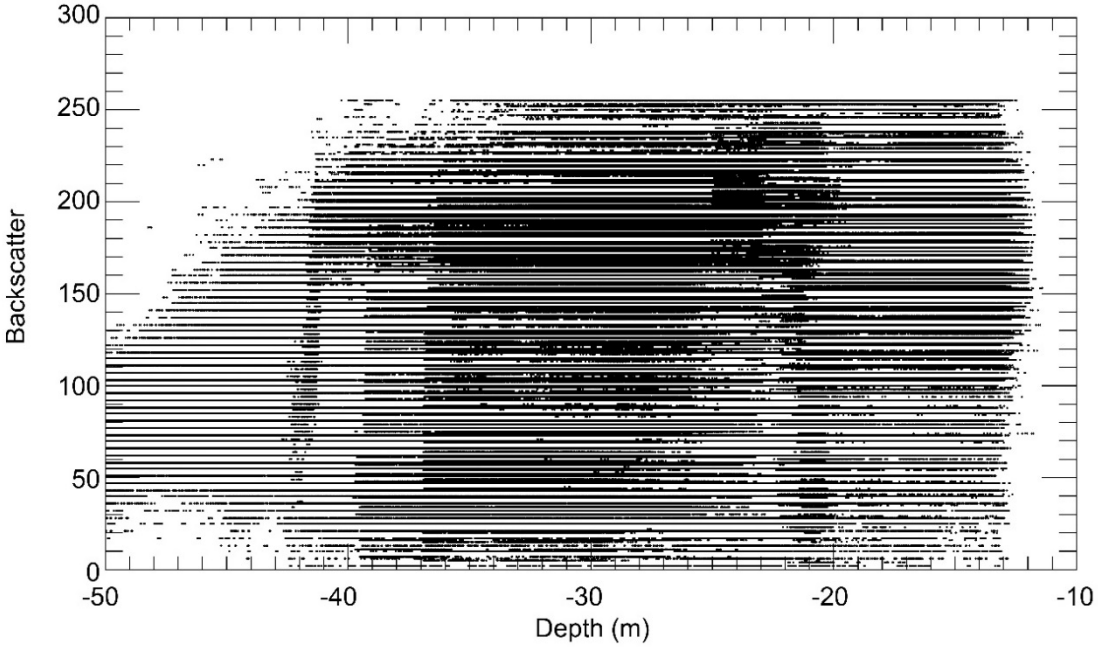

4.0 Creation of 50 m UTM Grid Framework

A second initial step was to create a 50 m UTM grid framework, which will serve as the primary sample units for the refined survey grid. This was constructed to nest perfectly within the current 100 m UTM grid (**Fig. 4.1**).

Figure 4.1. An example section showing the new 50 m grid (gray shaded squares) nested inside the current 100 m survey grid (lined squares) for southern Florida.

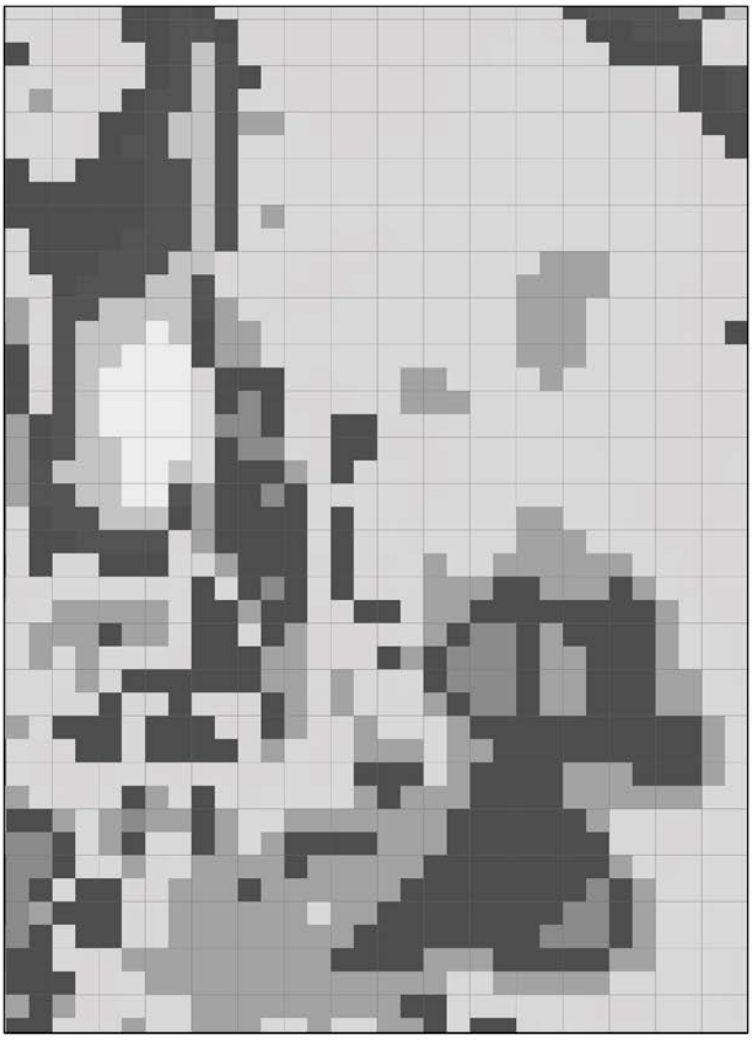

5.0 Designation of Species Life Stages for Design Analysis

Research for improving the optimal statistical design for RVC in southern Florida BFISH is focusing on potential refinements of the depth and substrate stratification variables (hardness, complexity) via analysis of species-depth-habitat associations. A first step in analyzing species-habitat associations was to determine whether shifts in spatial distribution occurred as animals progressed from smaller to larger sizes (and presumably younger to older ages). Identifying the size at which these shifts occurred enables the delineation of life stages of species for subsequent analyses, and prevents obscuring underlying habitat use patterns due to combining life stages that may occupy habitat differently. Target design species for RVC surveys in

Florida and the U.S. Caribbean are listed in **Table 5.1**. Data for analyzing species-depth-habitat associations were from RVC surveys in Dry Tortugas National Park (DRTO) during 2011-2014 (**Table 5.2**). The DRTO subregion is unique in the southern Florida survey frame in that it contains the full range of classified habitats and depths, and has relatively low fishing pressure. Sufficient data for analysis were available for 9 of the 12 species in **Table 5.1**.

Methods are illustrated for Black Grouper. Stratified random survey estimates of population abundance at size were computed at the stratum level for the 12 habitat-depth strata described in **Table 5.2**. For each 5 cm length interval, the proportion of abundance was computed among the 12 habitat-depth types. A matrix of proportion abundance arranged in rows of length intervals by columns of habitat-depth types was analyzed using principal components analysis. The plot of principal component 2 vs. principal component 1 is shown in **Fig. 5.1A**. Interestingly, the length classes from 15 to 45 cm were negative with respect to principal component 1, whereas length classes from 60 to 85cm were positive. The transition from smaller to larger size classes seemed to occur between 50 and 55 cm. The estimated L_{hab}, the length at which a shift in habitat use occurs, was 52.5 cm (**Fig. 5.1B**). Preliminary work on other reef fish species has indicated that L_{hab} denotes the transition from juveniles to subadults-adults, corresponding to the onset of sexual maturation.

Using the principal components analysis results, two life stages were delineated for Black Grouper: juveniles, <52.5 cm; and subadults-adults, ≥52.5 cm. Proportion abundance among habitats are shown in **Fig. 5.2** for these two life stages, along with the proportion of the survey area for the respective habitat (dashes). Cases where the abundance was disproportionately higher than the proportion of area denote positive habitat association, and vice-versa for negative association. Neutral association was inferred when the proportion abundance and proportion habitat area were similar. Both depth and vertical relief appeared to be important factors in habitat use of black grouper. Juveniles and subadults-adults were generally positively associated with moderate relief reefs. Habitat associations for juveniles were neutral or positive in low-relief shallow habitats, whereas subadults-adults were mostly negatively associated with these types. Habitat use of subadults-adults was positively associated with high-relief reefs, both contiguous and isolated.

Analysis of additional design species identified a specific L_{hab} and corresponding shift in life stage habitat use in each case: Red Grouper (**Figs. 5.3 & 5.4**), Mutton Snapper (**Figs. 5.5 & 5.6**), Hogfish (**Figs. 5.7 & 5.8**), Yellowtail Snapper (**Figs. 5.9 & 5.10**), French Grunt (**Figs. 5.11 & 5.12**), Stoplight Parrotfish (**Figs. 5.13 & 5.14**), Blue Tang (**Figs. 5.15 & 5.16**), and Foureye Butterflyfish (**Figs. 5.17 & 5.18**).

Table 5.1. Sampling design target species for diver surveys in southern Florida and the U.S. Caribbean.

Common	Latin	Family	Location/Type
Foureye Butterflyfish	*Chaetodon capistratus*	Butterflyfishes	Caribbean, Non-Target
			Florida, Non-Target
Black Grouper	*Mycteroperca bonaci*	Groupers	Florida, Exploited
Coney	*Cephalopholis fulva*	Groupers	Caribbean, Exploited
Red Grouper	*Epinephelus morio*	Groupers	Florida, Exploited
Red Hind	*Epinephelus guttatus*	Groupers	Caribbean, Exploited
French Grunt	*Haemulon flavolineatum*	Grunts	Caribbean, Exploited
			Florida, Non-Target
Stoplight Parrotfish	*Sparisoma viride*	Parrotfishes	Caribbean, Exploited
			Florida, Non-Target
Mutton Snapper	*Lutjanus analis*	Snappers	Florida, Exploited
Yellowtail Snapper	*Ocyurus chrysurus*	Snappers	Caribbean, Exploited
			Florida, Exploited
Blue Tang	*Acanthurus coeruleus*	Surgeonfishes	Caribbean, Exploited
			Florida, Non-Target
Queen Triggerfish	*Balistes vetula*	Triggerfishes	Caribbean, Exploited
Hogfish	*Lachnolaimus maximus*	Wrasses	Florida, Exploited

Table 5.2. Reef habitats in Dry Tortugas National Park, and survey sample sizes for 2011-2014. Total pooled sample size for fish-habitat analyses was n=1,434 buddy pair dives.

Habitat	Reef	Vertical Relief	Depth	Proportion of	Sample Sizes		
Code	Morphology	Category	Category	Survey Area	2011	2012	2014
CLS	Contiguous	Low	Shallow	0.1408	55	65	58
CLM	Contiguous	Low	Mid-Depth	0.2135	42	41	30
CLD	Contiguous	Low	Deep	0.0664	10	8	6
CMA	Contiguous	Moderate	All	0.0842	90	116	134
CHA	Contiguous	High	All	0.0289	53	43	35
ILS	Isolated Structures	Low	Shallow	0.0804	30	39	13
ILD	Isolated Structures	Low	Deep	0.0771	14	23	22
IMS	Isolated Structures	Moderate	Shallow	0.0981	15	28	12
IMD	Isolated Structures	Moderate	Deep	0.0900	38	13	31
IHA	Isolated Structures	High	All	0.0290	78	117	97
SMA	Spur-Groove	Moderate	All	0.0712	10	26	8
SHA	Spur-Groove	High	All	0.0204	10	6	18

Figure 5.1. (A) Scatterplot of principal components (PC) 2 vs. 1 for Black Grouper proportion abundance data by length class among habitat-depth strata; the red line separates length classes along the PC1 axis into smaller (15-45 cm) and larger (60-85 cm) groups that have differing spatial abundance patterns. **(B)** Population length frequency of Black Grouper; the dashed line denotes L_{hab}, the length at which a shift in habitat use occurs, possibly denoting the transition from juveniles to subadults-adults.

(A)

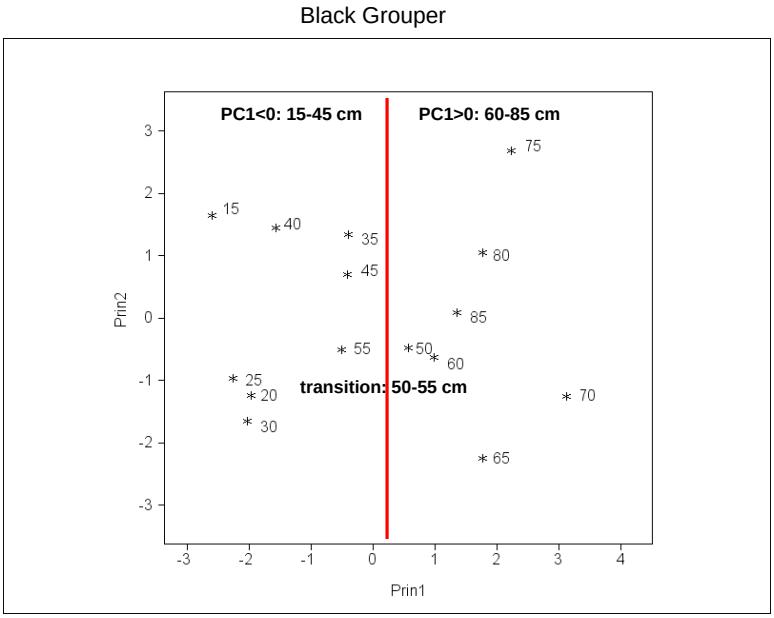

(B)

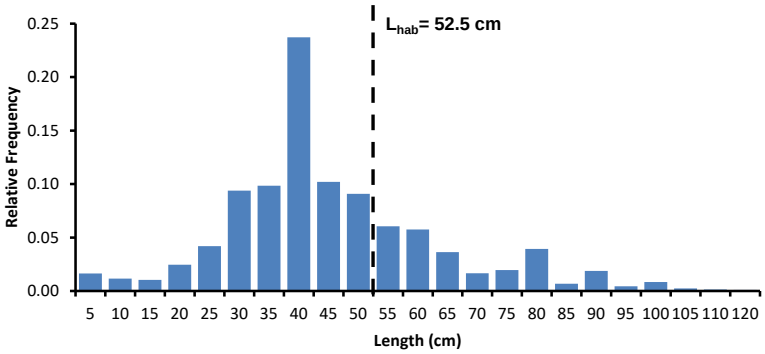

Figure 5.2. Proportion abundance by habitat type for juvenile and subadult-adult Black Grouper. Black dashes denote the proportion of habitat area in the survey domain; see Table 5.2 for habitat codes.

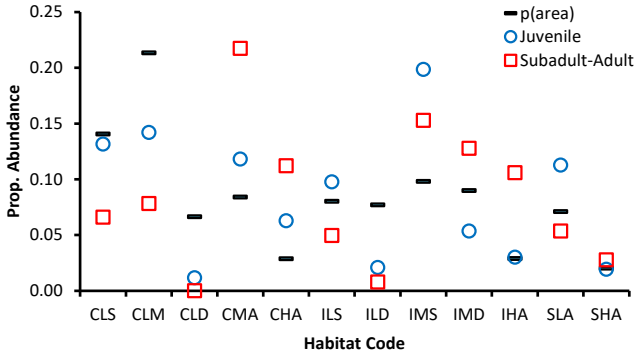

Figure 5.3. (A) Scatterplot of principal components (PC) 2 vs. 1 for Red Grouper proportion abundance data by length class among habitat-depth strata; the red line separates length classes along the PC1 axis into smaller (10-20 cm) and larger (25-75 cm) groups that have differing spatial abundance patterns. **(B)** Population length frequency of Red Grouper; the dashed line denotes L_{hab}, the length at which a shift in habitat use occurs, possibly denoting the transition from juveniles to subadults-adults.

(A)

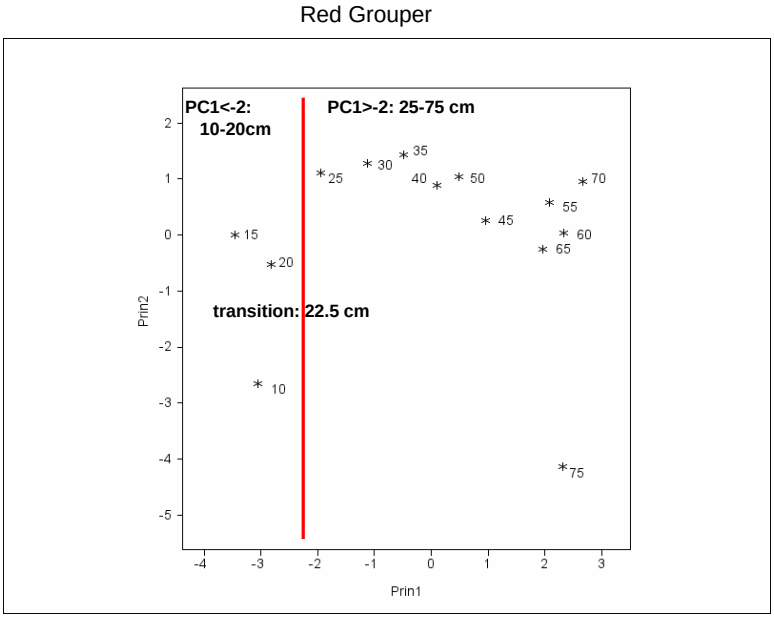

(B)

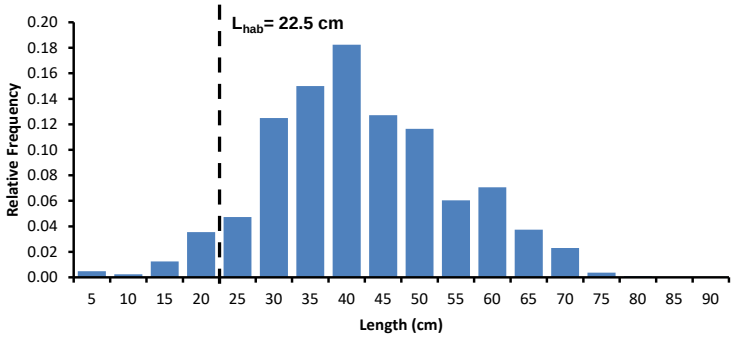

Figure 5.4. Proportion abundance by habitat type for juvenile and subadult-adult Red Grouper. Black dashes denote the proportion of habitat area in the survey domain; see Table 5.2 for habitat codes.

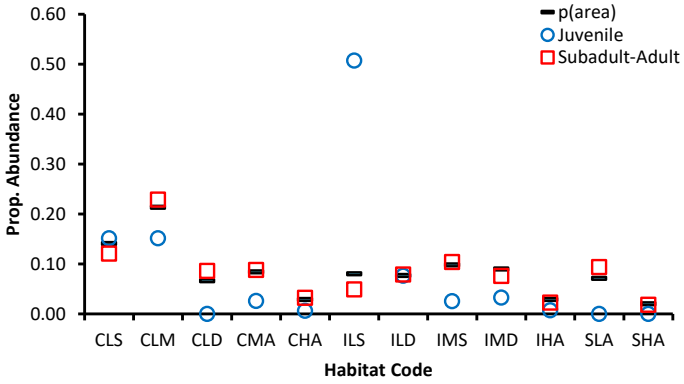

Figure 5.5. (A) Scatterplot of principal components (PC) 2 vs. 1 for Mutton Snapper proportion abundance data by length class among habitat-depth strata; the red line separates length classes along the PC1 axis into smaller (25 cm) and larger (30-75 cm) groups that have differing spatial abundance patterns. **(B)** Population length frequency of Mutton Snapper; the dashed line denotes L_{hab}, the length at which a shift in habitat use occurs, possibly denoting the transition from juveniles to subadults-adults.

(A)

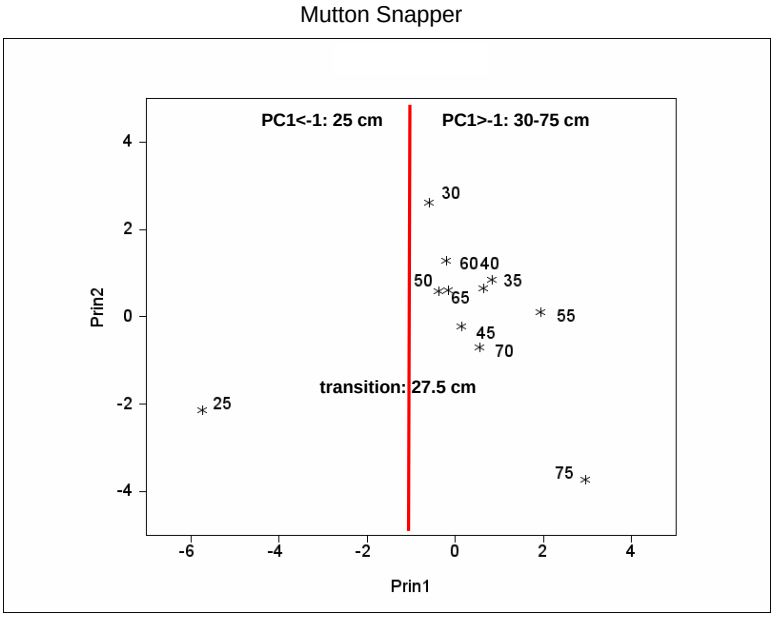

(B)

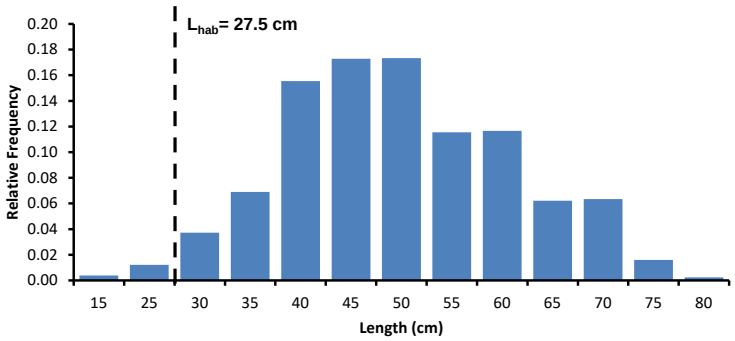

Figure 5.6. Proportion abundance by habitat type for juvenile and subadult-adult Mutton Snapper. Black dashes denote the proportion of habitat area in the survey domain; see Table 5.2 for habitat codes.

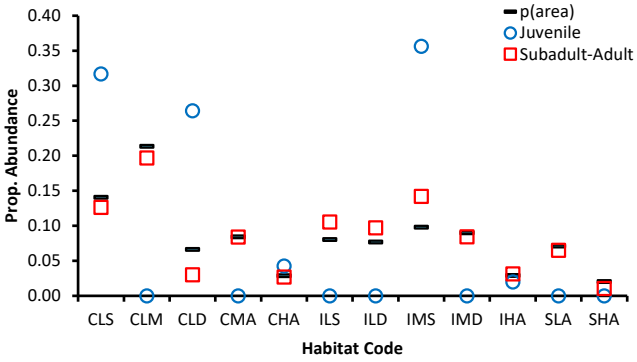

Figure 5.7. (A) Scatterplot of principal components (PC) 2 vs. 1 for Hogfish proportion abundance data by length class among habitat-depth strata; the red line separates length classes along the PC1 axis into smaller (10 cm) and larger (15-65 cm) groups that have differing spatial abundance patterns. **(B)** Population length frequency of Hogfish; the dashed line denotes L_{hab}, the length at which a shift in habitat use occurs, possibly denoting the transition from juveniles to subadults-adults.

(A)

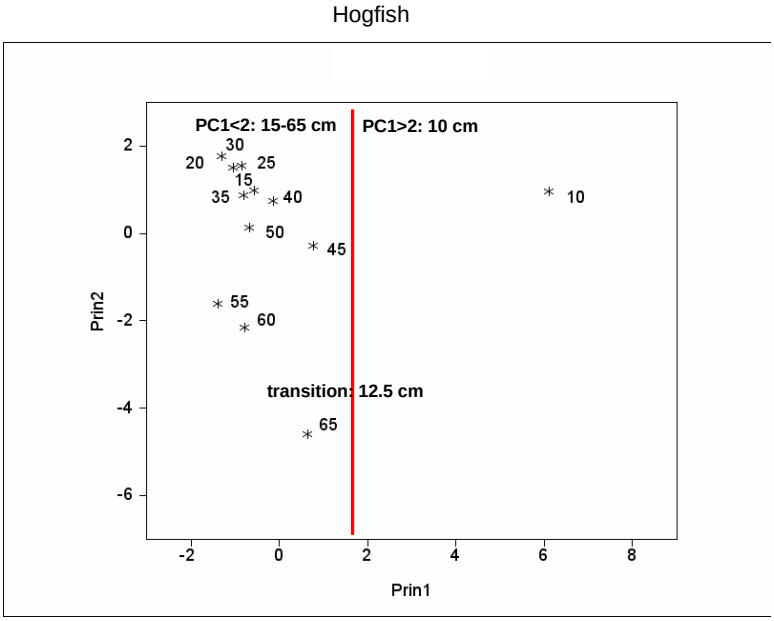

(B)

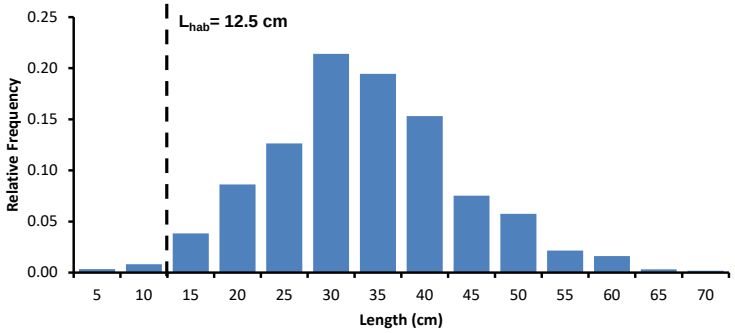

Figure 5.8. Proportion abundance by habitat type for juvenile and subadult-adult Hogfish. Black dashes denote the proportion of habitat area in the survey domain; see Table 5.2 for habitat codes.

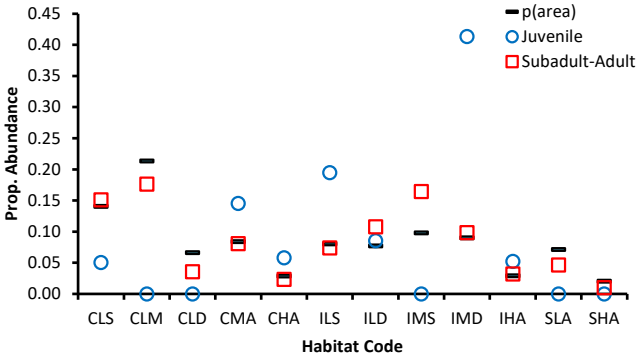

Figure 5.9. (A) Scatterplot of principal components (PC) 2 vs. 1 for Yellowtail Snapper proportion abundance data by length class among habitat-depth strata; the red line separates length classes along the PC2 axis into smaller (10-14 cm) and larger (16-38 cm) groups that have differing spatial abundance patterns. **(B)** Population length frequency of Yellowtail Snapper; the dashed line denotes L_{hab}, the length at which a shift in habitat use occurs, possibly denoting the transition from juveniles to subadults-adults.

(A)

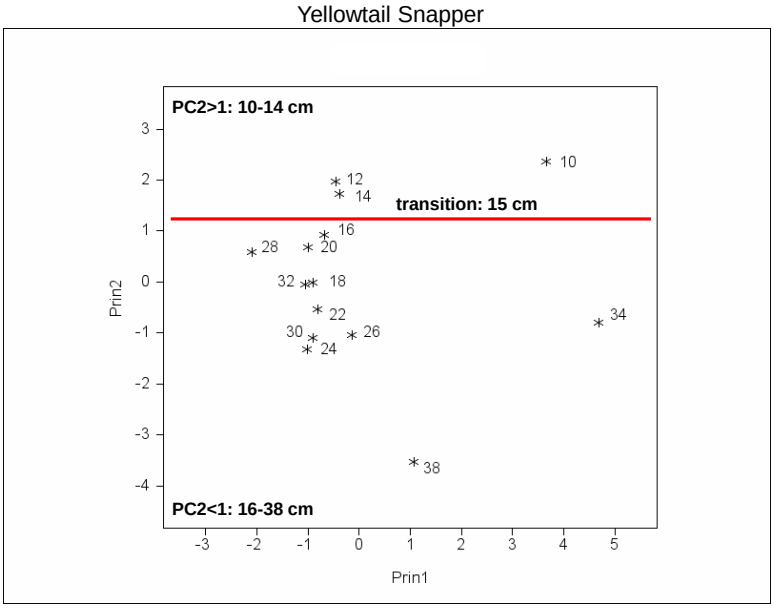

(B)

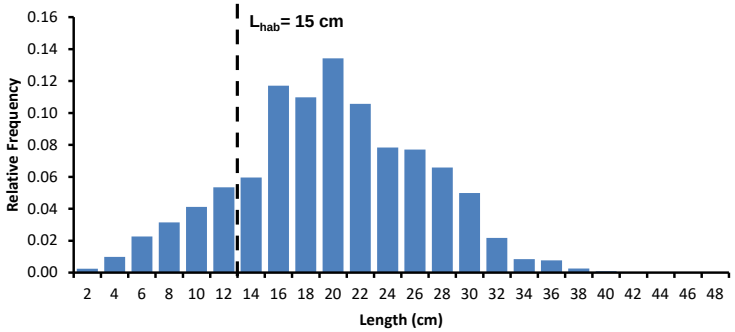

Figure 5.10. Proportion abundance by habitat type for juvenile and subadult-adult Yellowtail Snapper. Black dashes denote the proportion of habitat area in the survey domain; see Table 5.2 for habitat codes.

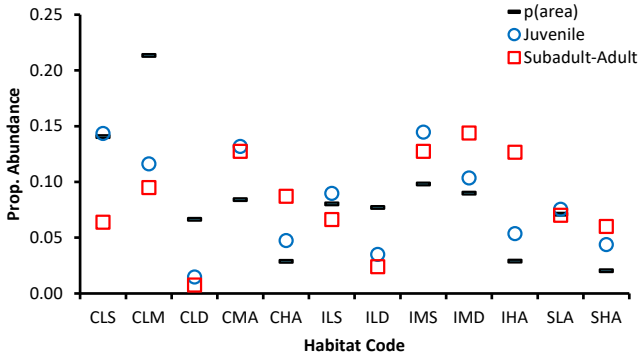

Figure 5.11. (A) Scatterplot of principal components (PC) 2 vs. 1 for French Grunt proportion abundance data by length class among habitat-depth strata; the solid red line separates length classes by a combination of the PC1 and PC2 axes into smaller (4-12 cm) and larger (14-26 cm) groups that have differing spatial abundance patterns. **(B)** Population length frequency of French Grunt; the dashed line denotes L_{hab}, the length at which a shift in habitat use occurs, possibly denoting the transition from juveniles to subadults-adults.

(A)

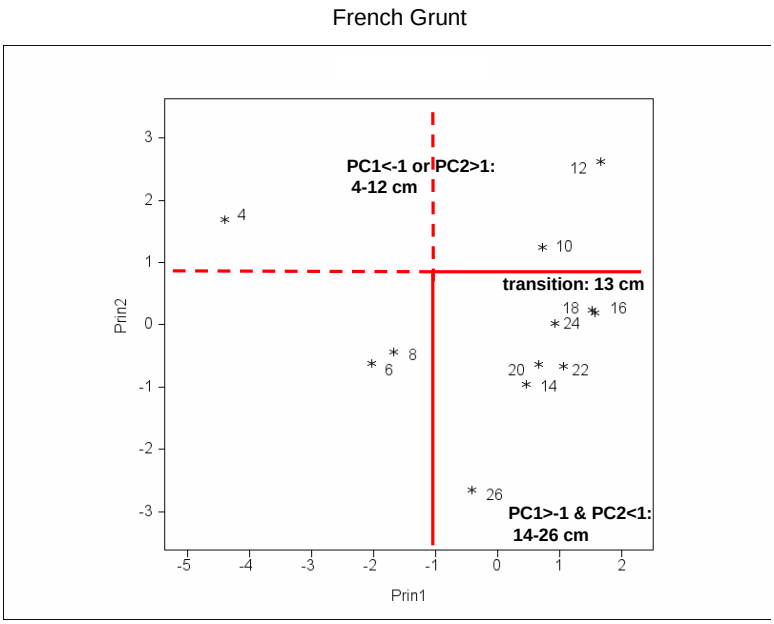

(B)

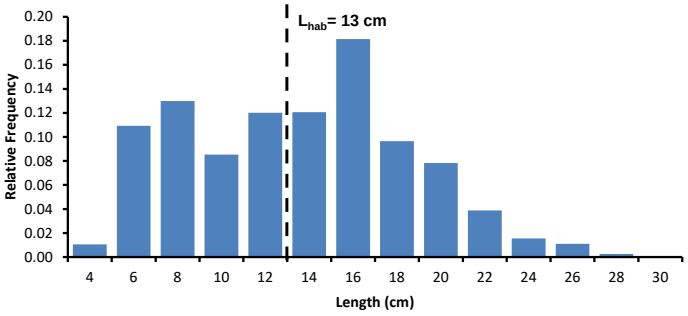

Figure 5.12. Proportion abundance by habitat type for juvenile and subadult-adult French Grunt. Black dashes denote the proportion of habitat area in the survey domain; see Table 5.2 for habitat codes.

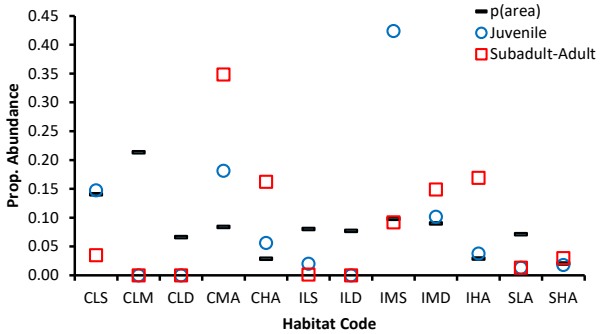

Figure 5.13. (A) Scatterplot of principal components (PC) 2 vs. 1 for Stoplight Parrotfish proportion abundance data by length class among habitat-depth strata; the red line separates length classes along PC1 into smaller (4-18 cm) and larger (20-40 cm) groups that have differing spatial abundance patterns. **(B)** Population length frequency of Stoplight Parrotfish; the dashed line denotes L_{hab}, the length at which a shift in habitat use occurs, possibly denoting the transition from juveniles to subadults-adults.

(A)

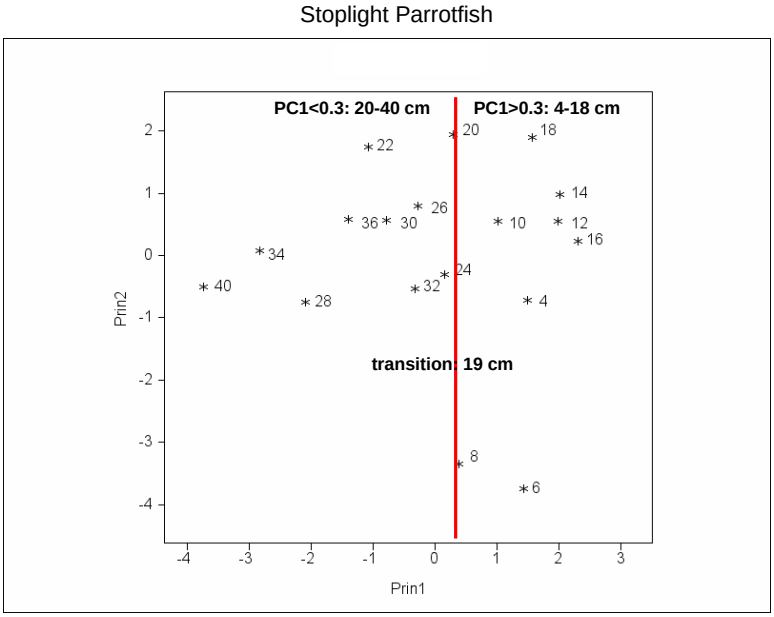

(B)

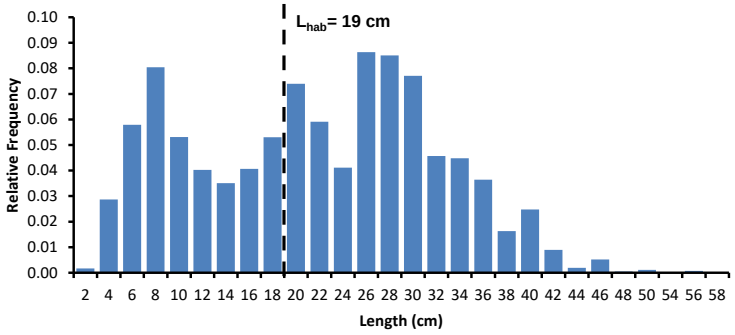

Figure 5.14. Proportion abundance by habitat type for juvenile and subadult-adult Stoplight Parrotfish. Black dashes denote the proportion of habitat area in the survey domain; see Table 5.2 for habitat codes.

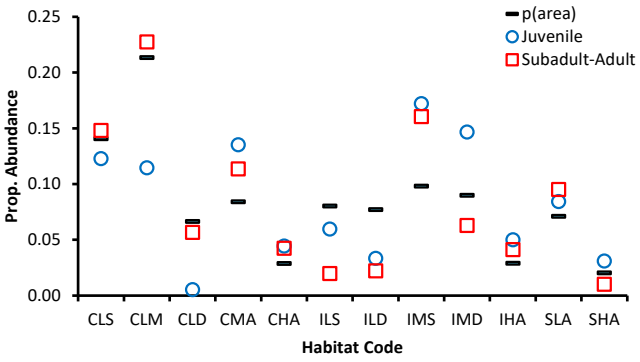

Figure 5.15. (A) Scatterplot of principal components (PC) 2 vs. 1 for Blue Tang proportion abundance data by length class among habitat-depth strata; the the solid red line separates length classes by a combination of the PC1 and PC2 axes into smaller (4-14 cm) and larger (16-30 cm) groups that have differing spatial abundance patterns. **(B)** Population length frequency of Blue Tang; the dashed line denotes L_{hab}, the length at which a shift in habitat use occurs, possibly denoting the transition from juveniles to subadults-adults.

(A)

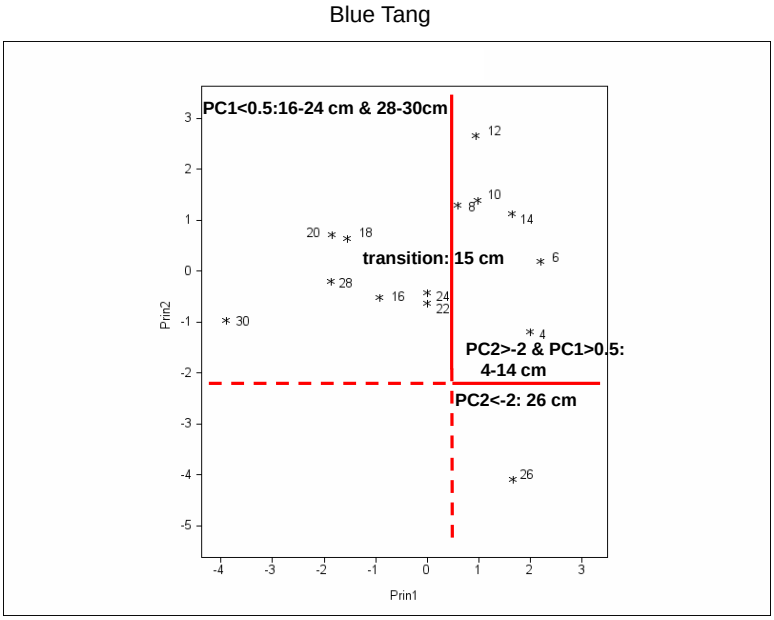

(B)

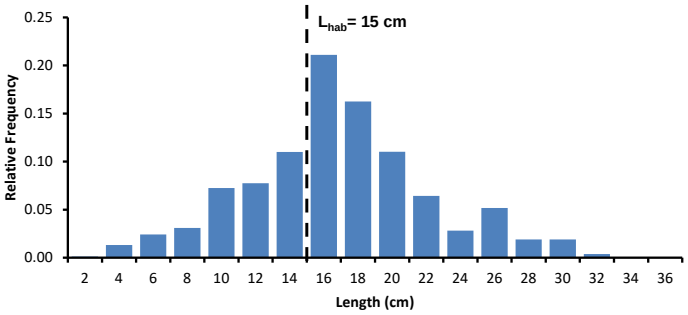

Figure 5.16. Proportion abundance by habitat type for juvenile and subadult-adult Blue Tang. Black dashes denote the proportion of habitat area in the survey domain; see Table 5.2 for habitat codes.

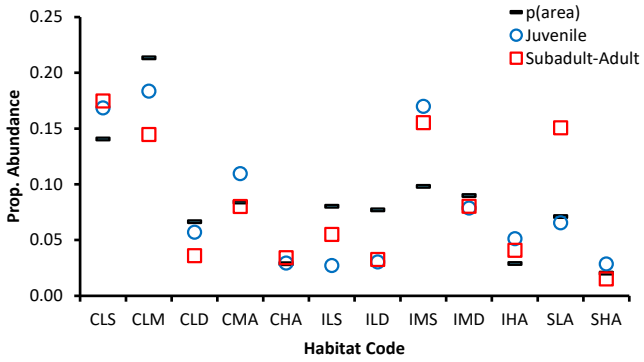

Figure 5.17. (A) Scatterplot of principal components (PC) 2 vs. 1 for Foureye Butterflyfish proportion abundance data by length class among habitat-depth strata; the the red line separates length classes along PC1 into smaller (3-5 cm) and larger (6-13 cm) groups that have differing spatial abundance patterns. **(B)** Population length frequency of Foureye Butterflyfish; the dashed line denotes L_{hab}, the length at which a shift in habitat use occurs, possibly denoting the transition from juveniles to subadults-adults.

(A)

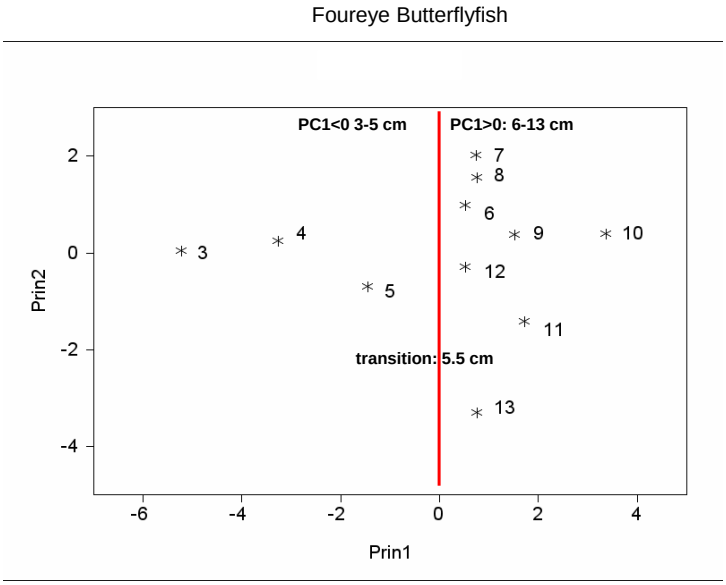

(B)

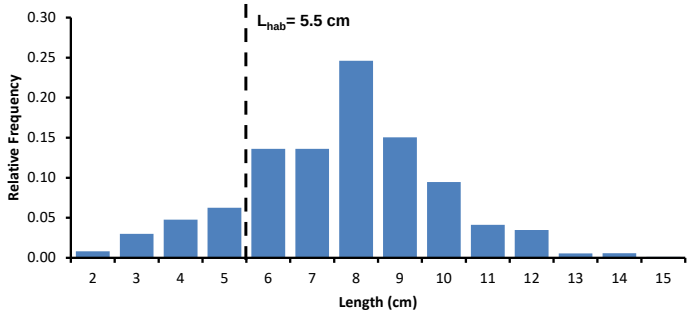

Figure 5.18. Proportion abundance by habitat type for juvenile and subadult-adult Foureye Butterflyfish. Black dashes denote the proportion of habitat area in the survey domain; see Table 5.2 for habitat codes.

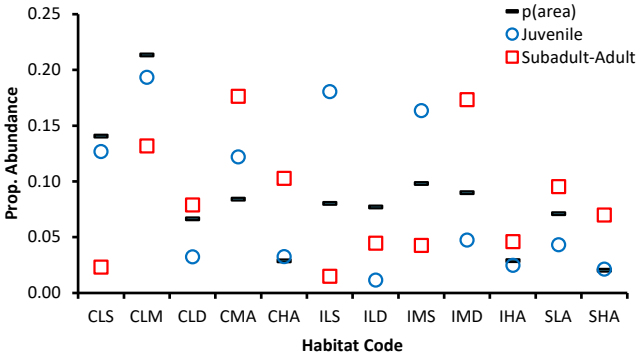

6.0 Regression Analysis: Depth Stratification

Analyses focused on specifying appropriate depth strata for the juvenile and subadult-adult life stages of the 9 design species. Logistic regression models were used to evaluate species occurrence as a function of depth. For exploratory model-building, the initial step converted depth from a continuous explanatory variable into categorical variables comprised of depth intervals. Relationships between fish occurrence p and depth intervals i=1,2,...,k were evaluated using the model

$$\text{logit}(p) = \alpha + b_1 X_1 + \cdots + b_{k-1} X_{k-1} + \varepsilon \quad , \qquad (1)$$

where logit $(p) = \left(\frac{p}{1-p}\right)$, X_i are discrete categorical variables for depth intervals, α is the intercept, b_i are the depth interval coefficients, and ε is the residual error. Estimates of p_i, the mean occurrence for interval i, are given by

$$p_i = \frac{e^{\alpha+b_i}}{1+e^{\alpha+b_i}} \quad . \qquad (2)$$

Depth intervals were constructed for 1 m increments along the sampled range of 1 to 30 m, combining the intervals as necessary to obtain a target minimum sample size of 30 observations. Three rugosity strata, low (L), moderate (M), and high (H), based on diver measurements of substrate vertical relief, were included in the model as covariates to control for the substrate complexity main effect on occurrence, enabling a detailed evaluation of the depth main effect on occurrence.

As shown in **Fig. 6.1A**, logistic regression point estimates of logit(p) for juvenile Black Grouper were generally higher for depths shallower than 10 m, and higher in depths deeper than 10 m. The substrate rugosity main effect was highly significant ($p<0.001$; **Table 6.1**); the graph of **Fig. 6.1B** shows higher logit(p) estimates for moderate and high rugosity compared to low rugosity. The point estimates of logit(p) from Fig. 6.1A were used to guide the construction of two different logistic regression models for juvenile Black Grouper occurrence as a function of depth (**Fig. 6.2**). The first was a continuous function, shown in **Figures 6.2A** (logit(p)-depth) and **6.2C** (back-transformed occurrence (p)-depth), which illustrates the general form of the occurrence-depth relationship. The second was a categorical function, shown in **Figures 6.2B** and **6.2D**, which illustrates depth strata that describe the occurrence-depth relationship. The depth strata were constructed such that model-fitting diagnostics (i.e., log-likelihood and AIC) were either similar to or outperformed the continuous model. These results will serve as the basis for exploring more effective depth stratification for future RVC surveys. In addition, the depth strata will be used as covariates to control for the depth main effect on abundance metrics in model-based analyses of potential substrate stratification variables.

Figure 6.1. Logistic regression point estimates of juvenile Black Grouper logit(p) for (A) depth intervals and (B) substrate habitat classes (L=low rugosity; M=moderate rugosity; H=high rugosity). Data were from 2011-2014 surveys in Dry Tortugas National Park. Each point estimate for depth was based on 30 or more observations.

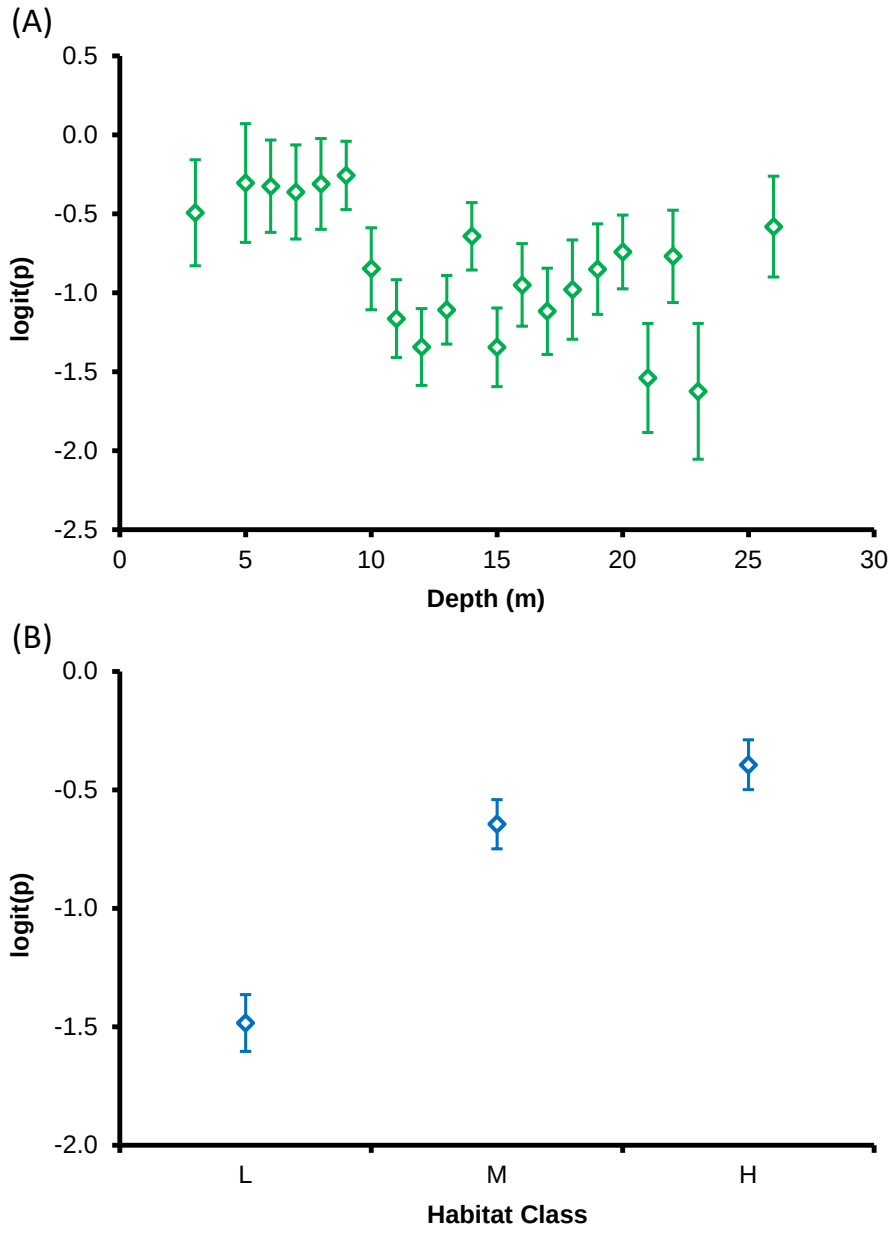

Figure 6.2. Logistic regression modeling for juvenile Black Grouper (A-B) logit(p) and (C-D) occurrence p as a function of depth. Logit(p) point estimates and regression functions are shown for (A) continuous depth and (B) depth strata models. Back-transformed occurrence regression functions are shown for (C) continuous depth and (D) depth strata models.

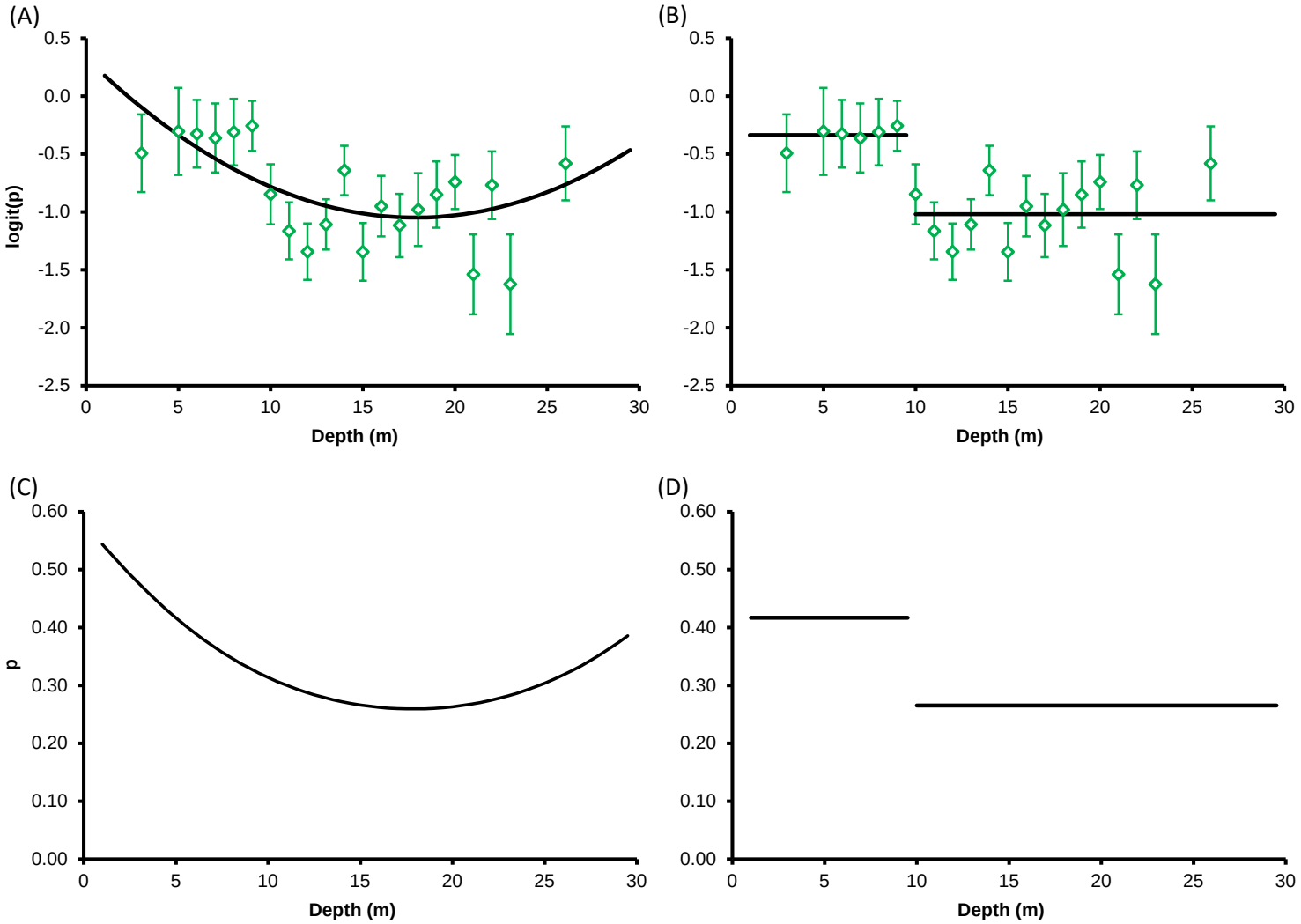

Similar analyses of relationships between abundance metrics and depth were conducted for subadult-adult Black Grouper (**Figs. 6.3-6.4**), and life stages of the other design species: Red Grouper (**Figs. 6.5-6.8**), Mutton Snapper (**Figs. 6.9-6.10**), Hogfish (**Figs. 6.11-6.12**), Yellowtail Snapper (**Figs. 6.13-6.16**), French Grunt (**Figs. 6.17-6.20**), Stoplight Parrotfish (**Figs. 6.21-6.24**), Blue Tang (**Figs. 6.25-6.28**), and Foureye Butterflyfish (**Figs. 6.29-6.32**). Data were insufficient to analyze the juvenile life stages of Mutton Snapper and Hogfish. A summary of logistic regression results for the 9 design species is provided in **Table 6.1**. The rugosity covariates were significant for all but one species life stage (juvenile Foureye Butterflyfish), and some form of depth stratification was indicated for all but two species life stages (adult Black Grouper and juvenile Foureye Butterflyfish).

Table 6.1. Summary of logistic regression results for depth stratification for target species and life stages in Dry Tortugas National Park. Diver-measured habitat rugosity was included as a covariate where appropriate (i.e., significant).

	Life	Rugosity	Continuous	Depth Strata Model	
Species	**Stage**	**Covariate Sig.**	**Depth Model**	**No. of Strata**	**Sig.**
Black Grouper	J	p<0.001	quadratic	2	p<0.001
	A	p<0.001	intercept only	1	ns
Red Grouper	J	p<0.001	linear	2	p<0.001
	A	p<0.05	quadratic	3	p<0.01
Mutton Snapper	A	ns	linear	2	p<0.01
Hogfish	A	ns	linear	2	p<0.01
Yellowtail Snapper	J	p<0.01	quadratic	3	p<0.001
	A	p<0.001	intercept only	2	p<0.05
French Grunt	J	p<0.001	linear	3	p<0.001
	A	p<0.001	linear	3	p<0.001
Stoplight Parrotfish	J	p<0.001	quadratic	3	p<0.001
	A	p<0.001	quadratic	3	p<0.001
Blue Tang	J	p<0.001	quadratic	3	p<0.001
	A	p<0.001	quadratic	2	p<0.001
Foureye Butterflyfish	J	ns	intercept only	1	ns
	A	p<0.001	quadratic	3	p<0.001

Figure 6.3. Logistic regression point estimates of subadult-adult Black Grouper logit(p) for (A) depth intervals and (B) substrate habitat classes (L=low rugosity; M=moderate rugosity; H=high rugosity). Data were from 2011-2014 surveys in Dry Tortugas National Park. Each point estimate for depth was based on 30 or more observations.

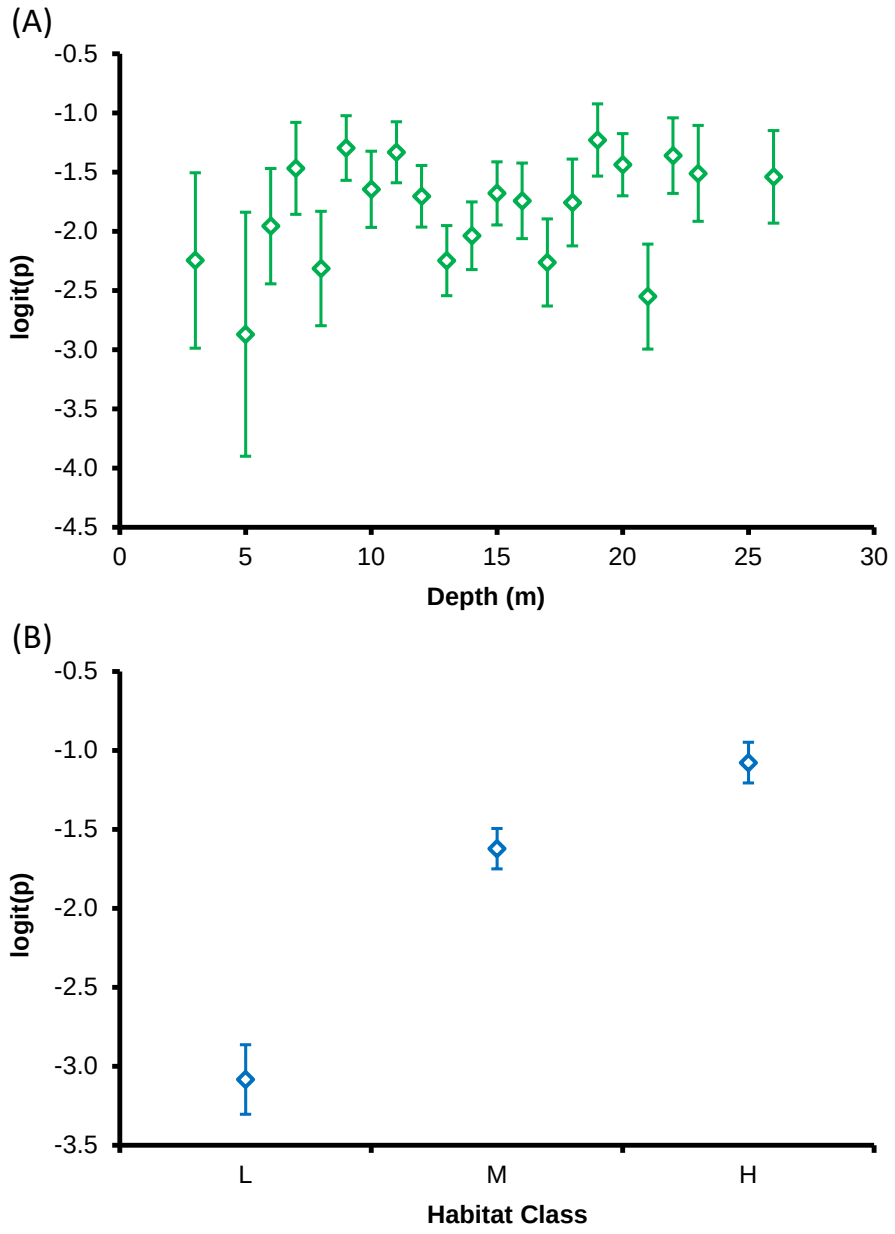

Figure 6.4. Logistic regression modeling for subadult-adult Black Grouper (A) logit(p) and (B) occurrence p as a function of depth. Logit(p) point estimates and regression function are shown for the (A) continuous depth model, which was identical to the strata depth model (1-strata). The back-transformed occurrence regression function is shown in (B).

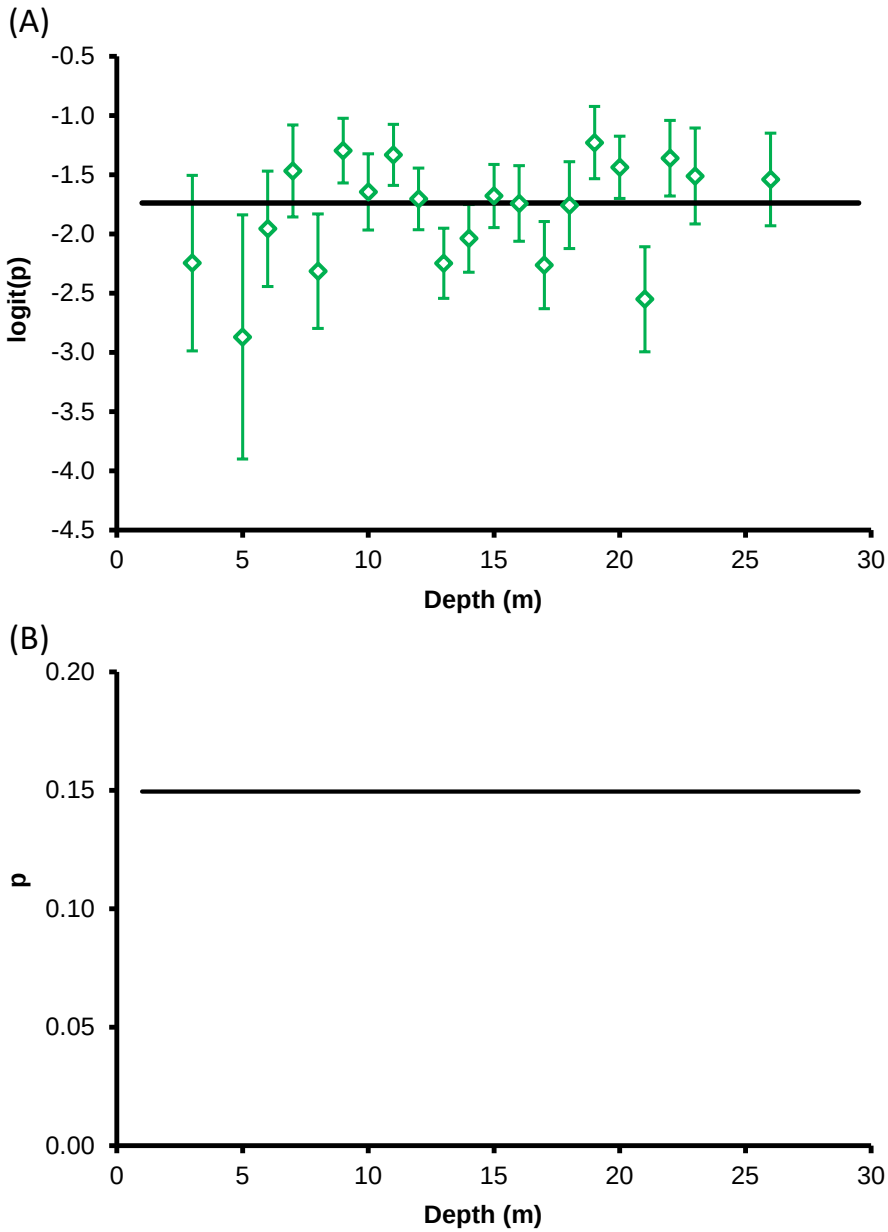

Figure 6.5. Logistic regression point estimates of juvenile Red Grouper logit(p) for (A) depth intervals and (B) substrate habitat classes (L=low rugosity; M=moderate rugosity; H=high rugosity). Data were from 2011-2014 surveys in Dry Tortugas National Park. Each point estimate for depth was based on 30 or more observations.

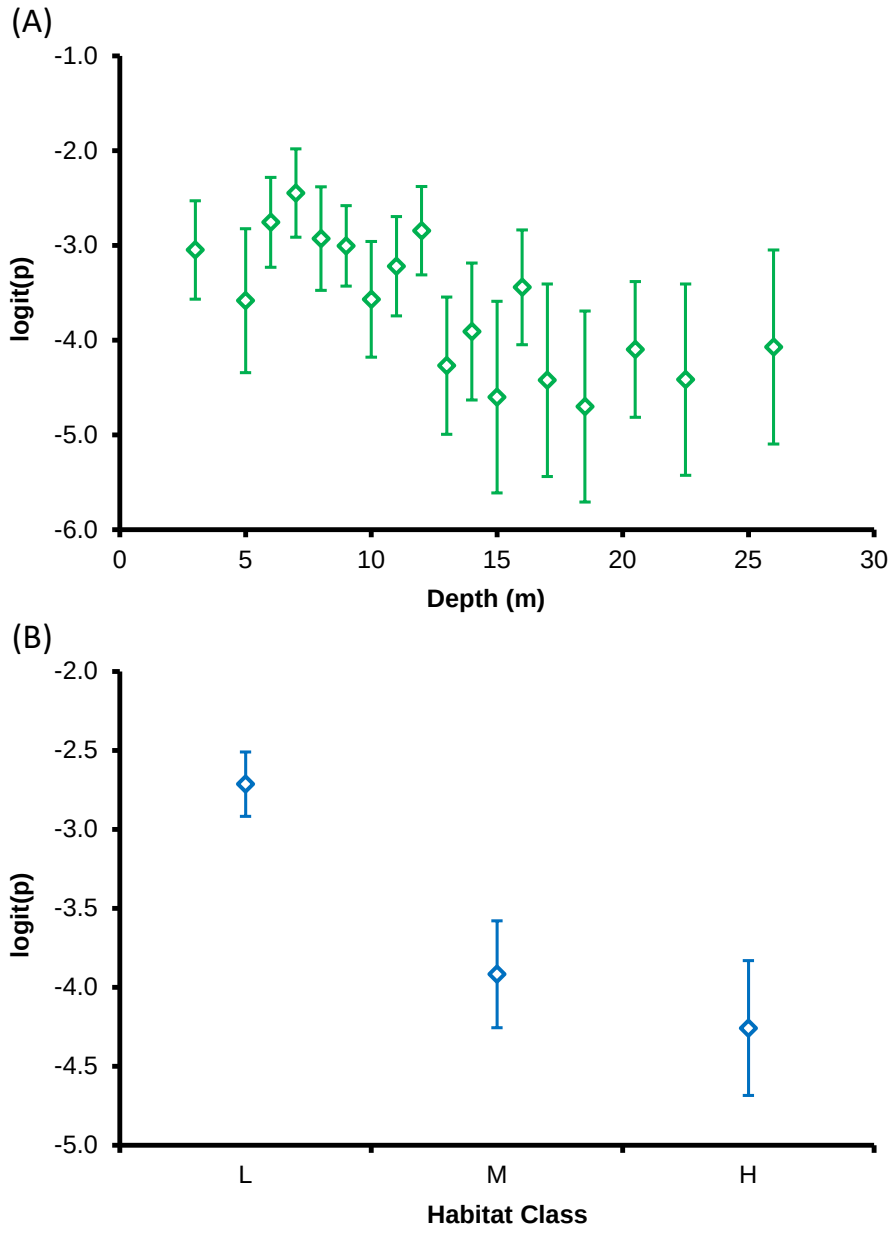

Figure 6.6. Logistic regression modeling for juvenile Red Grouper (A-B) logit(p) and (C-D) occurrence p as a function of depth. Logit(p) point estimates and regression functions are shown for (A) continuous depth and (B) depth strata models. Back-transformed occurrence regression functions are shown for (C) continuous depth and (D) depth strata models.

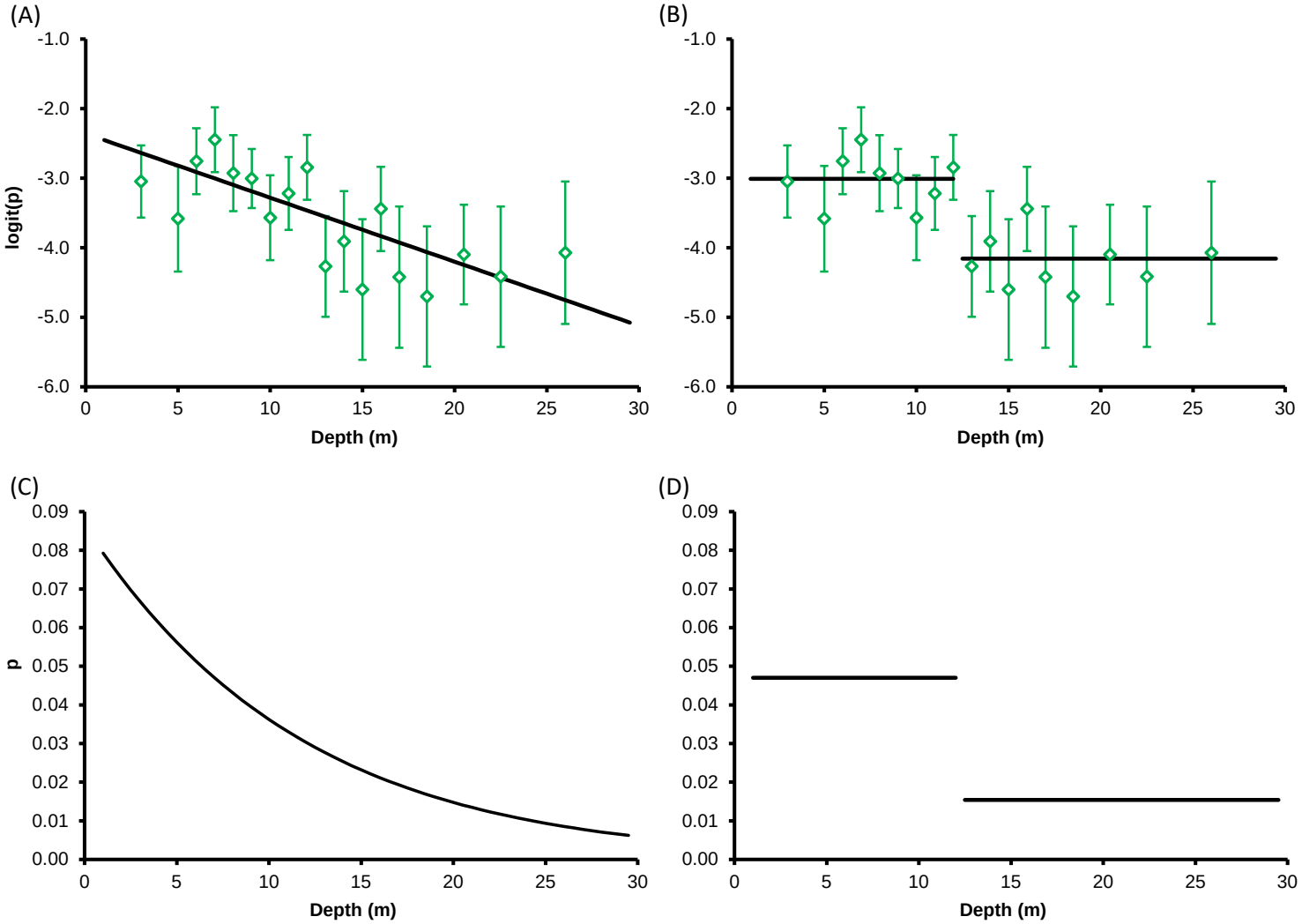

Figure 6.7. Logistic regression point estimates of subadult-adult Red Grouper logit(p) for (A) depth intervals and (B) substrate habitat classes (L=low rugosity; M=moderate rugosity; H=high rugosity). Data were from 2011-2014 surveys in Dry Tortugas National Park. Each point estimate for depth was based on 30 or more observations.

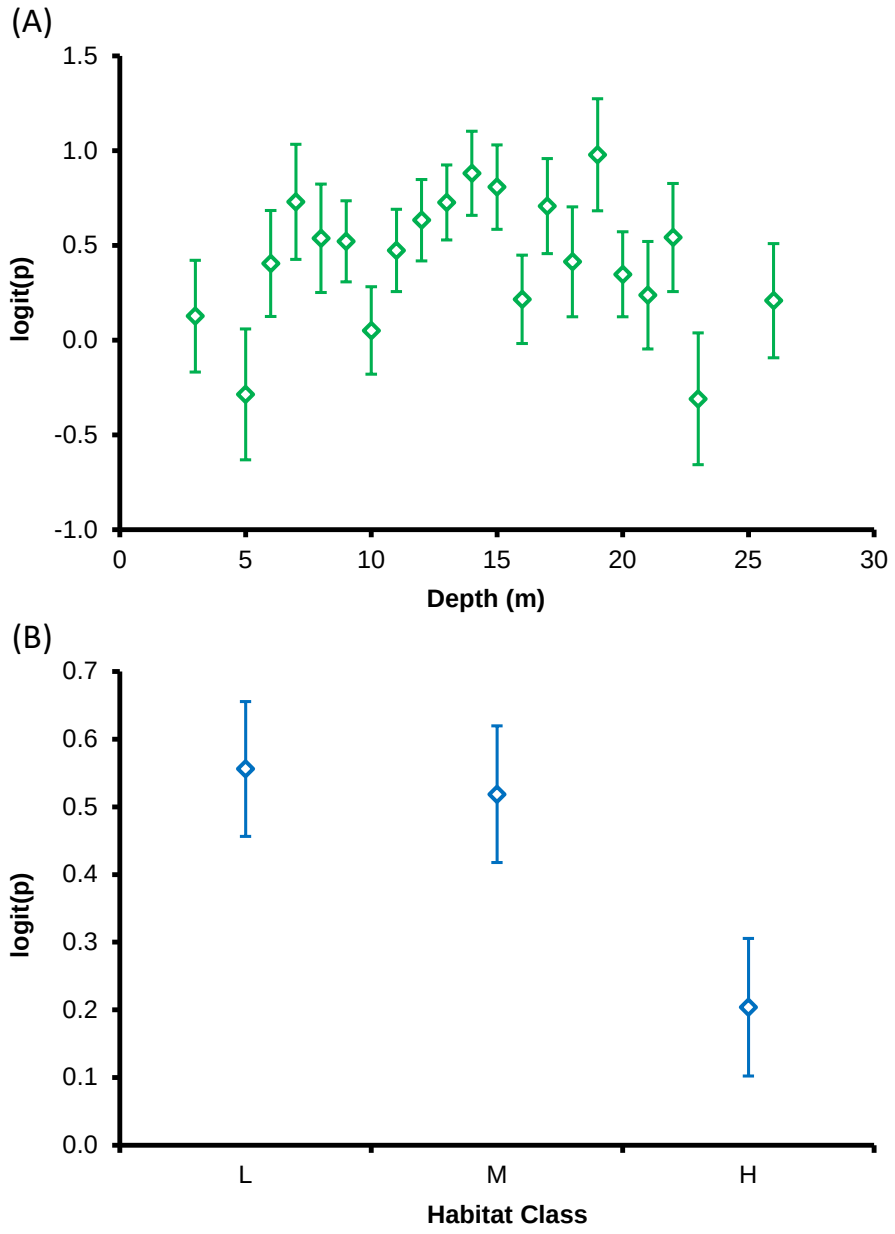

Figure 6.8. Logistic regression modeling for subadult-adult Red Grouper (A-B) logit(p) and (C-D) occurrence p as a function of depth. Logit(p) point estimates and regression functions are shown for (A) continuous depth and (B) depth strata models. Back-transformed occurrence regression functions are shown for (C) continuous depth and (D) depth strata models.

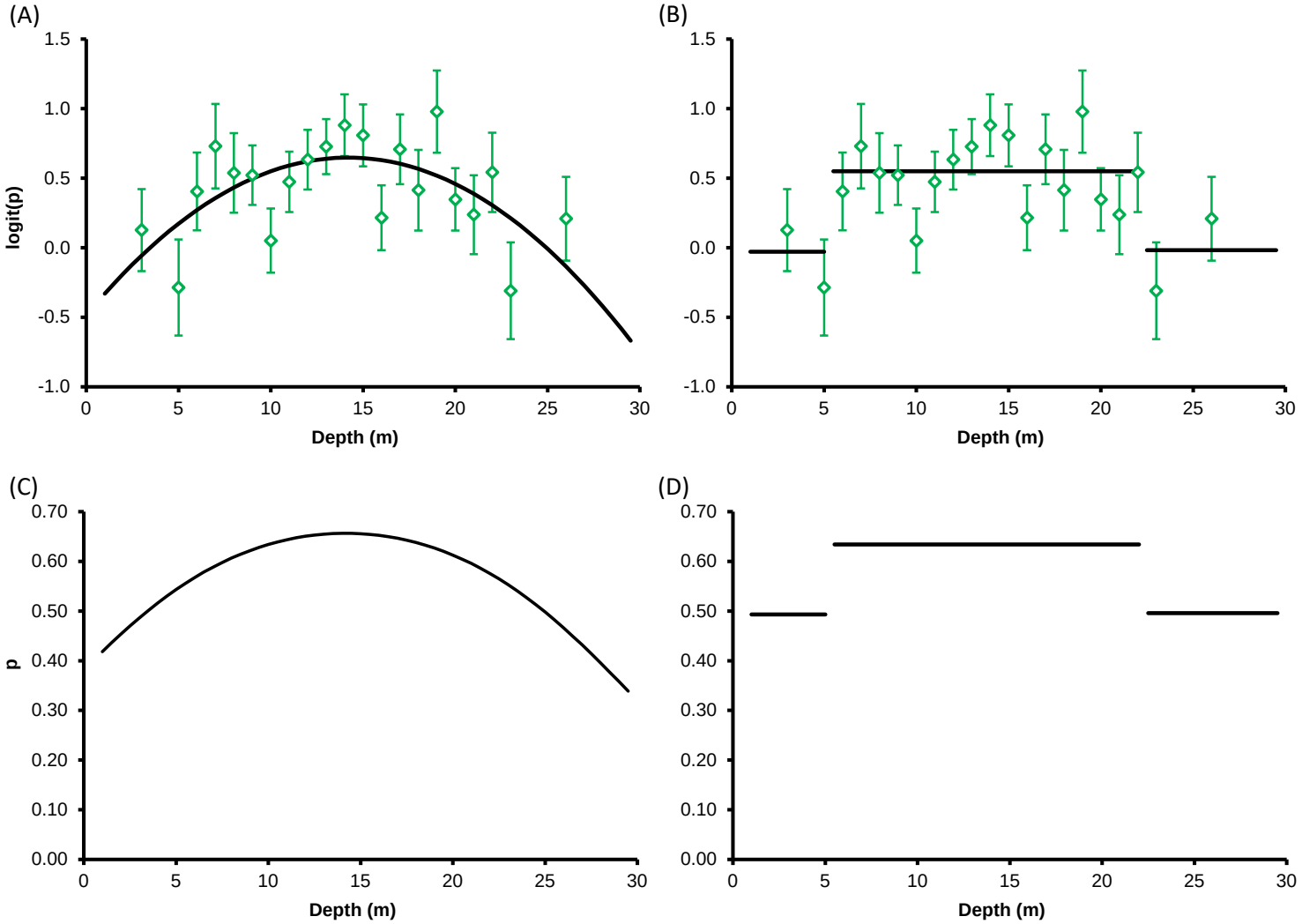

Figure 6.9. Logistic regression point estimates of subadult-adult Mutton Snapper logit(p) for (A) depth intervals and (B) substrate habitat classes (L=low rugosity; M=moderate rugosity; H=high rugosity). Data were from 2011-2014 surveys in Dry Tortugas National Park. Each point estimate for depth was based on 30 or more observations.

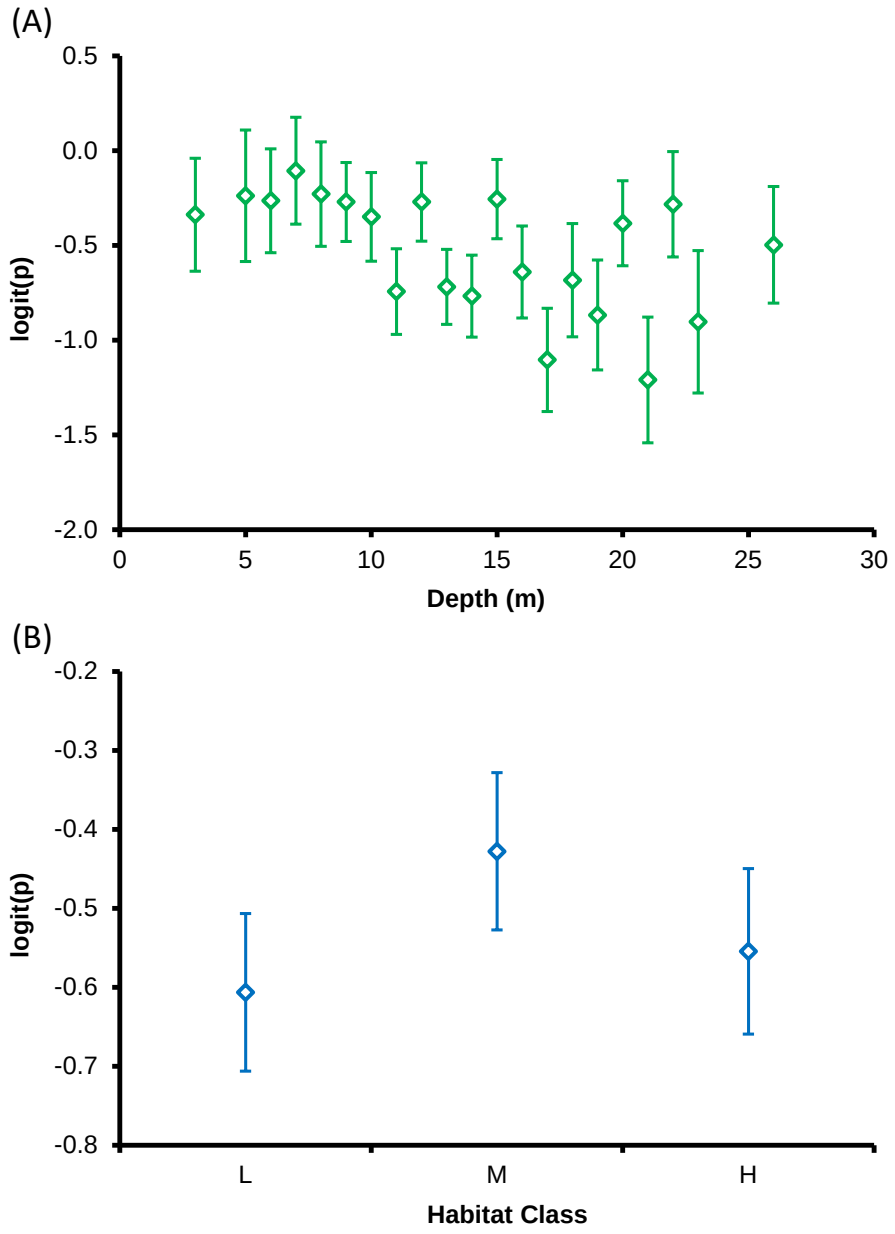

Figure 6.10. Logistic regression modeling for subadult-adult Mutton Snapper (A-B) logit(p) and (C-D) occurrence p as a function of depth. Logit(p) point estimates and regression functions are shown for (A) continuous depth and (B) depth strata models. Back-transformed occurrence regression functions are shown for (C) continuous depth and (D) depth strata models.

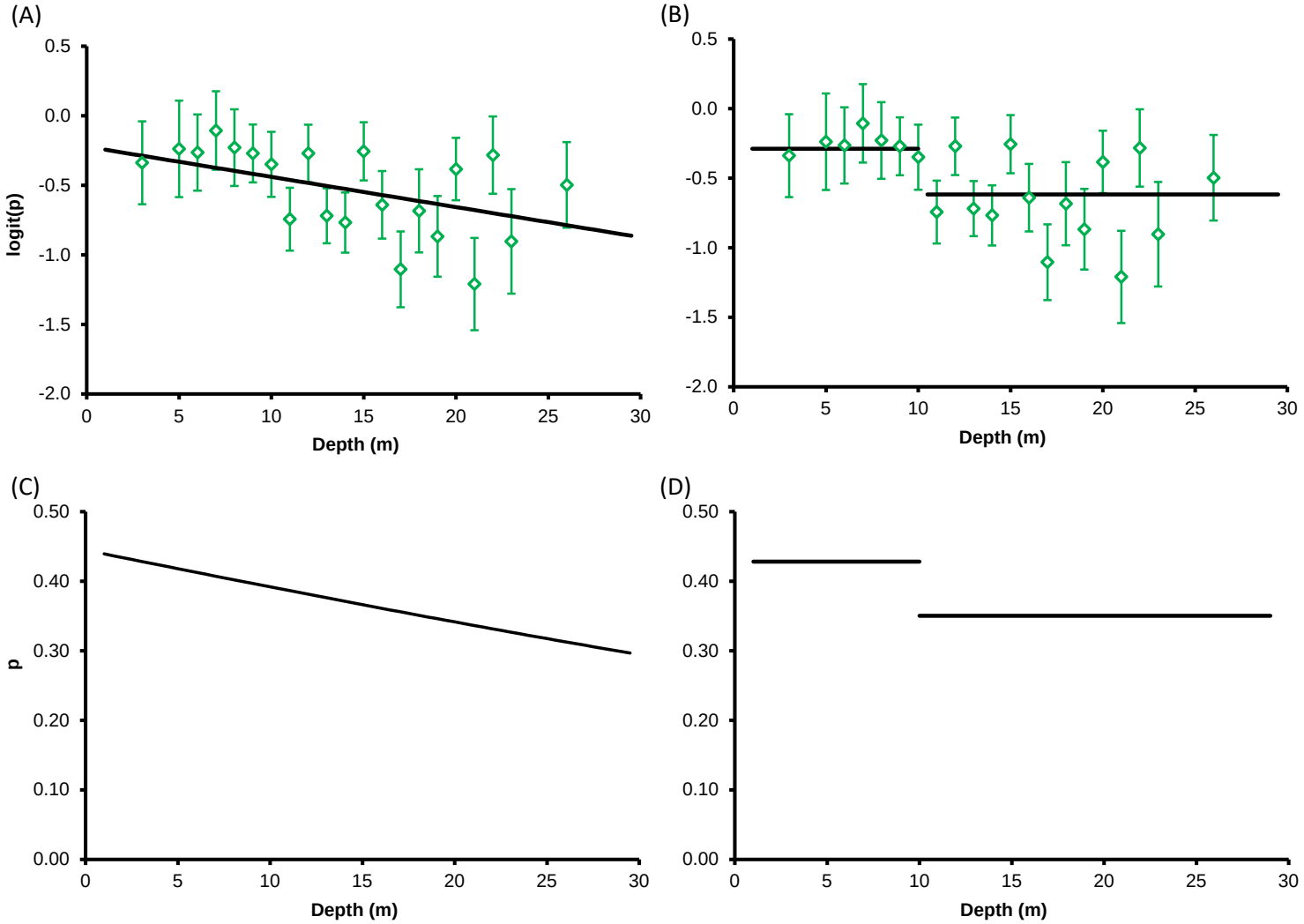

Figure 6.11. Logistic regression point estimates of subadult-adult Hogfish logit(p) for (A) depth intervals and (B) substrate habitat classes (L=low rugosity; M=moderate rugosity; H=high rugosity). Data were from 2011-2014 surveys in Dry Tortugas National Park. Each point estimate for depth was based on 30 or more observations.

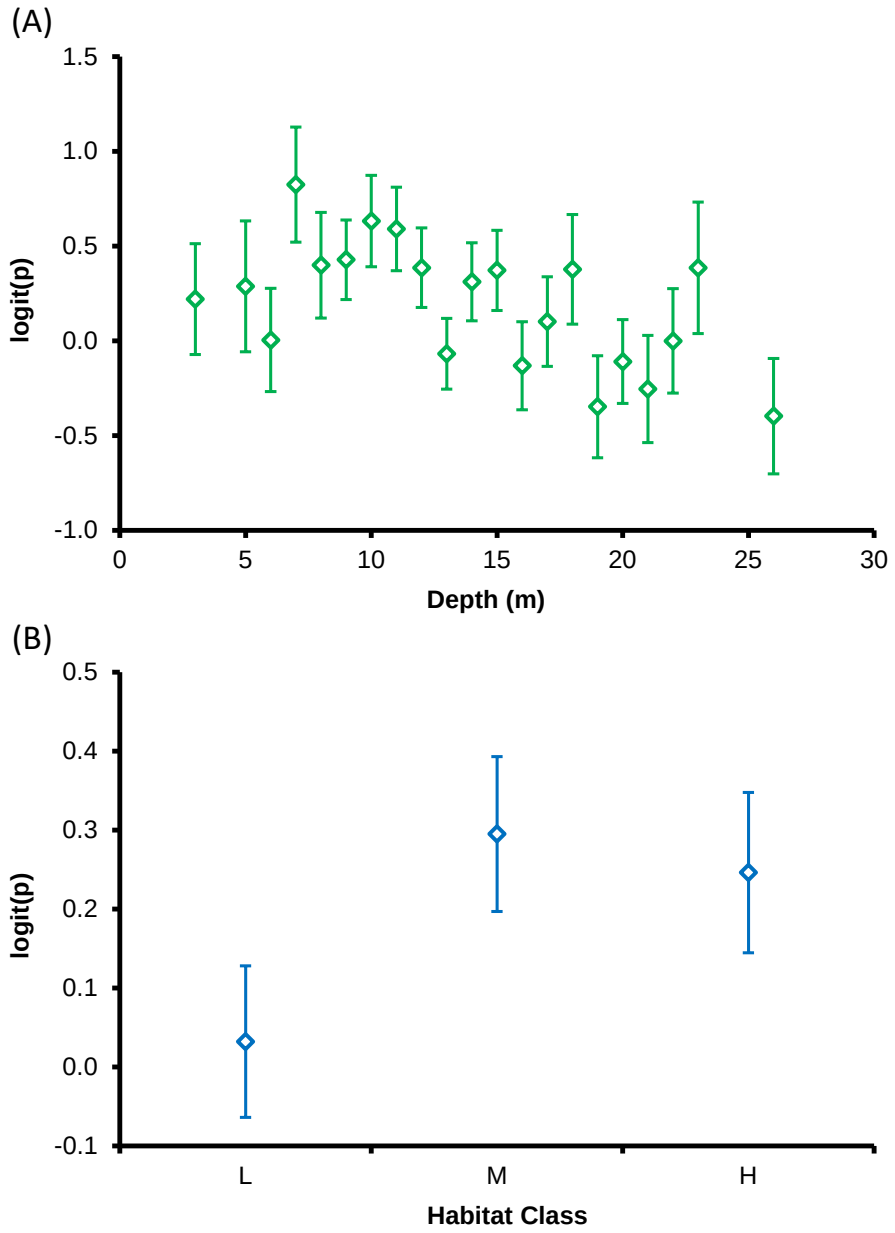

Figure 6.12. Logistic regression modeling for subadult-adult Hogfish (A-B) logit(p) and (C-D) occurrence p as a function of depth. Logit(p) point estimates and regression functions are shown for (A) continuous depth and (B) depth strata models. Back-transformed occurrence regression functions are shown for (C) continuous depth and (D) depth strata models.

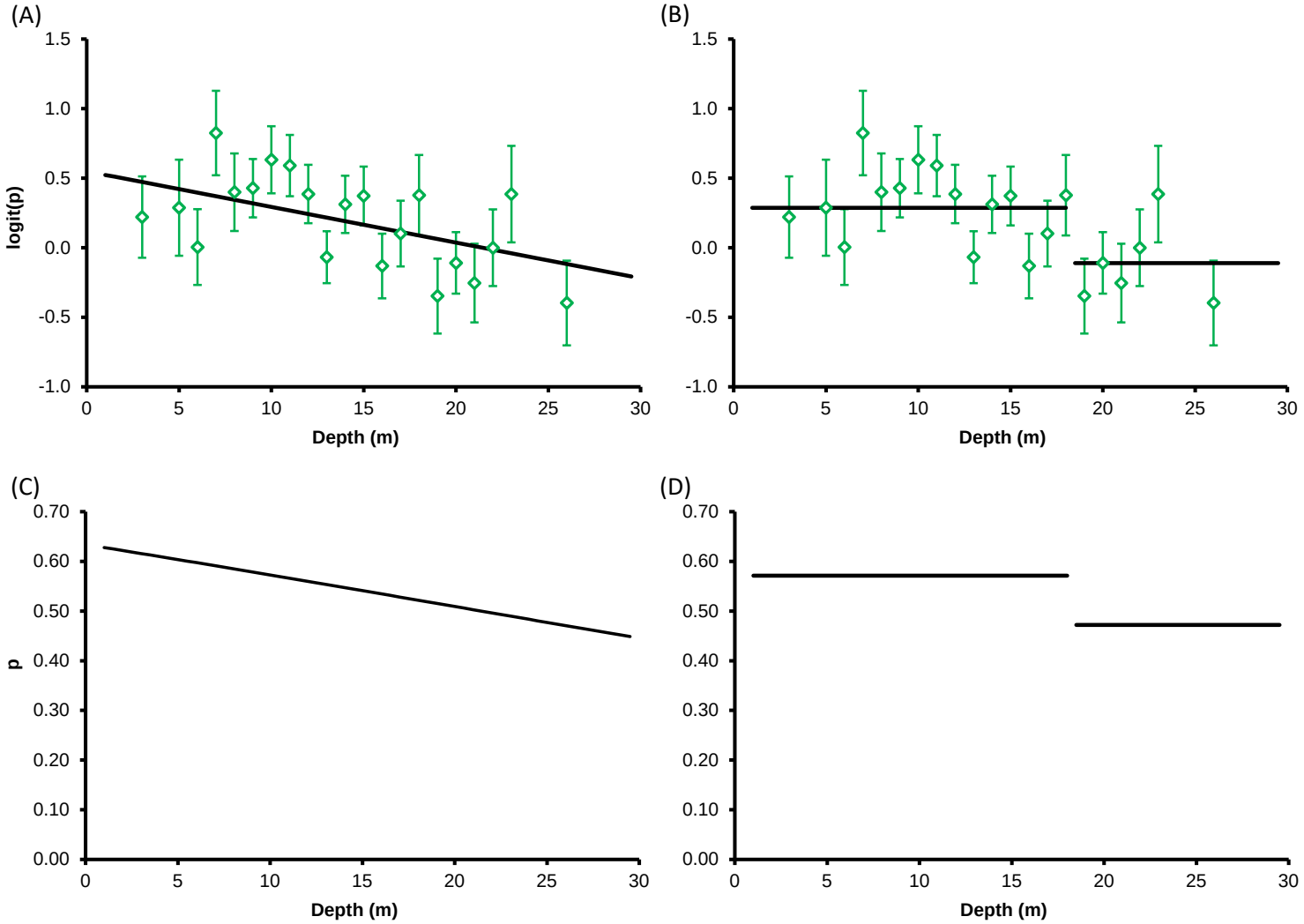

Figure 6.13. Logistic regression point estimates of juvenile Yellowtail Snapper logit(p) for (A) depth intervals and (B) substrate habitat classes (L=low rugosity; M=moderate rugosity; H=high rugosity). Data were from 2011-2014 surveys in Dry Tortugas National Park. Each point estimate for depth was based on 30 or more observations.

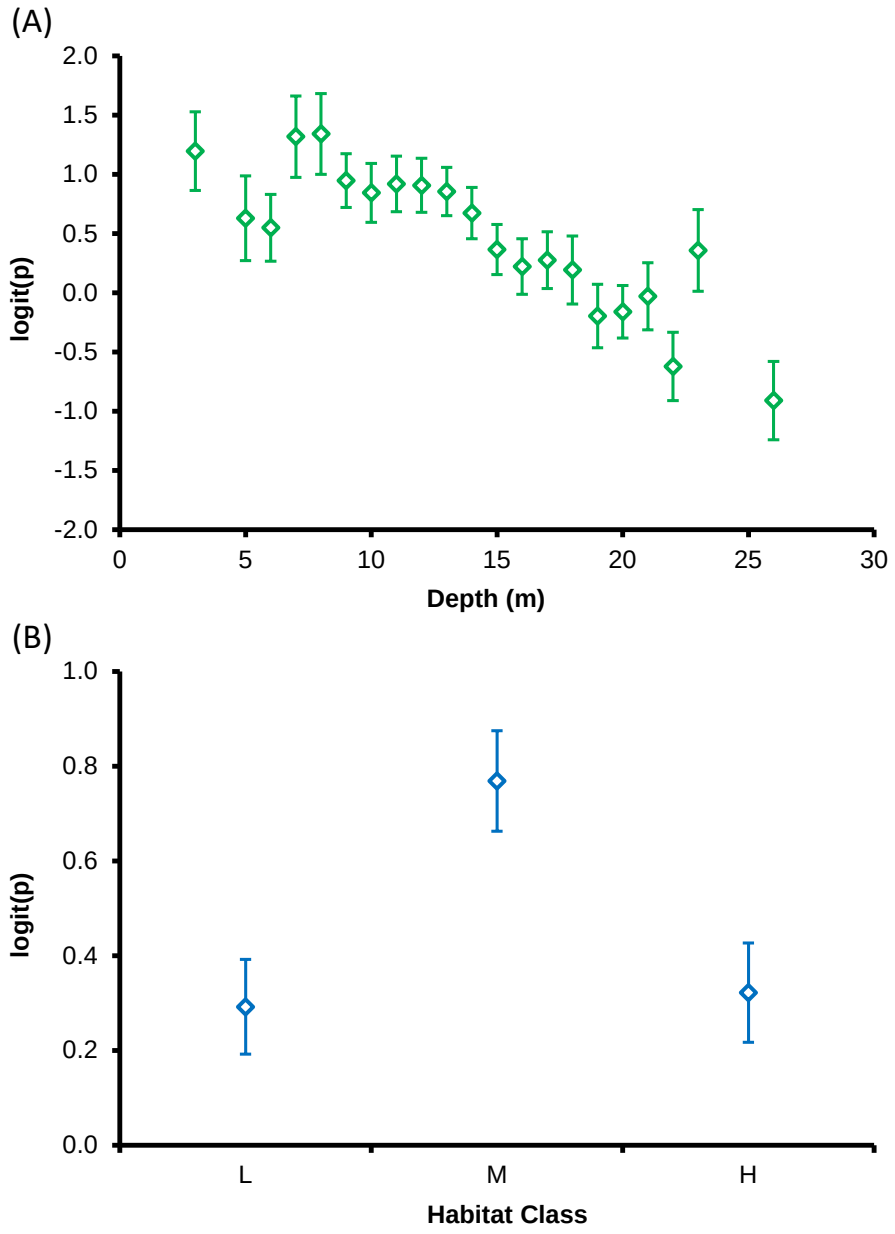

Figure 6.14. Logistic regression modeling for juvenile Yellowtail Snapper (A-B) logit(p) and (C-D) occurrence p as a function of depth. Logit(p) point estimates and regression functions are shown for (A) continuous depth and (B) depth strata models. Back-transformed occurrence regression functions are shown for (C) continuous depth and (D) depth strata models.

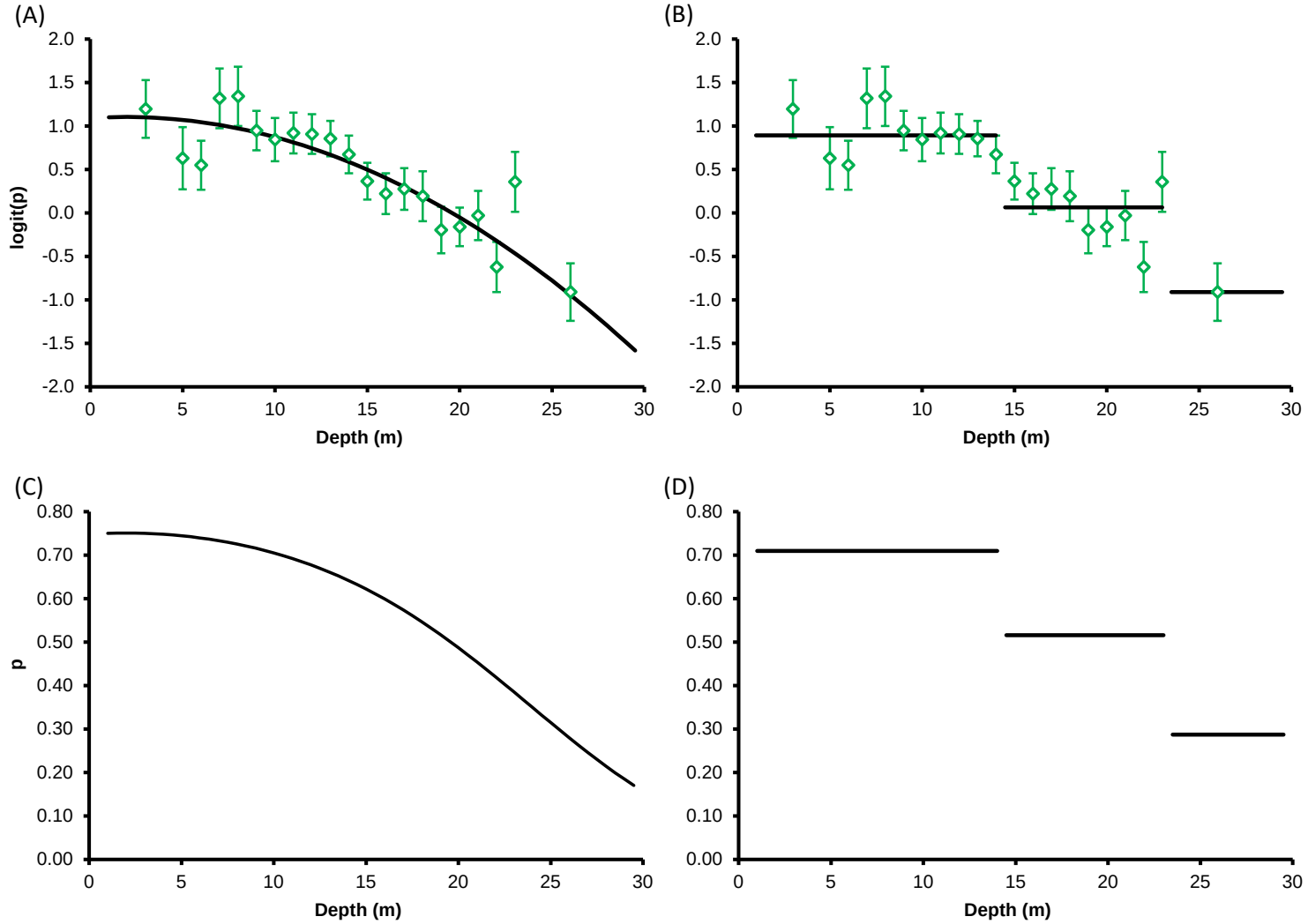

Figure 6.15. Logistic regression point estimates of subadult-adult Yellowtail Snapper logit(p) for (A) depth intervals and (B) substrate habitat classes (L=low rugosity; M=moderate rugosity; H=high rugosity). Data were from 2011-2014 surveys in Dry Tortugas National Park. Each point estimate for depth was based on 30 or more observations.

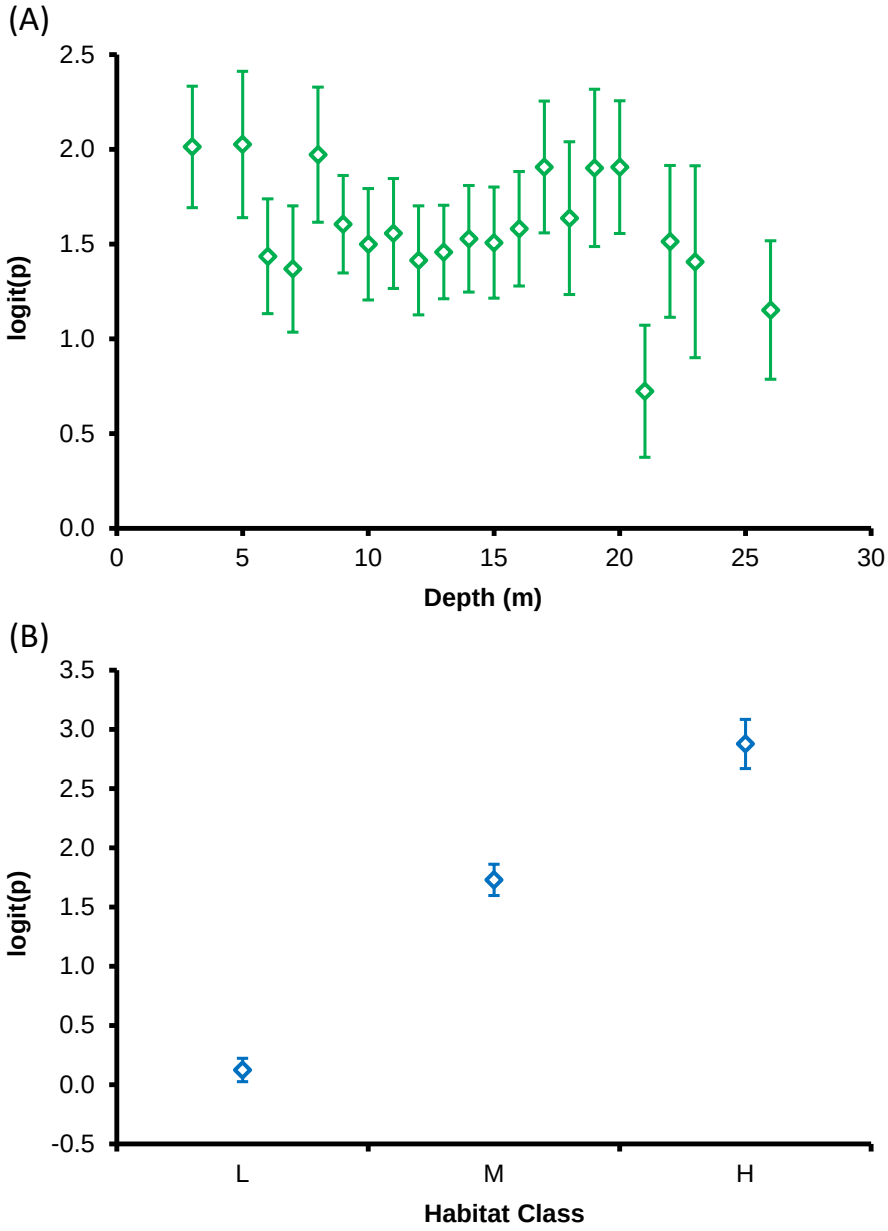

Figure 6.16. Logistic regression modeling for subadult-adult Yellowtail Snapper (A-B) logit(p) and (C-D) occurrence p as a function of depth. Logit(p) point estimates and regression functions are shown for (A) continuous depth and (B) depth strata models. Back-transformed occurrence regression functions are shown for (C) continuous depth and (D) depth strata models.

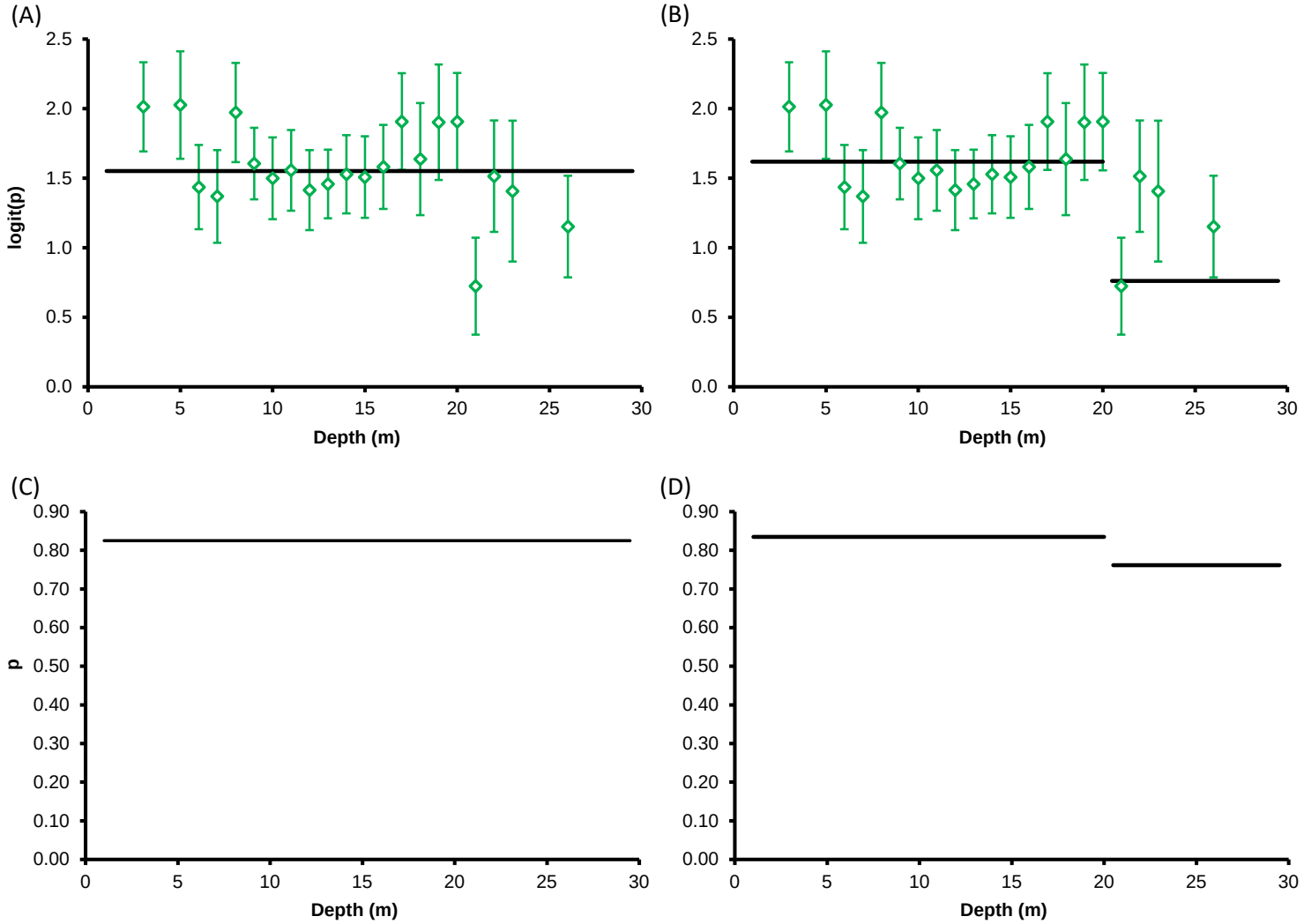

Figure 6.17. Logistic regression point estimates of juvenile French Grunt logit(p) for (A) depth intervals and (B) substrate habitat classes (L=low rugosity; M=moderate rugosity; H=high rugosity). Data were from 2011-2014 surveys in Dry Tortugas National Park. Each point estimate for depth was based on 30 or more observations.

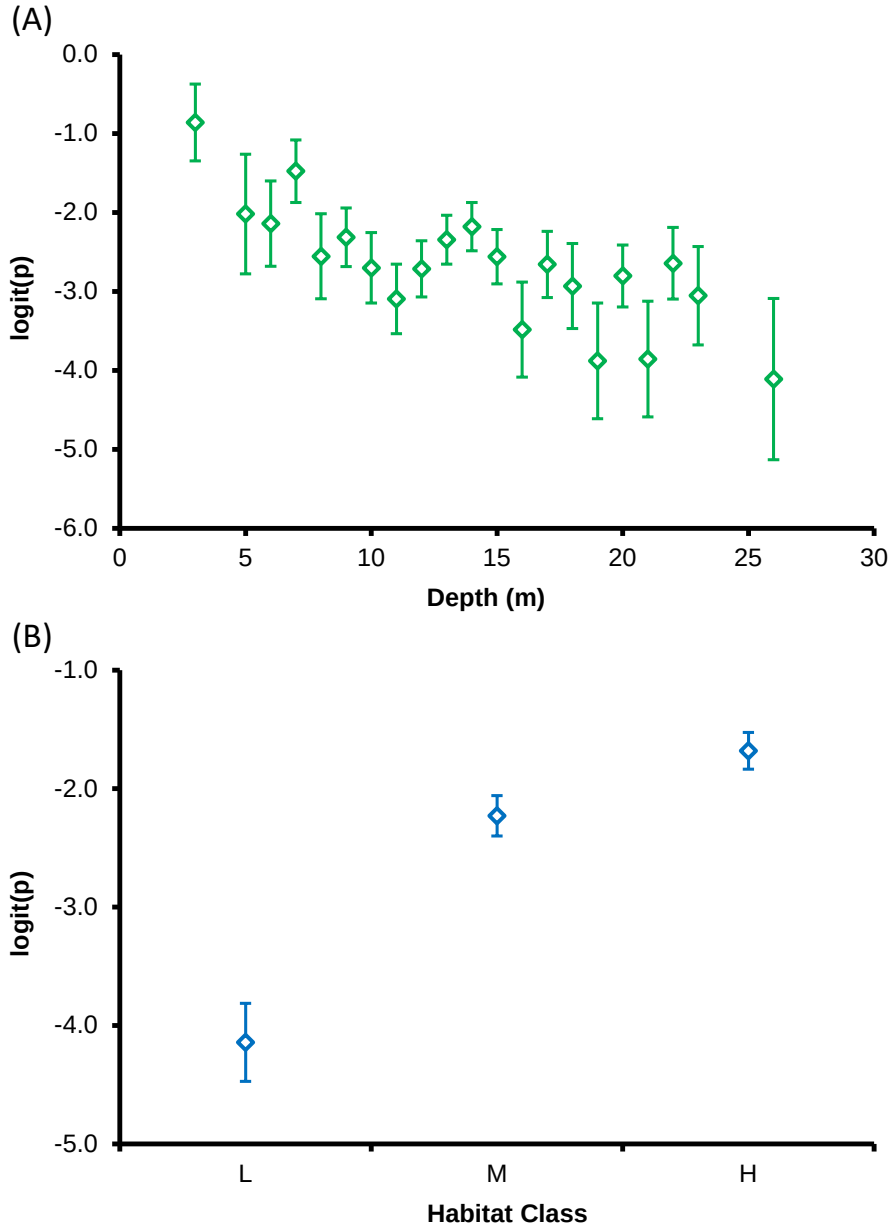

Figure 6.18. Logistic regression modeling for juvenile French Grunt (A-B) logit(p) and (C-D) occurrence p as a function of depth. Logit(p) point estimates and regression functions are shown for (A) continuous depth and (B) depth strata models. Back-transformed occurrence regression functions are shown for (C) continuous depth and (D) depth strata models.

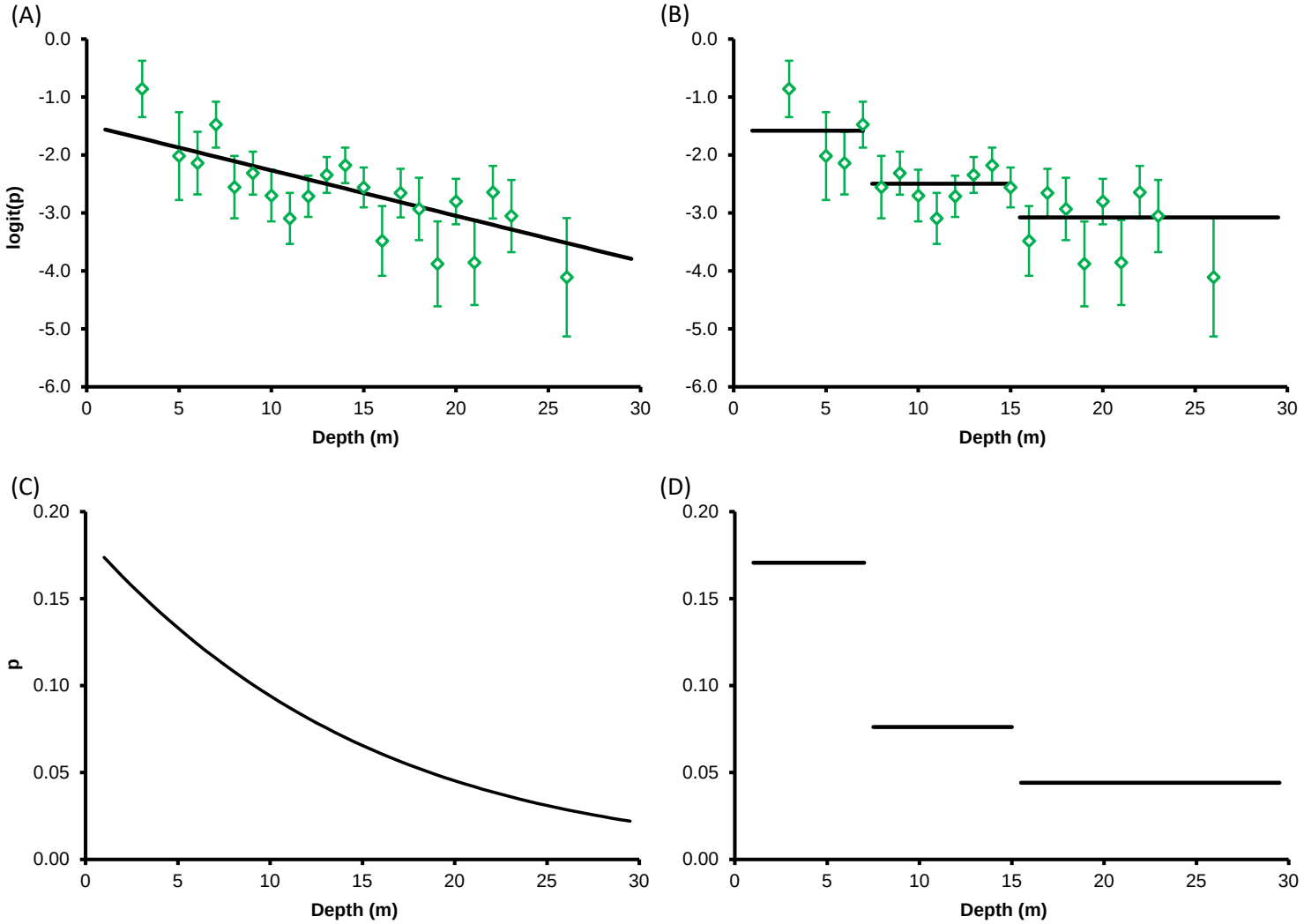

Figure 6.19. Logistic regression point estimates of subadult-adult French Grunt logit(p) for (A) depth intervals and (B) substrate habitat classes (L=low rugosity; M=moderate rugosity; H=high rugosity). Data were from 2011-2014 surveys in Dry Tortugas National Park. Each point estimate for depth was based on 30 or more observations.

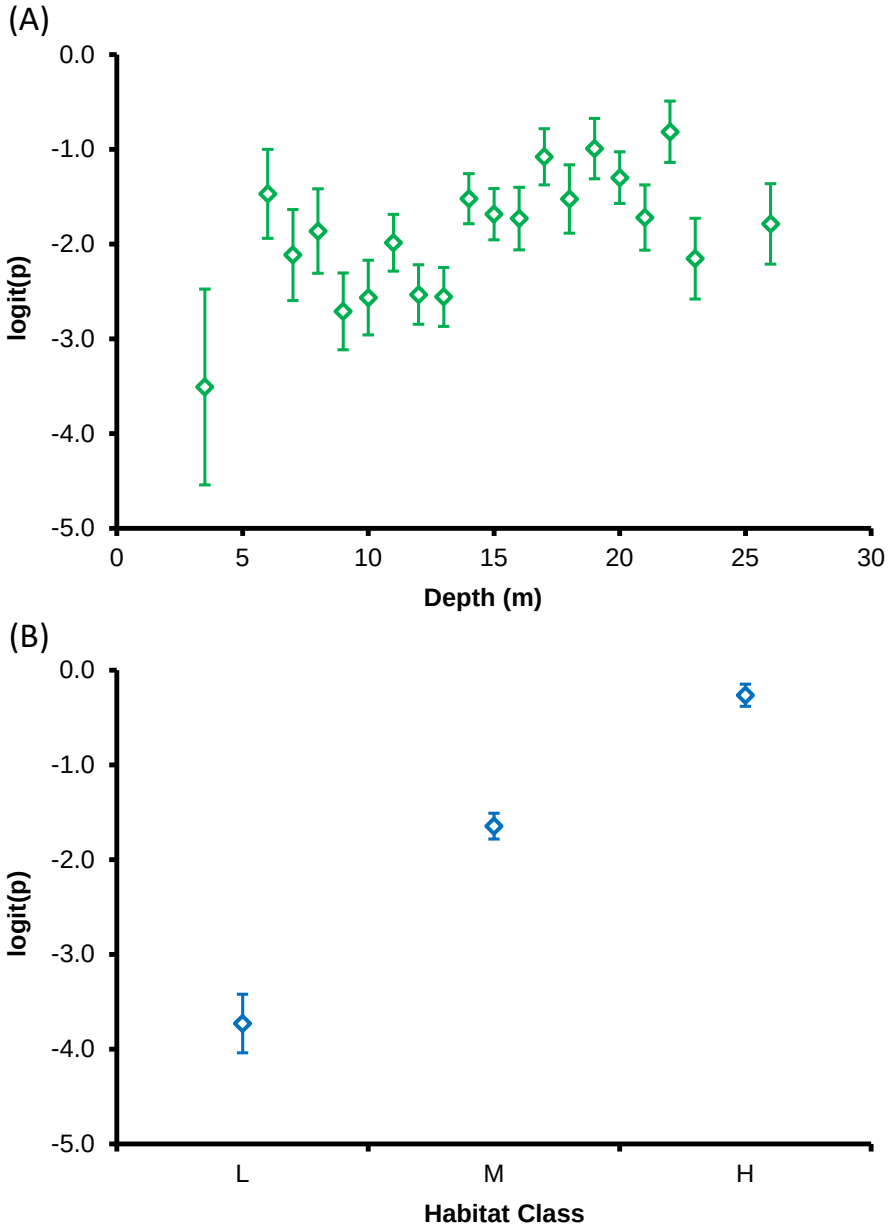

Figure 6.20. Logistic regression modeling for subadult-adult French Grunt (A-B) logit(p) and (C-D) occurrence p as a function of depth. Logit(p) point estimates and regression functions are shown for (A) continuous depth and (B) depth strata models. Back-transformed occurrence regression functions are shown for (C) continuous depth and (D) depth strata models.

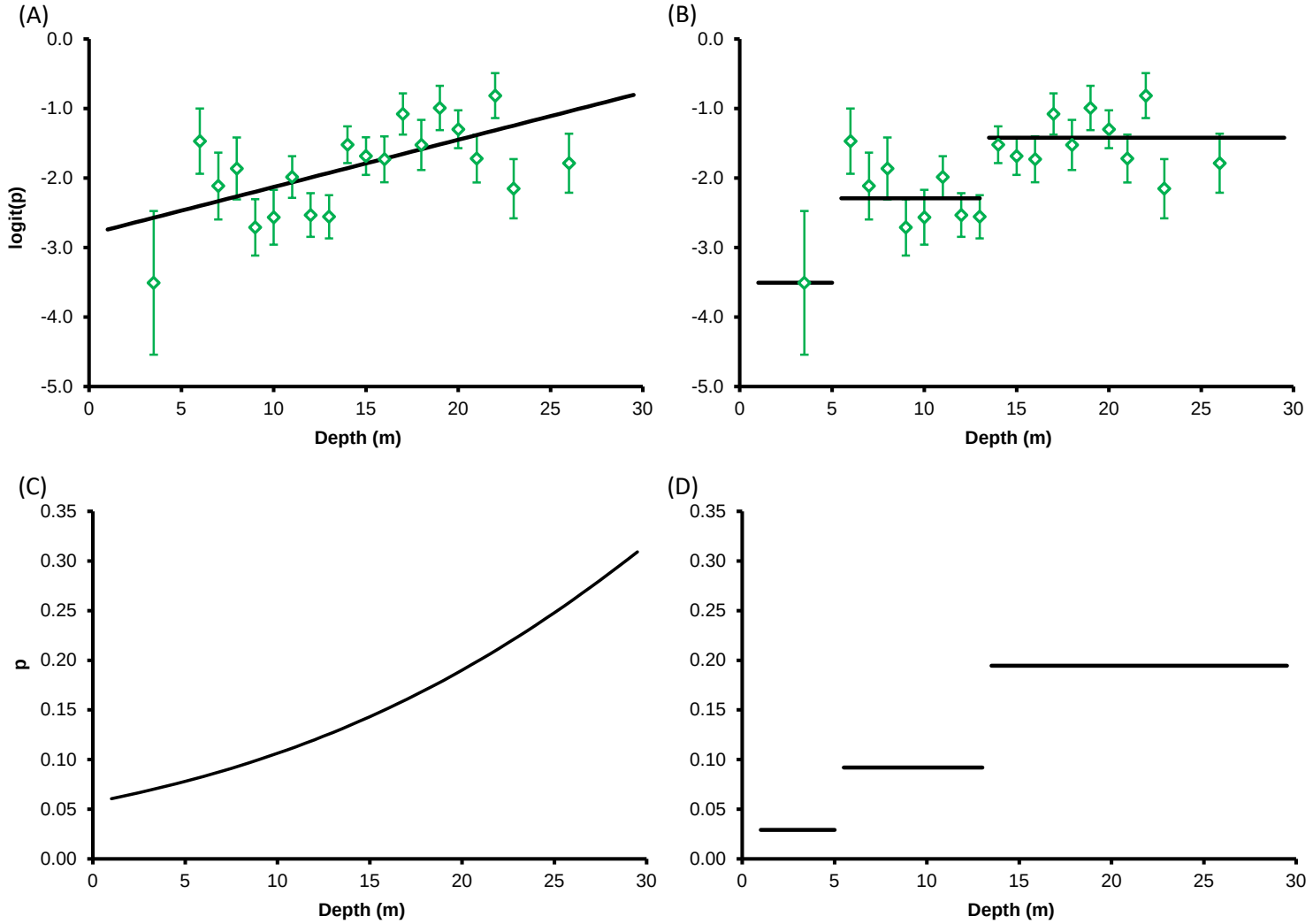

Figure 6.21. Logistic regression point estimates of juvenile Stoplight Parrotfish logit(p) for (A) depth intervals and (B) substrate habitat classes (L=low rugosity; M=moderate rugosity; H=high rugosity). Data were from 2011-2014 surveys in Dry Tortugas National Park. Each point estimate for depth was based on 30 or more observations.

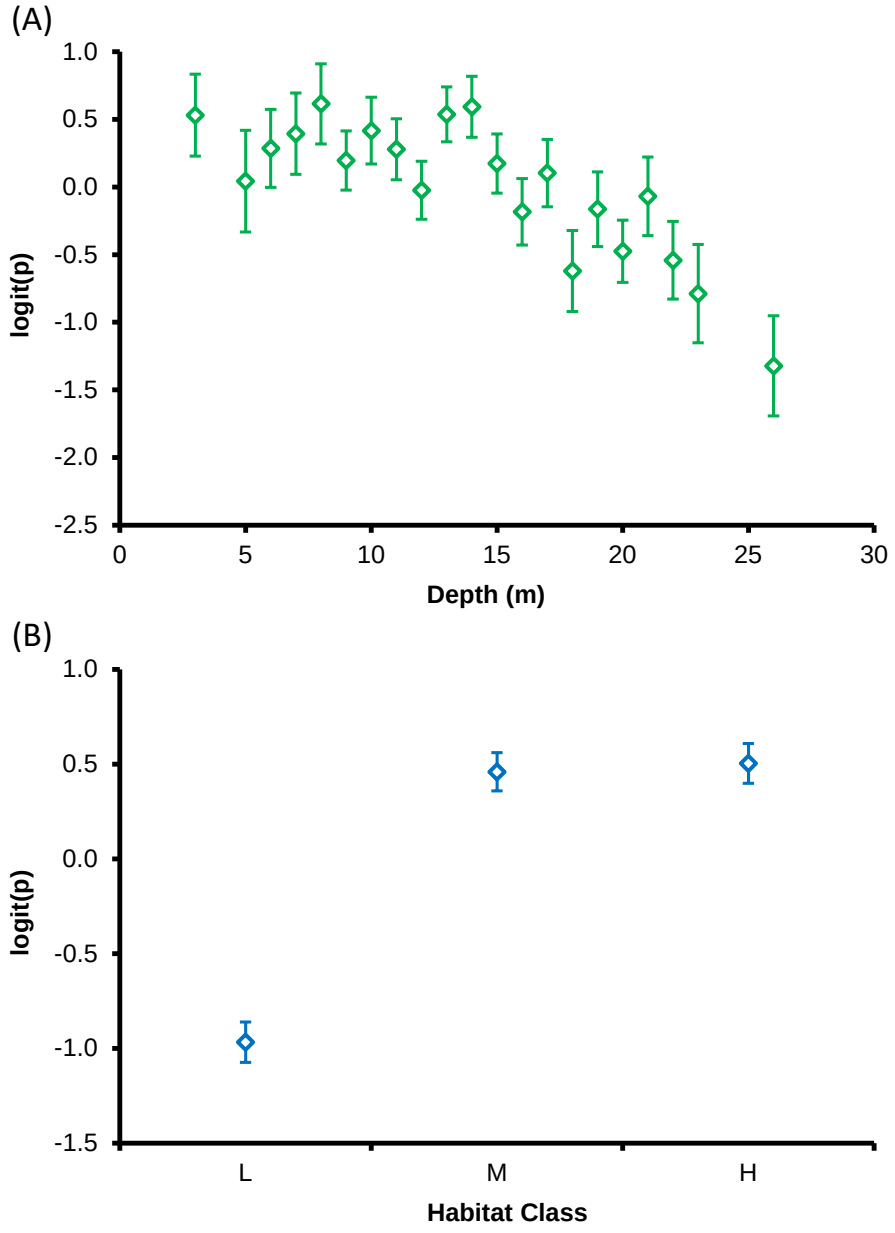

Figure 6.22. Logistic regression modeling for juvenile Stoplight Parrotfish (A-B) logit(p) and (C-D) occurrence p as a function of depth. Logit(p) point estimates and regression functions are shown for (A) continuous depth and (B) depth strata models. Back-transformed occurrence regression functions are shown for (C) continuous depth and (D) depth strata models.

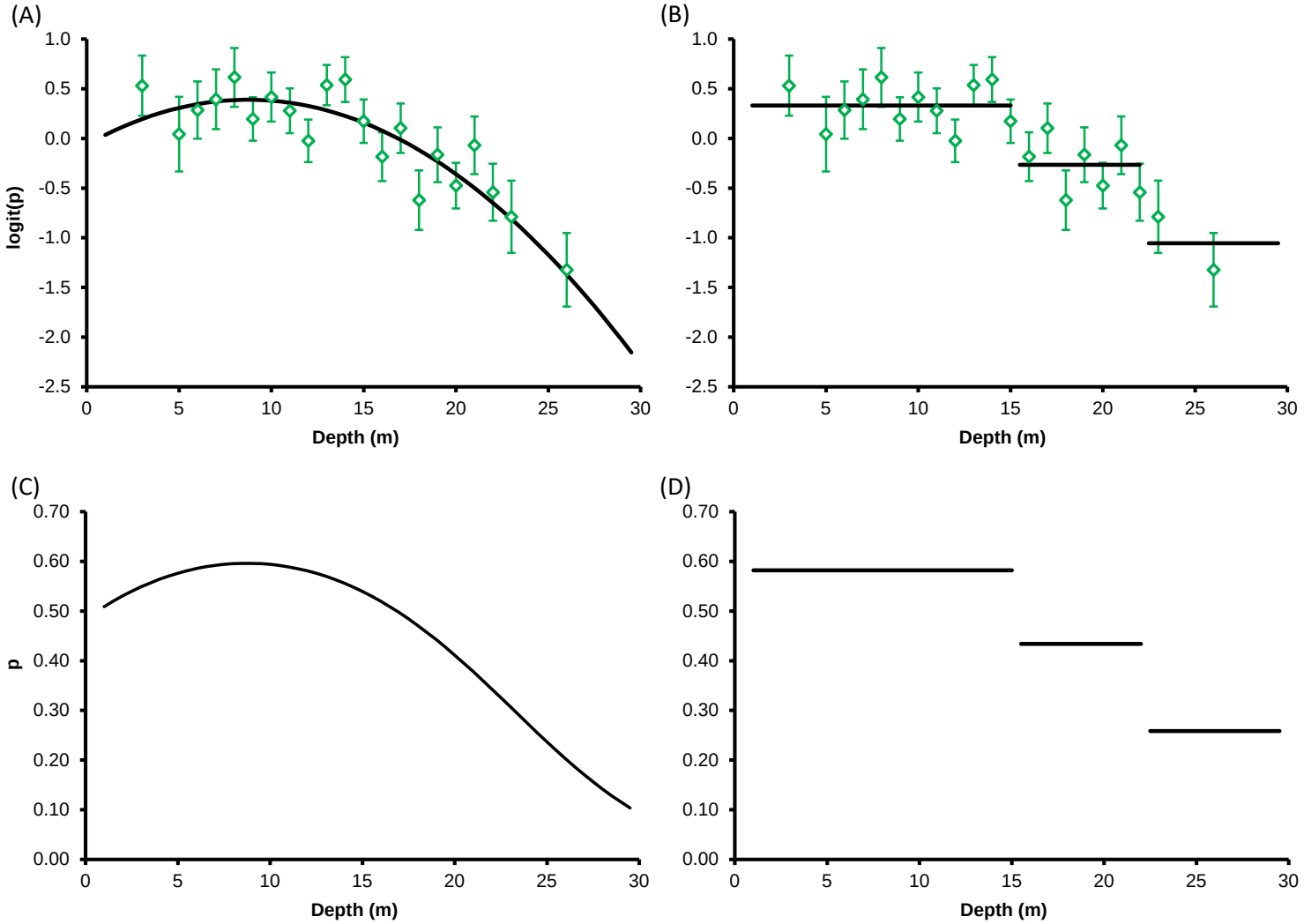

Figure 6.23. Logistic regression point estimates of subadult-adult Stoplight Parrotfish logit(p) for (A) depth intervals and (B) substrate habitat classes (L=low rugosity; M=moderate rugosity; H=high rugosity). Data were from 2011-2014 surveys in Dry Tortugas National Park. Each point estimate for depth was based on 30 or more observations.

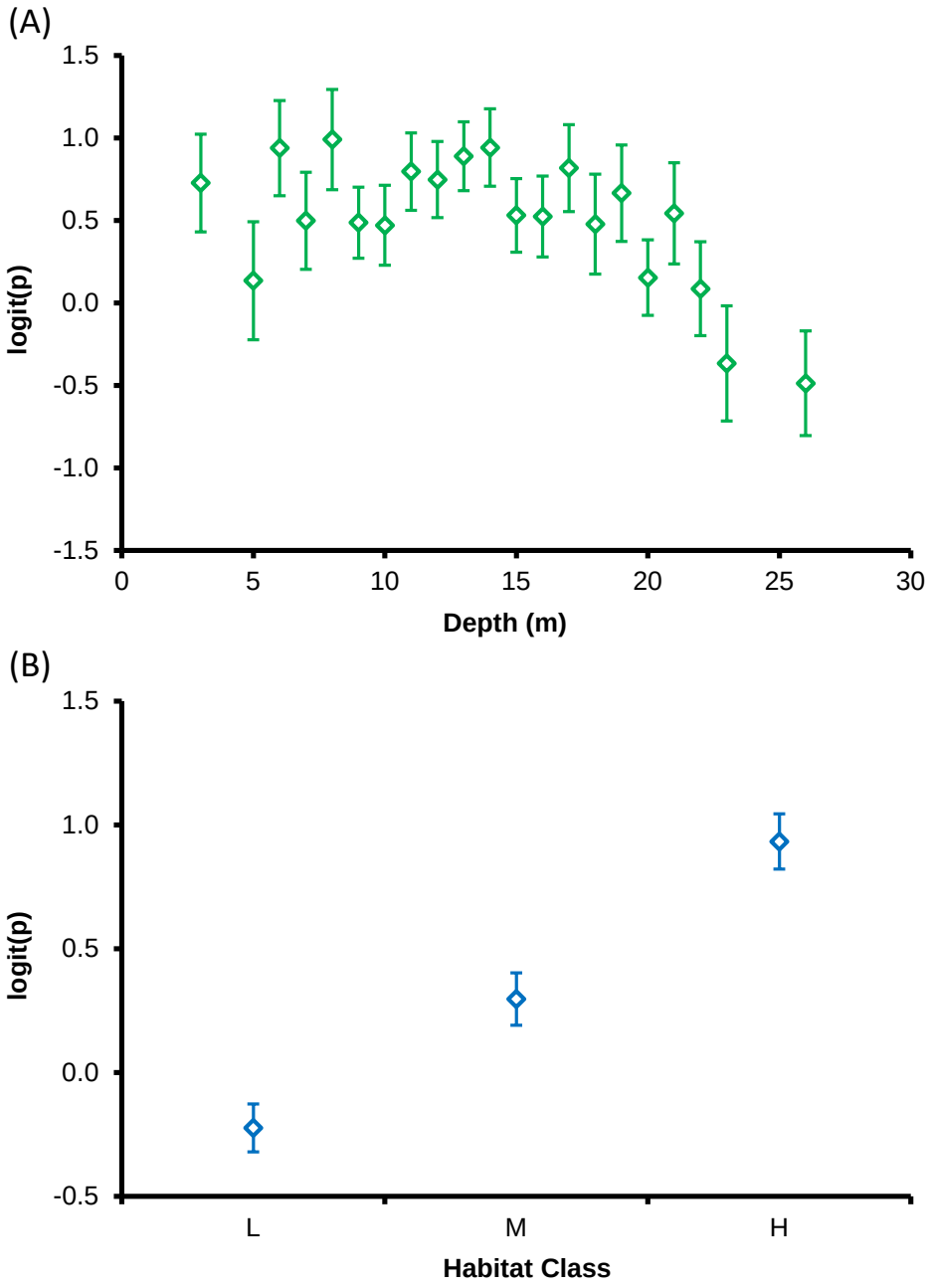

Figure 6.24. Logistic regression modeling for subadult-adult Stoplight Parrotfish (A-B) logit(p) and (C-D) occurrence p as a function of depth. Logit(p) point estimates and regression functions are shown for (A) continuous depth and (B) depth strata models. Back-transformed occurrence regression functions are shown for (C) continuous depth and (D) depth strata models.

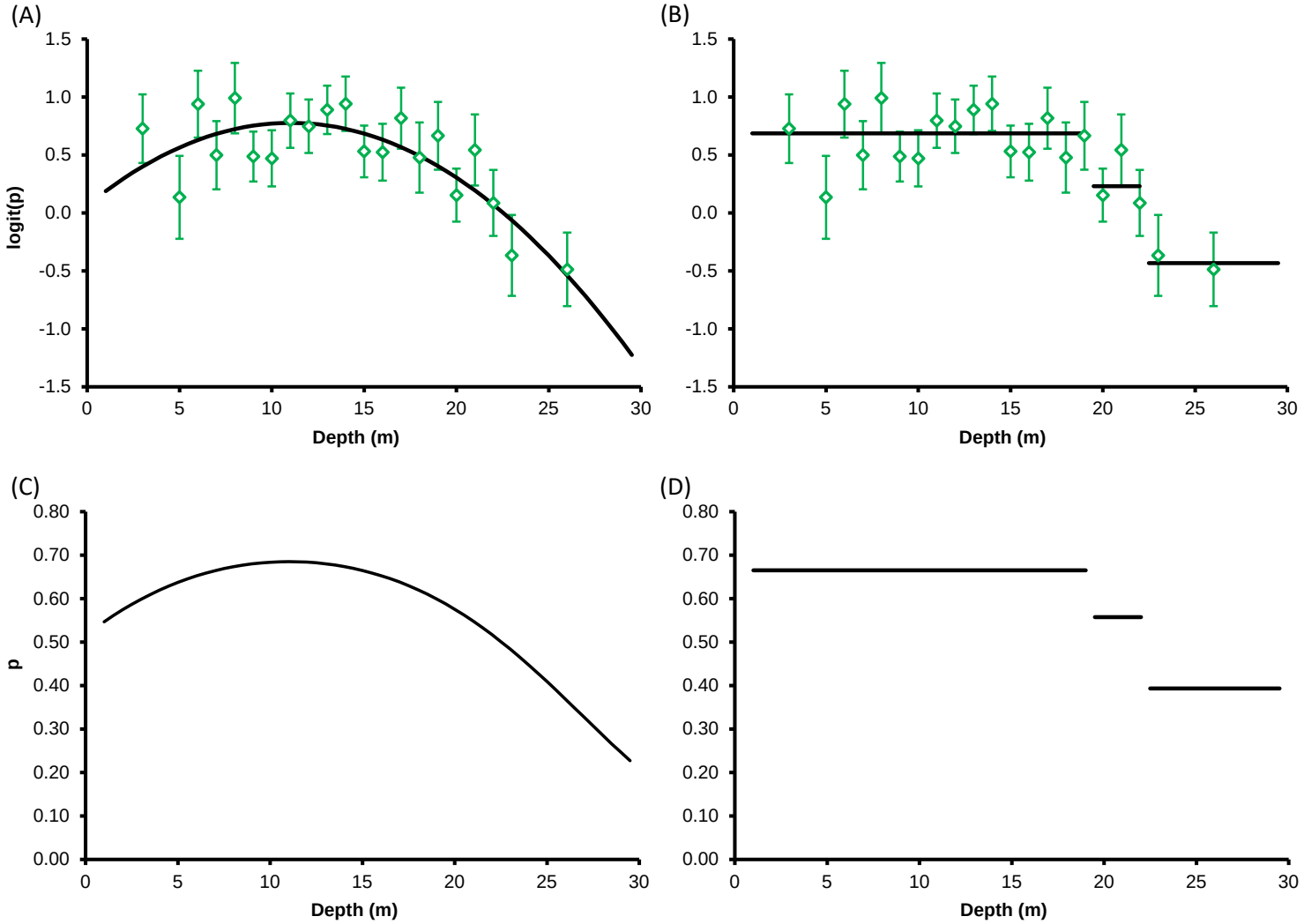

Figure 6.25. Logistic regression point estimates of juvenile Blue Tang logit(p) for (A) depth intervals and (B) substrate habitat classes (L=low rugosity; M=moderate rugosity; H=high rugosity). Data were from 2011-2014 surveys in Dry Tortugas National Park. Each point estimate for depth was based on 30 or more observations.

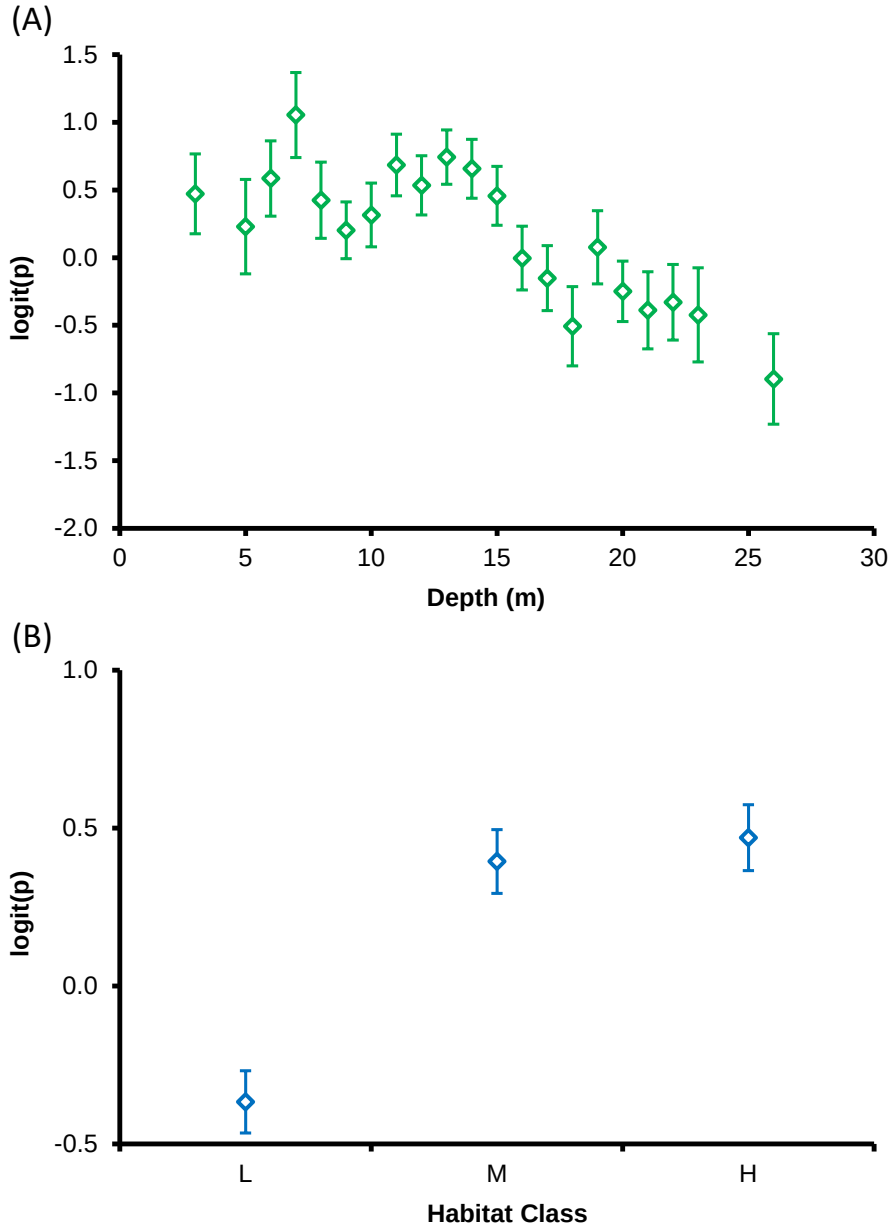

Figure 6.26. Logistic regression modeling for juvenile Blue Tang (A-B) logit(p) and (C-D) occurrence p as a function of depth. Logit(p) point estimates and regression functions are shown for (A) continuous depth and (B) depth strata models. Back-transformed occurrence regression functions are shown for (C) continuous depth and (D) depth strata models.

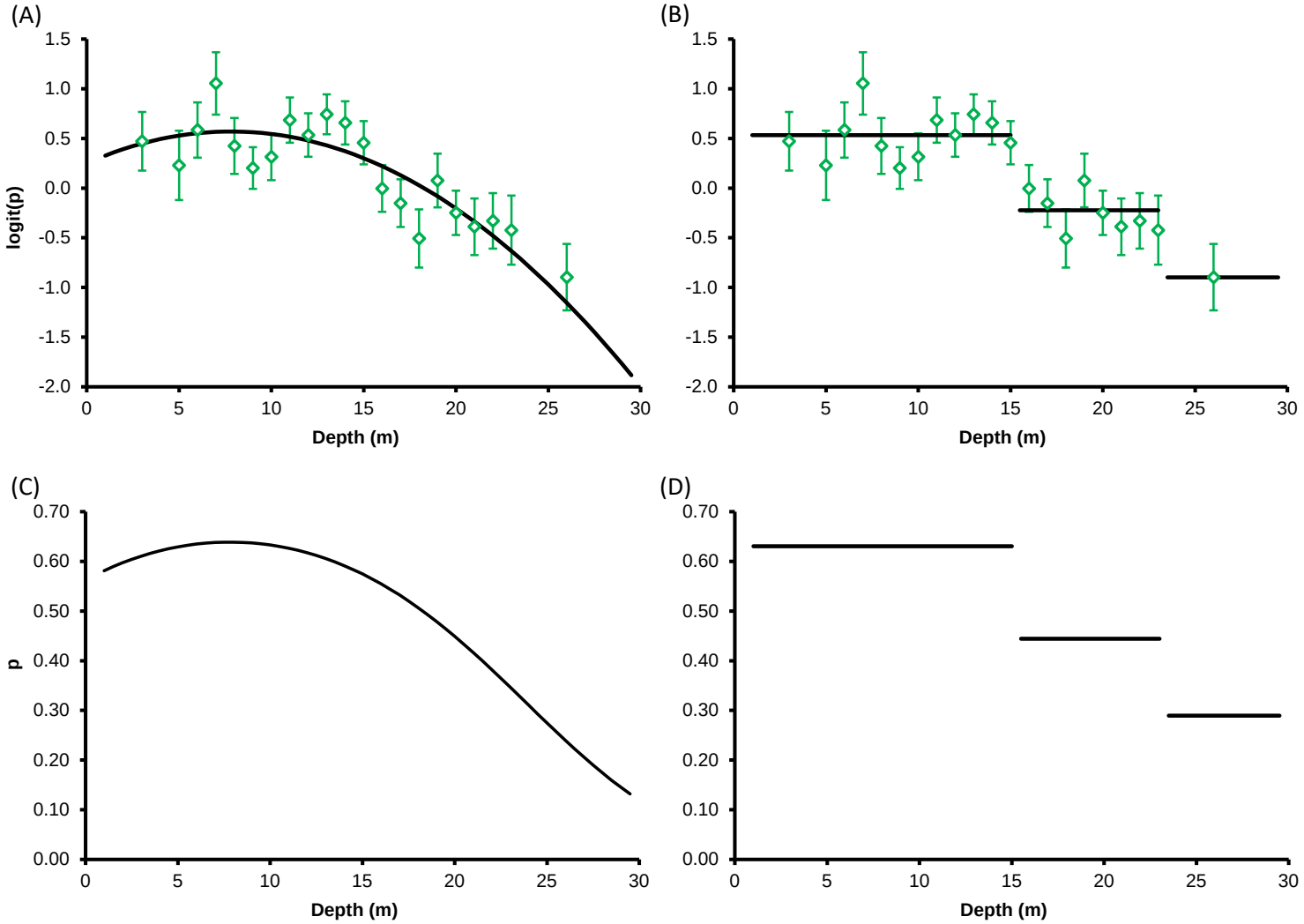

Figure 6.27. Logistic regression point estimates of subadult-adult Blue Tang logit(p) for (A) depth intervals and (B) substrate habitat classes (L=low rugosity; M=moderate rugosity; H=high rugosity). Data were from 2011-2014 surveys in Dry Tortugas National Park. Each point estimate for depth was based on 30 or more observations.

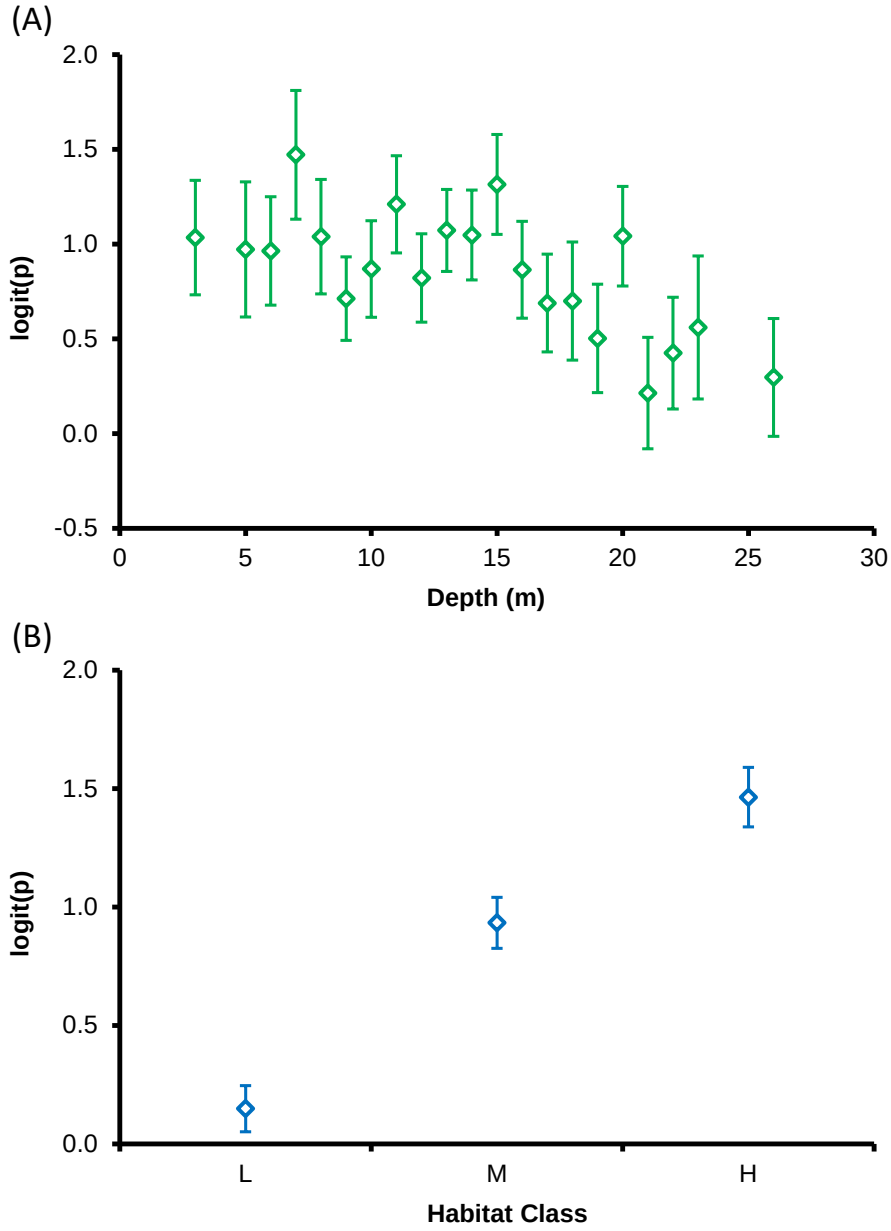

Figure 6.28. Logistic regression modeling for subadult-adult Blue Tang (A-B) logit(p) and (C-D) occurrence p as a function of depth. Logit(p) point estimates and regression functions are shown for (A) continuous depth and (B) depth strata models. Back-transformed occurrence regression functions are shown for (C) continuous depth and (D) depth strata models.

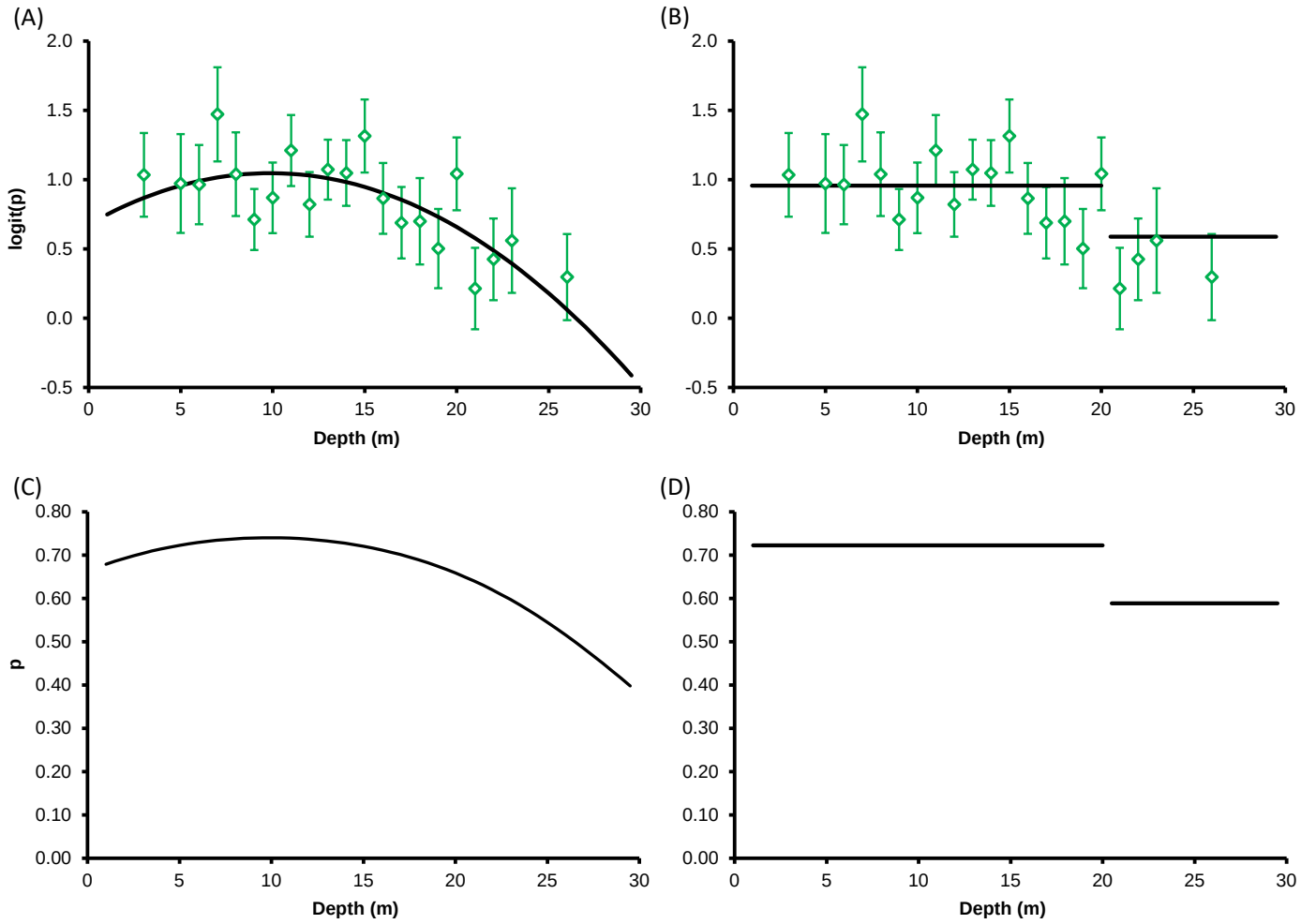

Figure 6.29. Logistic regression point estimates of juvenile Foureye Butterflyfish logit(p) for (A) depth intervals and (B) substrate habitat classes (L=low rugosity; M=moderate rugosity; H=high rugosity). Data were from 2011-2014 surveys in Dry Tortugas National Park. Each point estimate for depth was based on 30 or more observations.

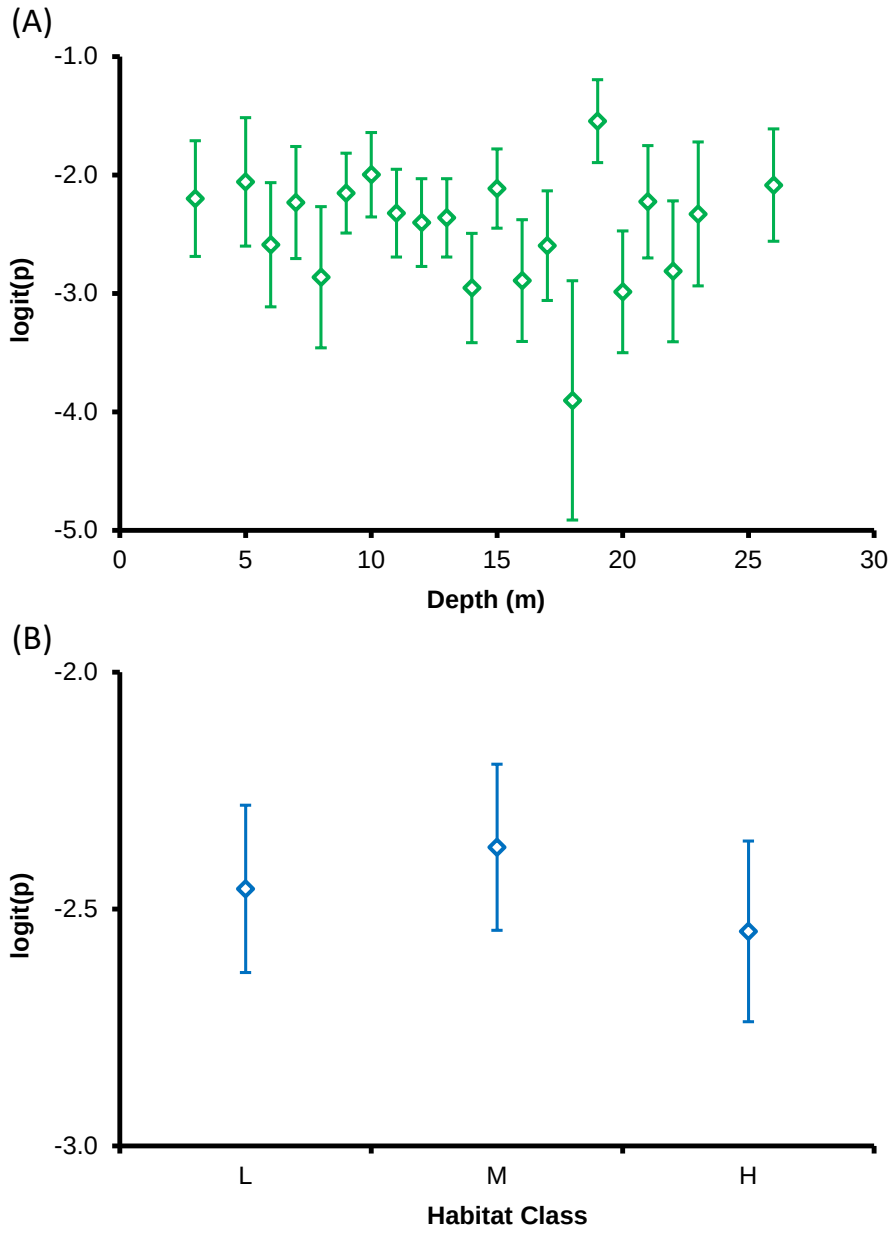

Figure 6.30. Logistic regression modeling for juvenile Foureye Butterflyfish (A) logit(p) and (B) occurrence p as a function of depth. Logit(p) point estimates and regression function are shown for the (A) continuous depth model, which was identical to the strata depth model (1-strata). The back-transformed occurrence regression function is shown in (B).

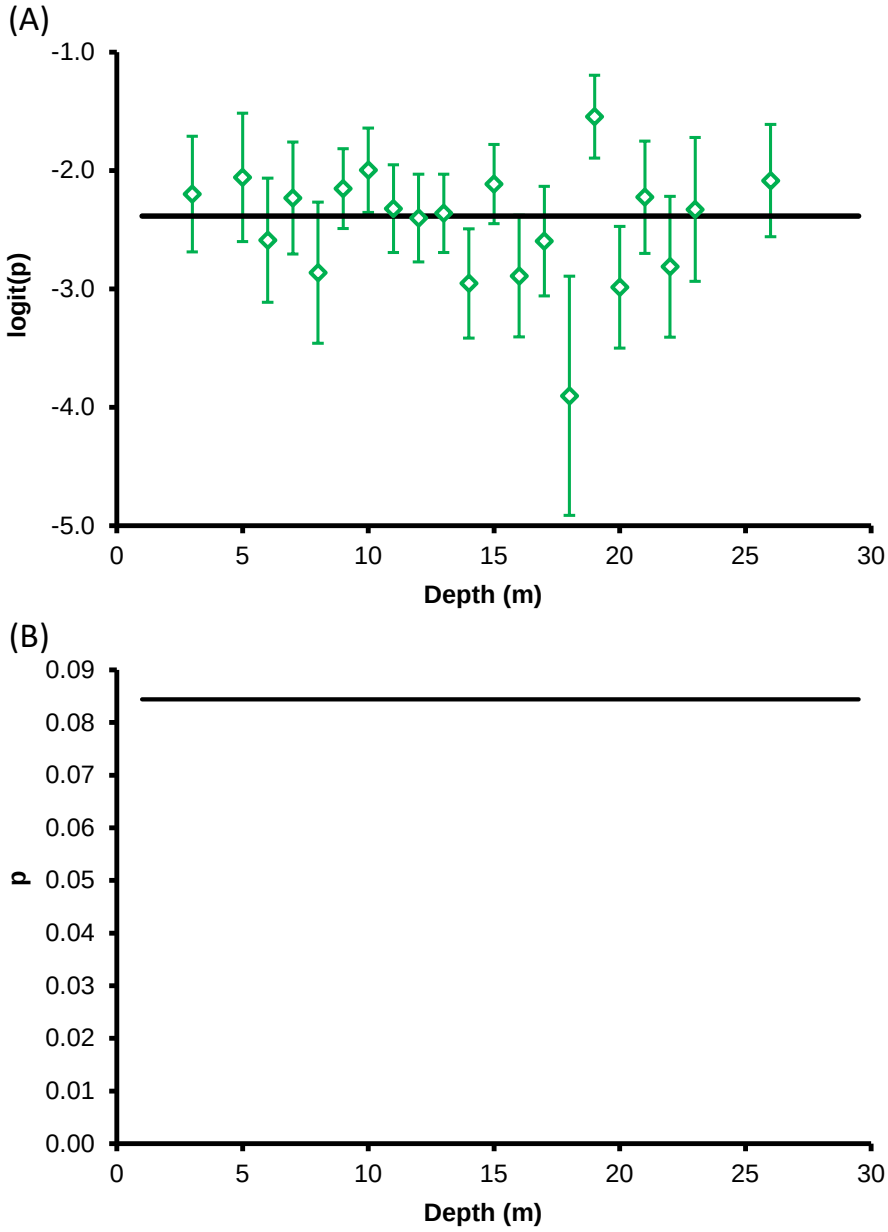

Figure 6.31. Logistic regression point estimates of subadult-adult Foureye Butterflyfish logit(p) for (A) depth intervals and (B) substrate habitat classes (L=low rugosity; M=moderate rugosity; H=high rugosity). Data were from 2011-2014 surveys in Dry Tortugas National Park. Each point estimate for depth was based on 30 or more observations.

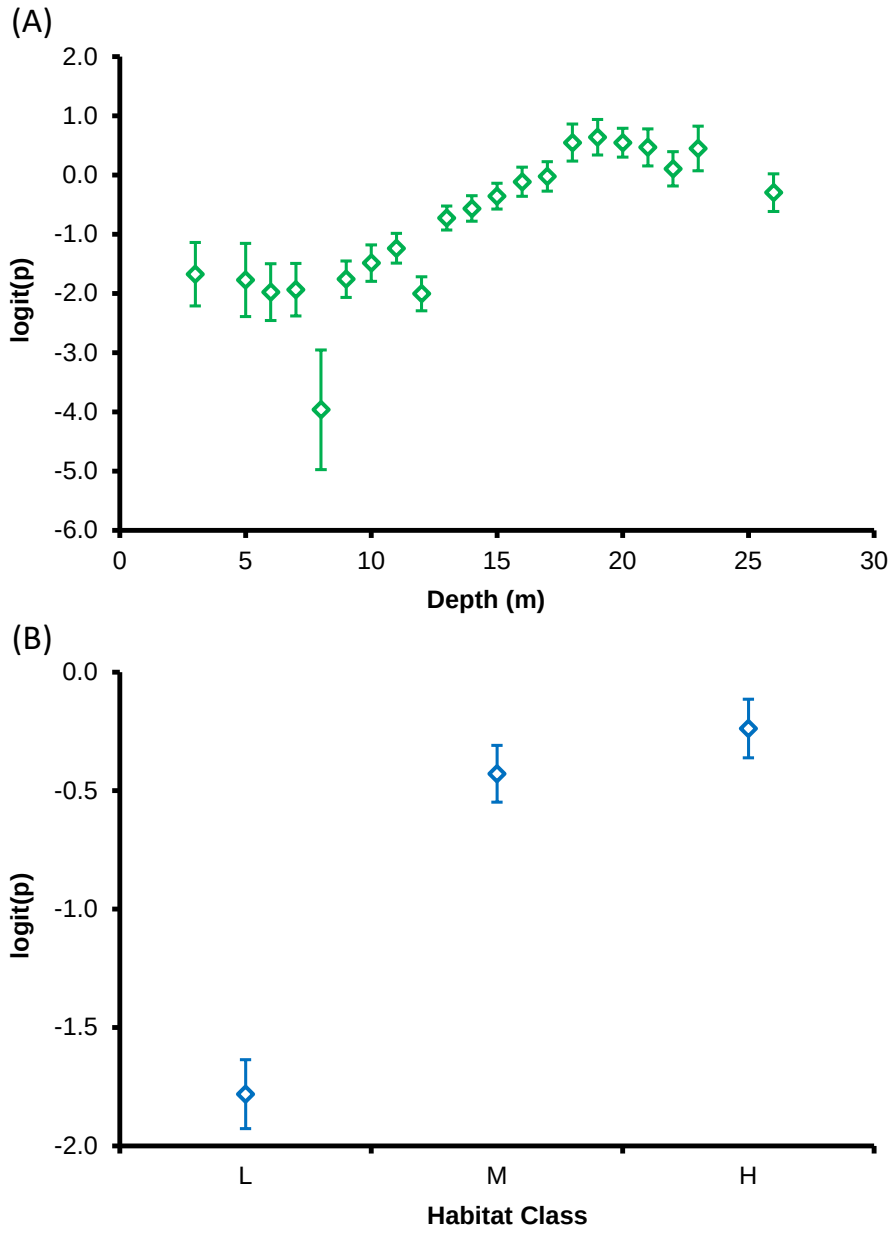

Figure 6.32. Logistic regression modeling for subadult-adult Foureye Butterflyfish (A-B) logit(p) and (C-D) occurrence p as a function of depth. Logit(p) point estimates and regression functions are shown for (A) continuous depth and (B) depth strata models. Back-transformed occurrence regression functions are shown for (C) continuous depth and (D) depth strata models.

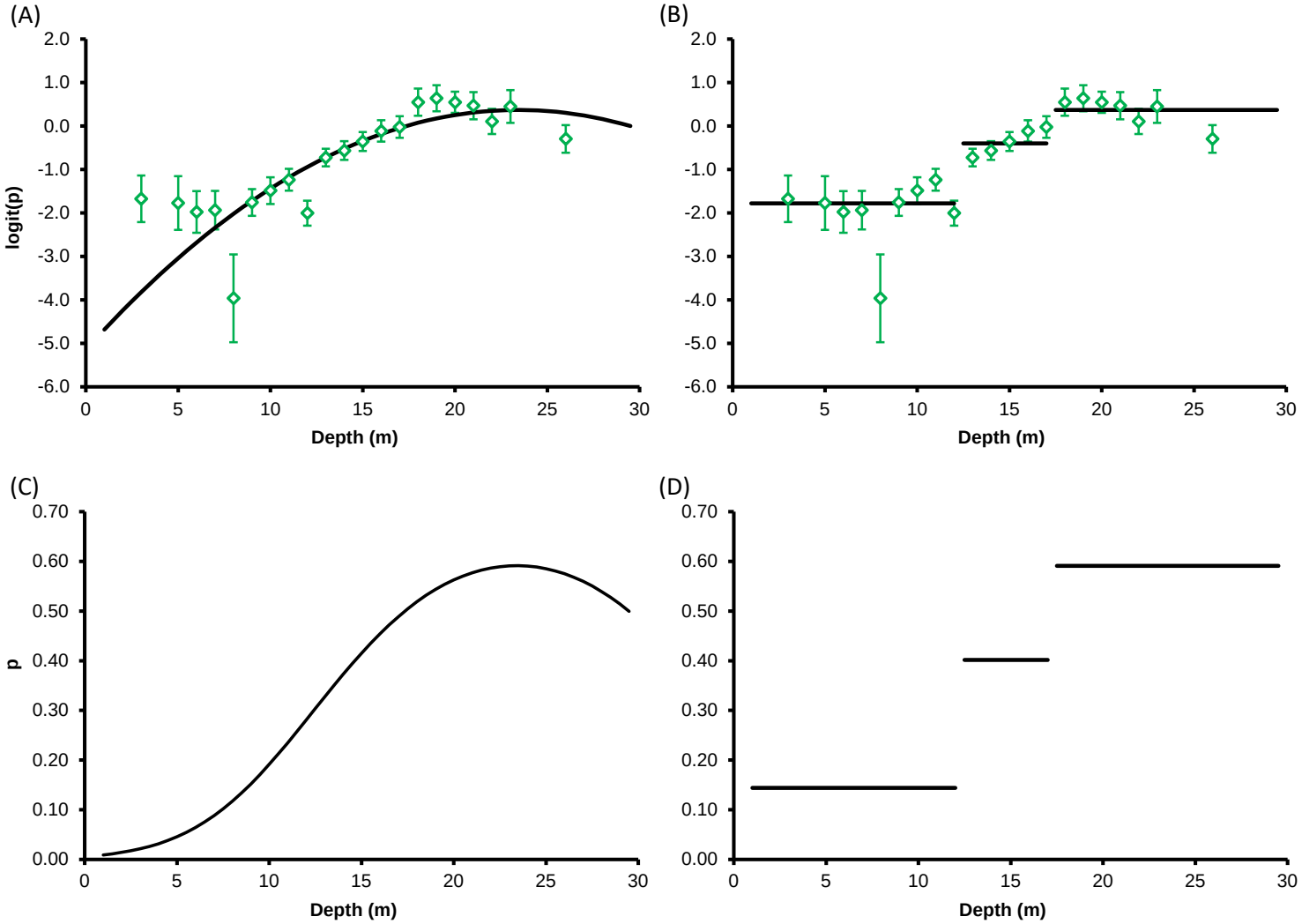

7.0 Regression Analysis: Diver-Measured Rugosity and Stratification

The analysis of section 6.0 showed a highly significant ($p<0.001$) main effect for the categorical rugosity covariate for 11 of 16 species life stages (**Table 6.1**). Logistic regression was employed to evaluate the relationship between occurrence and rugosity for these 11 species life stages. The species-specific depth strata identified in section 6.0 were included as categorical covariates in the logistic regression model. Rugosity observations at each sampling location comprised the weighted average of vertical relief based on frequency categories measured by divers (**Fig. 7.1**). Logistic regression point estimates by rugosity intervals and corresponding categorical rugosity strata models showed well-defined, increasing relationships of occurrence with rugosity for 10 of the 11 species life stages (**Figs. 7.2** to **7.11**). Red grouper juveniles were the exception, showing a decreasing relationship of occurrence with increasing rugosity (**Fig. 7.12**).

While logistic regression analyses identified stratification schemes for depth (section 6.0) and rugosity, the schemes for each variable differed among species. Composite stratification schemes for depth and rugosity were identified for the suite of 16 species life stages based on the single-species schemes. This was accomplished by evaluating the logistic regression models for the group of species life stages for a given variable, and identifying stratum levels coinciding with major changes in predicted logit(p) strata values across species. The procedure resulted in 3 composite depth strata and 4 composite rugosity strata for the 16 species life stages (**Table 7.1**). The underlying relative frequencies of vertical relief recorded by divers is shown in **Fig. 7.13** for each of the four composite rugosity strata, illustrating a clear progression of decreasing frequencies of lower relief categories and increasing frequencies of higher relief categories with increasing rugosity level (R1 to R4).

Figure 7.1. Illustration of procedure to calculate average vertical relief of hard substrate from diver data.

Diver Recorded Data **Computations**

max vertical relief (m)	1.8				
frequency of vertical relief			weighted average vertical relief (m)		
category	percent		midpoint (m)	weighting factor	w*midpoint
<0.2 m	45		0.1	0.45	0.0450
0.2 - 0.5 m	20		0.35	0.2	0.0700
0.5 - 1.0 m	15		0.75	0.15	0.1125
1.0 - 1.5 m	10		1.25	0.1	0.1250
>1.5 m	10		1.65	0.1	0.1650
Total	100		sum=	1	0.5175

midpoint of interval 1.5 m to max

average vertical relief

Figure 7.2. Logistic regression modeling for juvenile Black Grouper (A) logit(p) and (B) occurrence p as a function of diver rugosity (average vertical relief; see Fig. 7.1). Data were from 2011-2014 surveys in Dry Tortugas National Park. Each point estimate (A) for rugosity was based on 30 or more observations. Regression functions are shown for rugosity strata models.

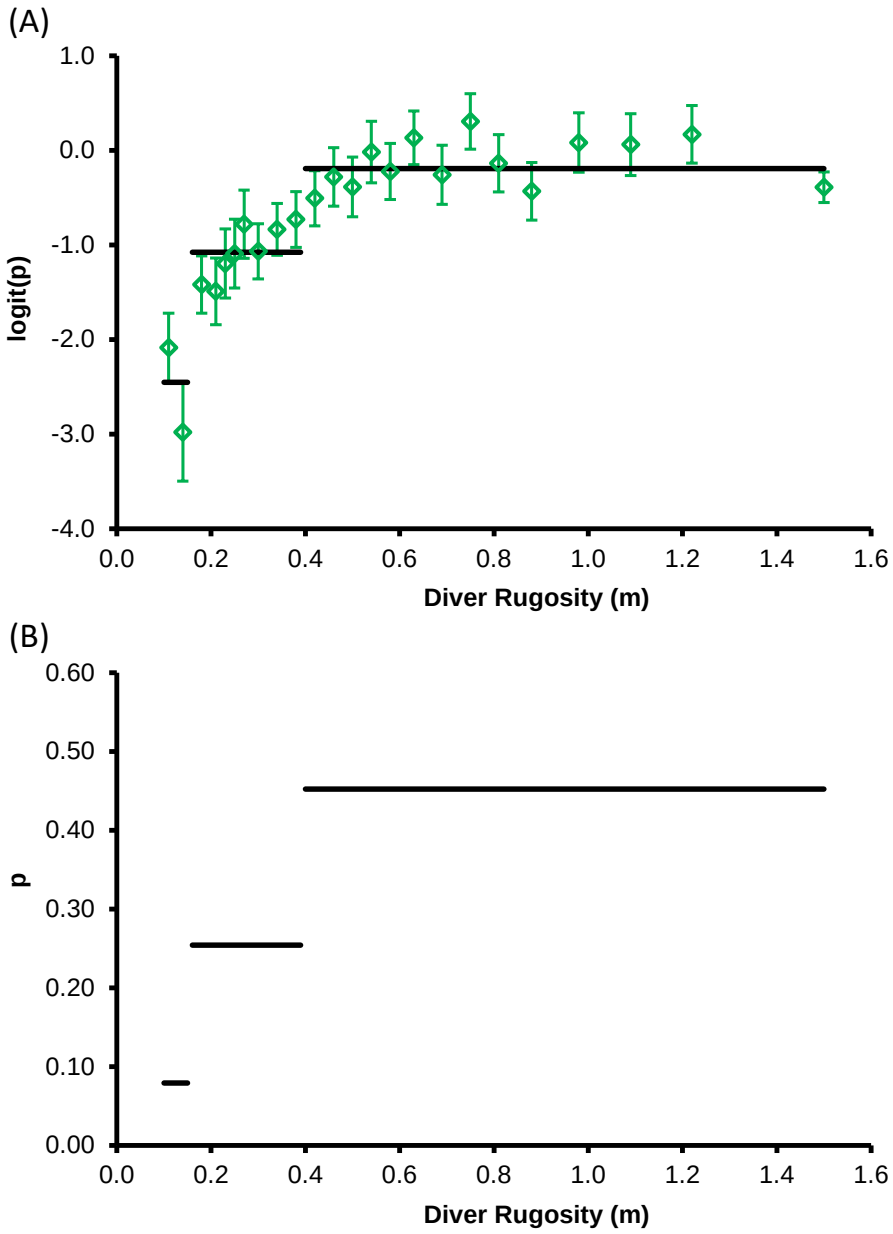

Figure 7.3. Logistic regression modeling for subadult-adult Black Grouper (A) logit(p) and (B) occurrence p as a function of diver rugosity (average vertical relief; see Fig. 7.1). Data were from 2011-2014 surveys in Dry Tortugas National Park. Each point estimate (A) for rugosity was based on 30 or more observations. Regression functions are shown for rugosity strata models.

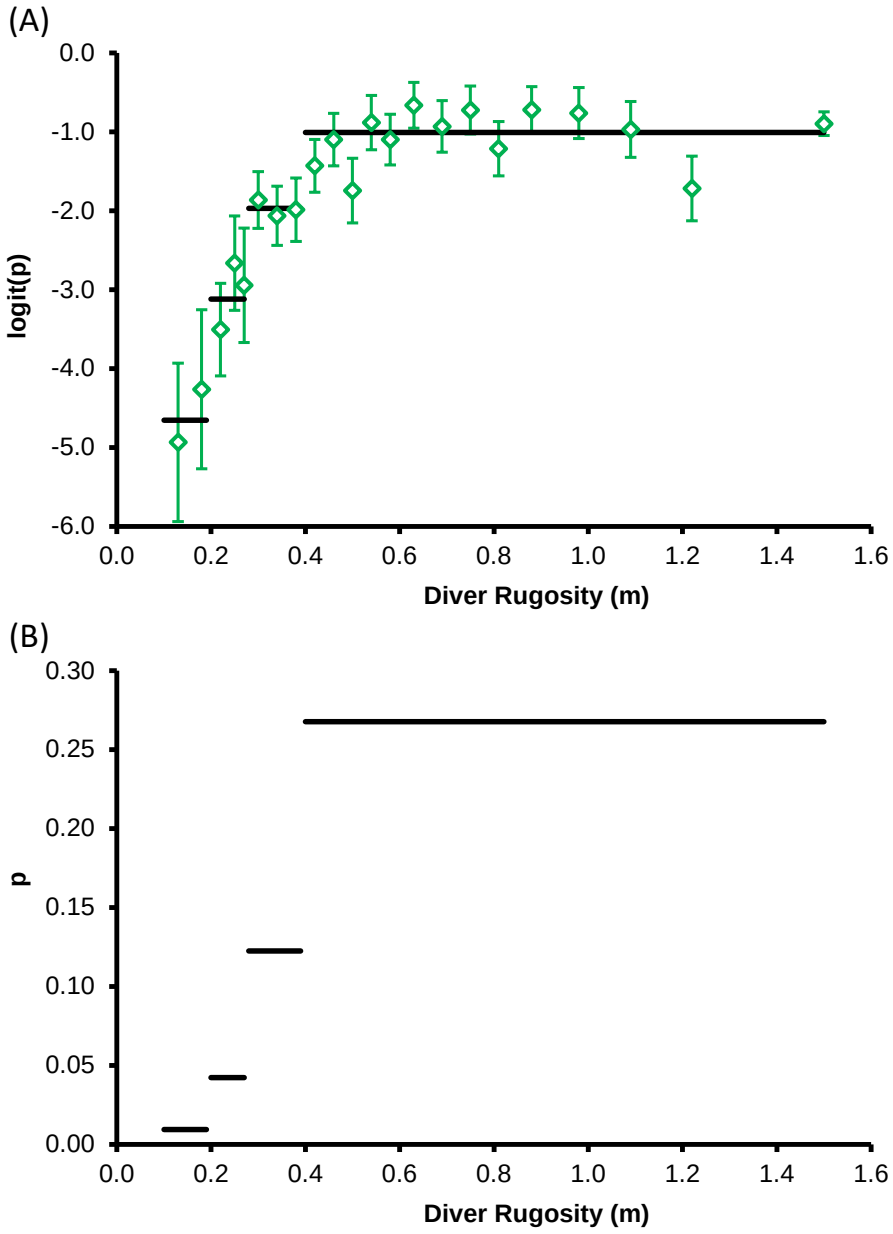

Figure 7.4. Logistic regression modeling for subadult-adult Yellowtail Snapper (A) logit(p) and (B) occurrence p as a function of diver rugosity (average vertical relief; see Fig. 7.1). Data were from 2011-2014 surveys in Dry Tortugas National Park. Each point estimate (A) for rugosity was based on 30 or more observations. Regression functions are shown for rugosity strata models.

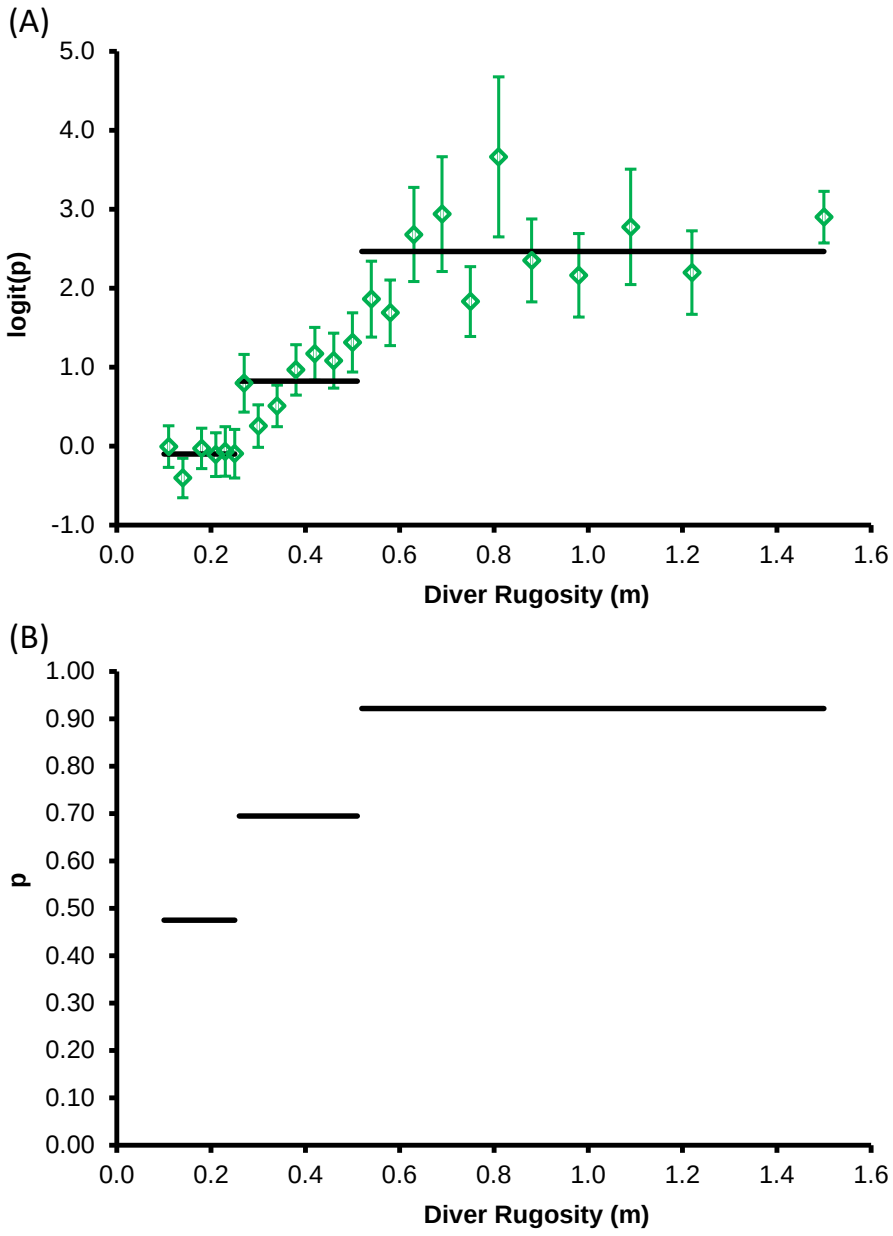

Figure 7.5. Logistic regression modeling for juvenile French Grunt (A) logit(p) and (B) occurrence p as a function of diver rugosity (average vertical relief; see Fig. 7.1). Data were from 2011-2014 surveys in Dry Tortugas National Park. Each point estimate (A) for rugosity was based on 30 or more observations. Regression functions are shown for rugosity strata models.

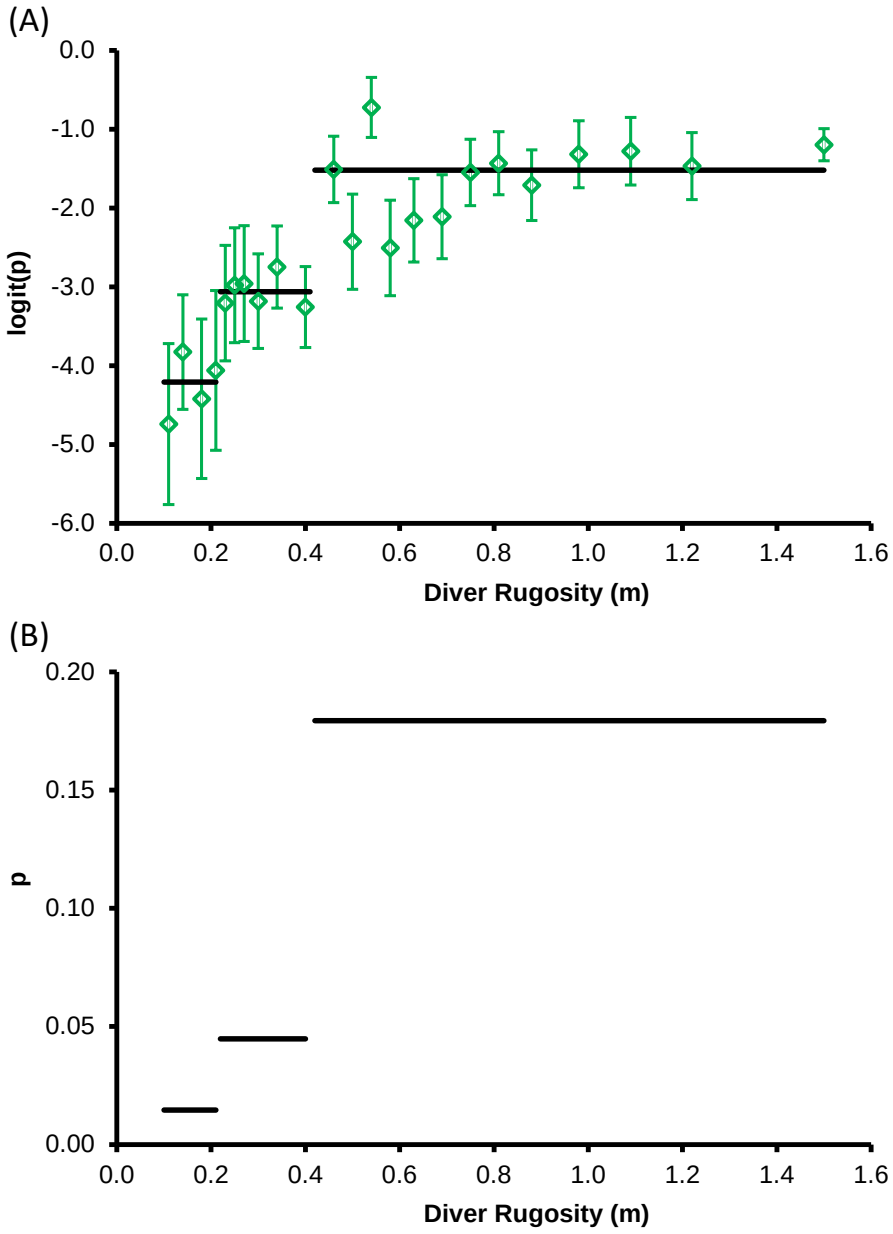

Figure 7.6. Logistic regression modeling for subadult-adult French Grunt (A) logit(p) and (B) occurrence p as a function of diver rugosity (average vertical relief; see Fig. 7.1). Data were from 2011-2014 surveys in Dry Tortugas National Park. Each point estimate (A) for rugosity was based on 30 or more observations. Regression functions are shown for rugosity strata models.

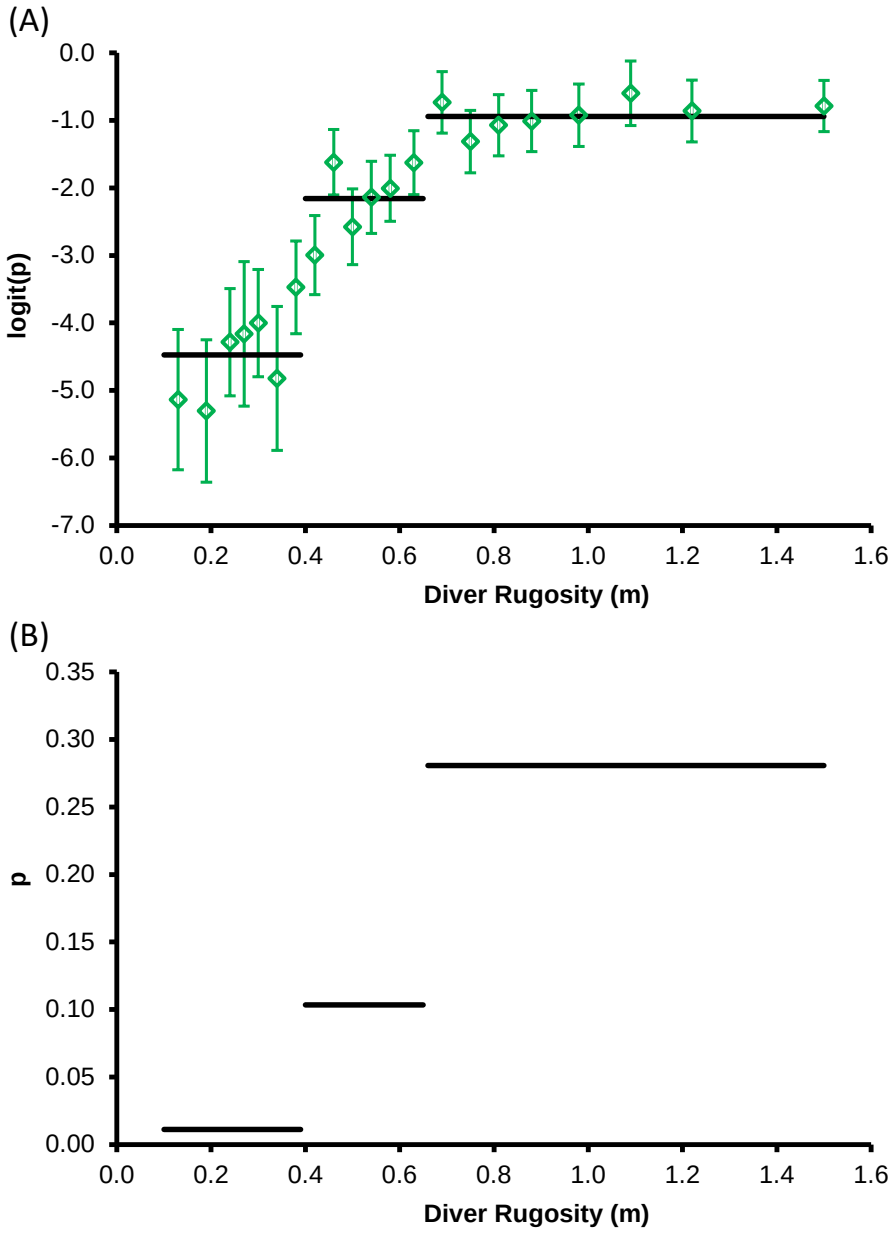

Figure 7.7. Logistic regression modeling for juvenile Stoplight Parrotfish (A) logit(p) and (B) occurrence p as a function of diver rugosity (average vertical relief; see Fig. 7.1). Data were from 2011-2014 surveys in Dry Tortugas National Park. Each point estimate (A) for rugosity was based on 30 or more observations. Regression functions are shown for rugosity strata models.

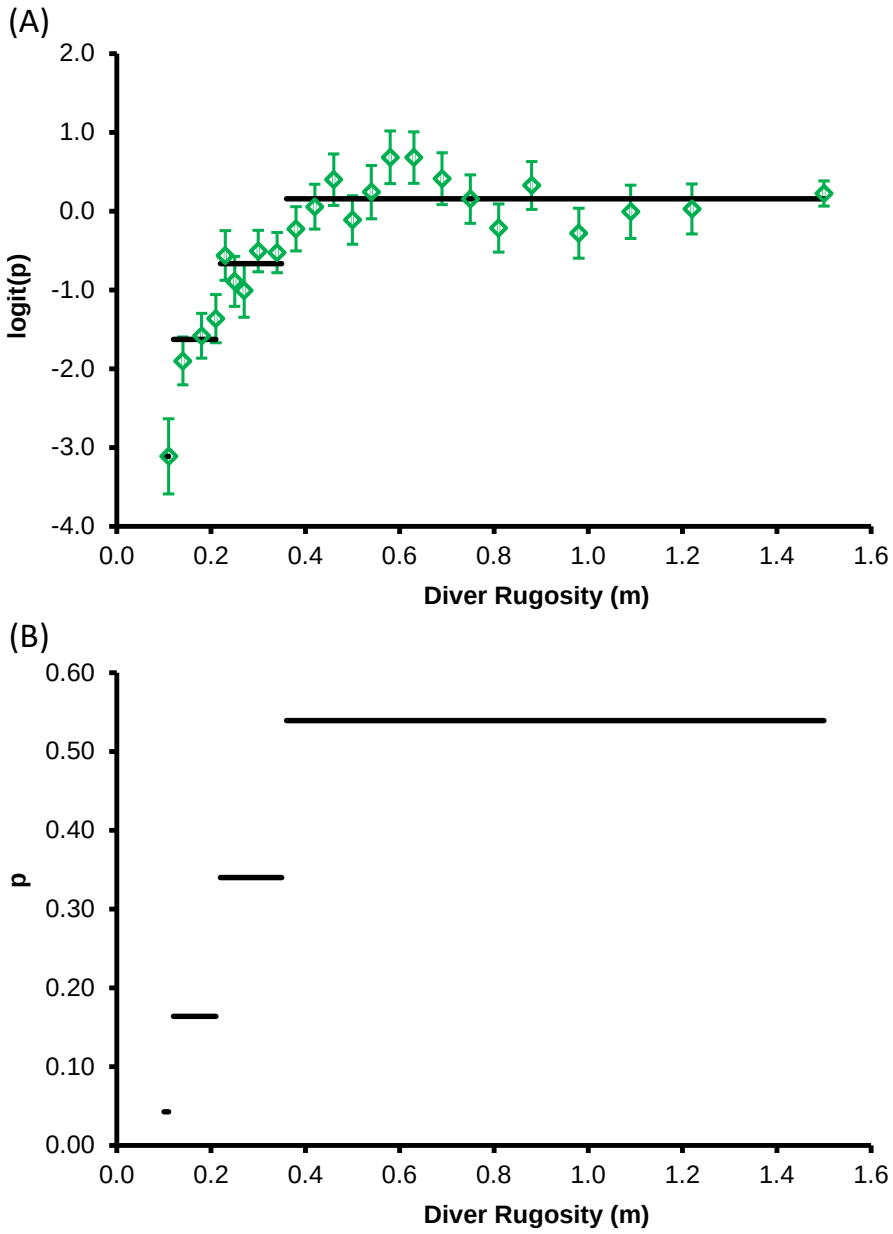

Figure 7.8. Logistic regression modeling for subadult-adult Stoplight Parrotfish (A) logit(p) and (B) occurrence p as a function of diver rugosity (average vertical relief; see Fig. 7.1). Data were from 2011-2014 surveys in Dry Tortugas National Park. Each point estimate (A) for rugosity was based on 30 or more observations. Regression functions are shown for rugosity strata models.

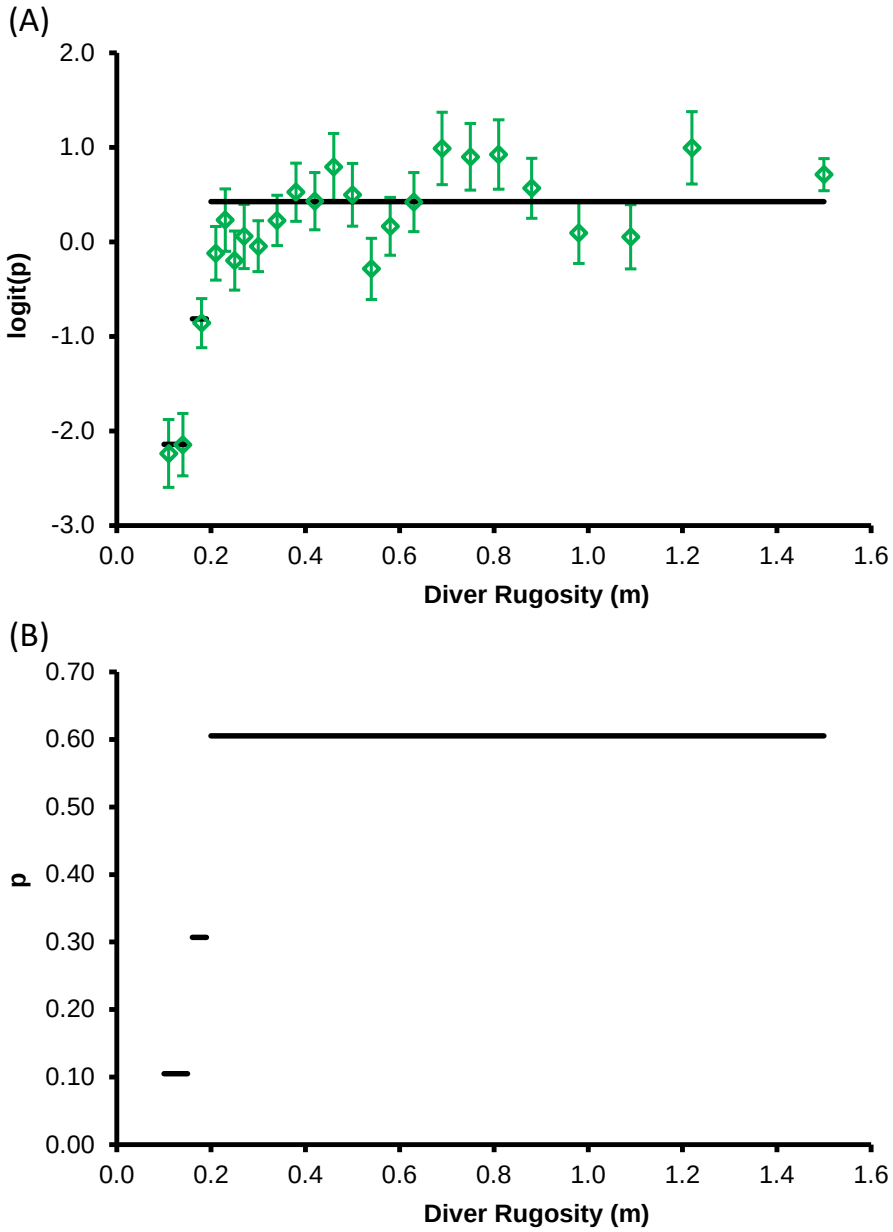

Figure 7.9. Logistic regression modeling for juvenile Blue Tang (A) logit(p) and (B) occurrence p as a function of diver rugosity (average vertical relief; see Fig. 7.1). Data were from 2011-2014 surveys in Dry Tortugas National Park. Each point estimate (A) for rugosity was based on 30 or more observations. Regression functions are shown for rugosity strata models.

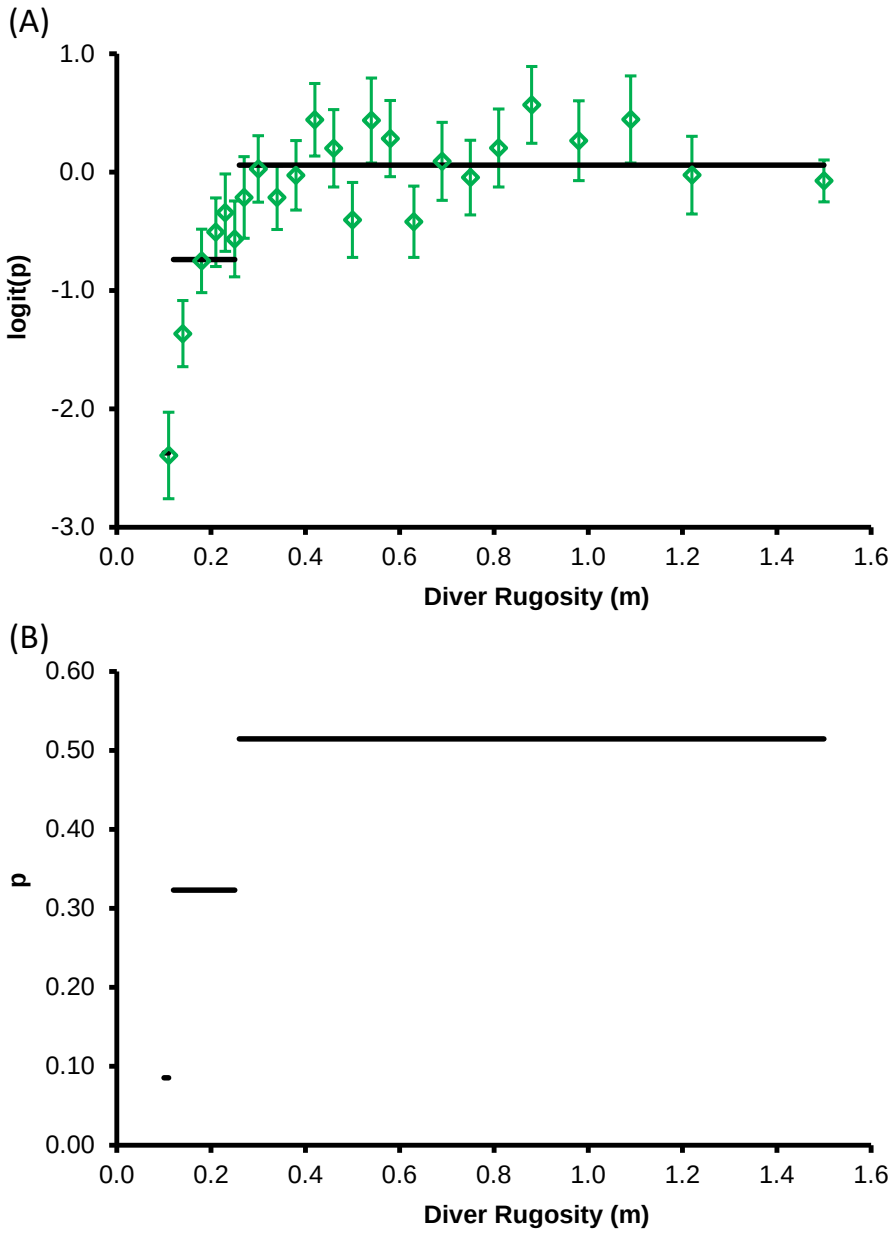

Figure 7.10. Logistic regression modeling for subadult-adult Blue Tang (A) logit(p) and (B) occurrence p as a function of diver rugosity (average vertical relief; see Fig. 7.1). Data were from 2011-2014 surveys in Dry Tortugas National Park. Each point estimate (A) for rugosity was based on 30 or more observations. Regression functions are shown for rugosity strata models.

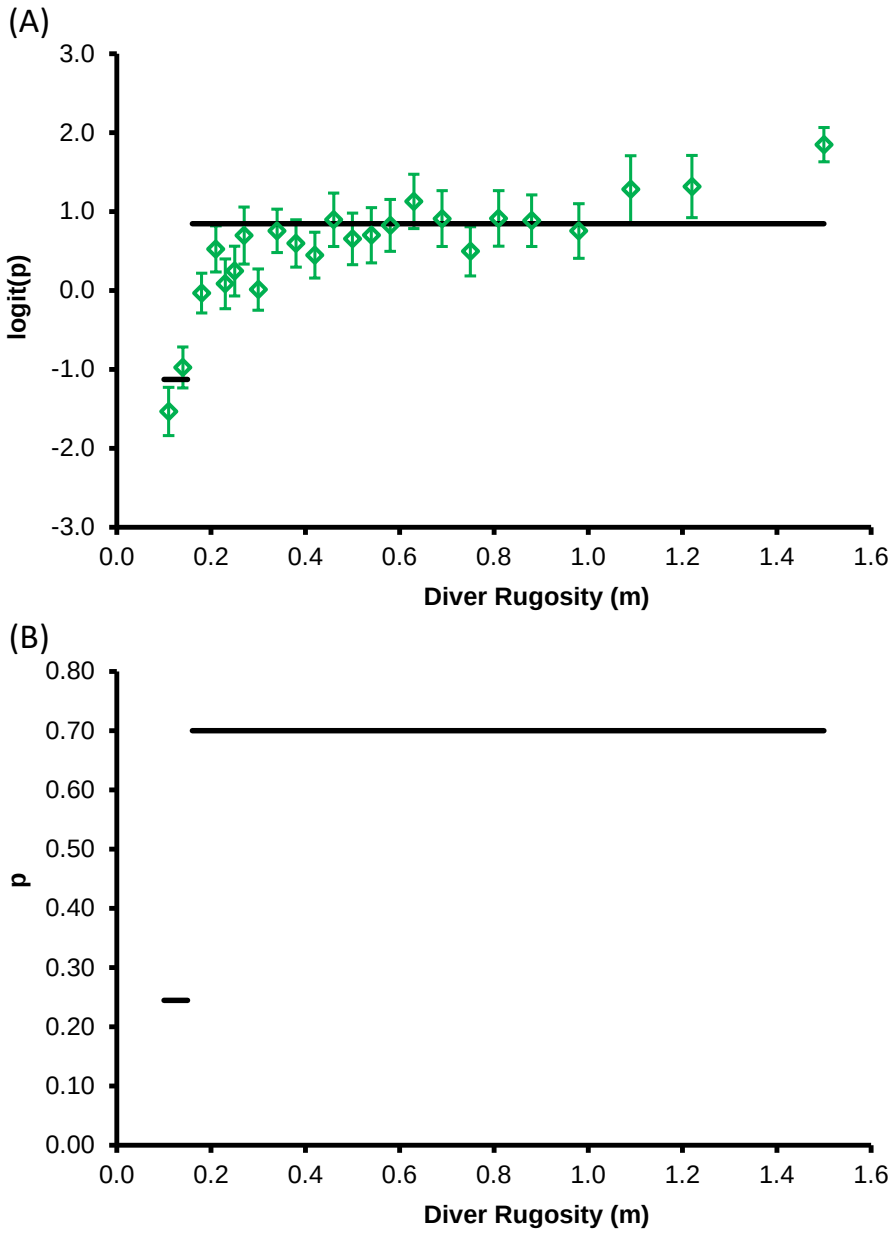

Figure 7.11. Logistic regression modeling for subadult-adult Foureye Butterflyfish (A) logit(p) and (B) occurrence p as a function of diver rugosity (average vertical relief; see Fig. 7.1). Data were from 2011-2014 surveys in Dry Tortugas National Park. Each point estimate (A) for rugosity was based on 30 or more observations. Regression functions are shown for rugosity strata models.

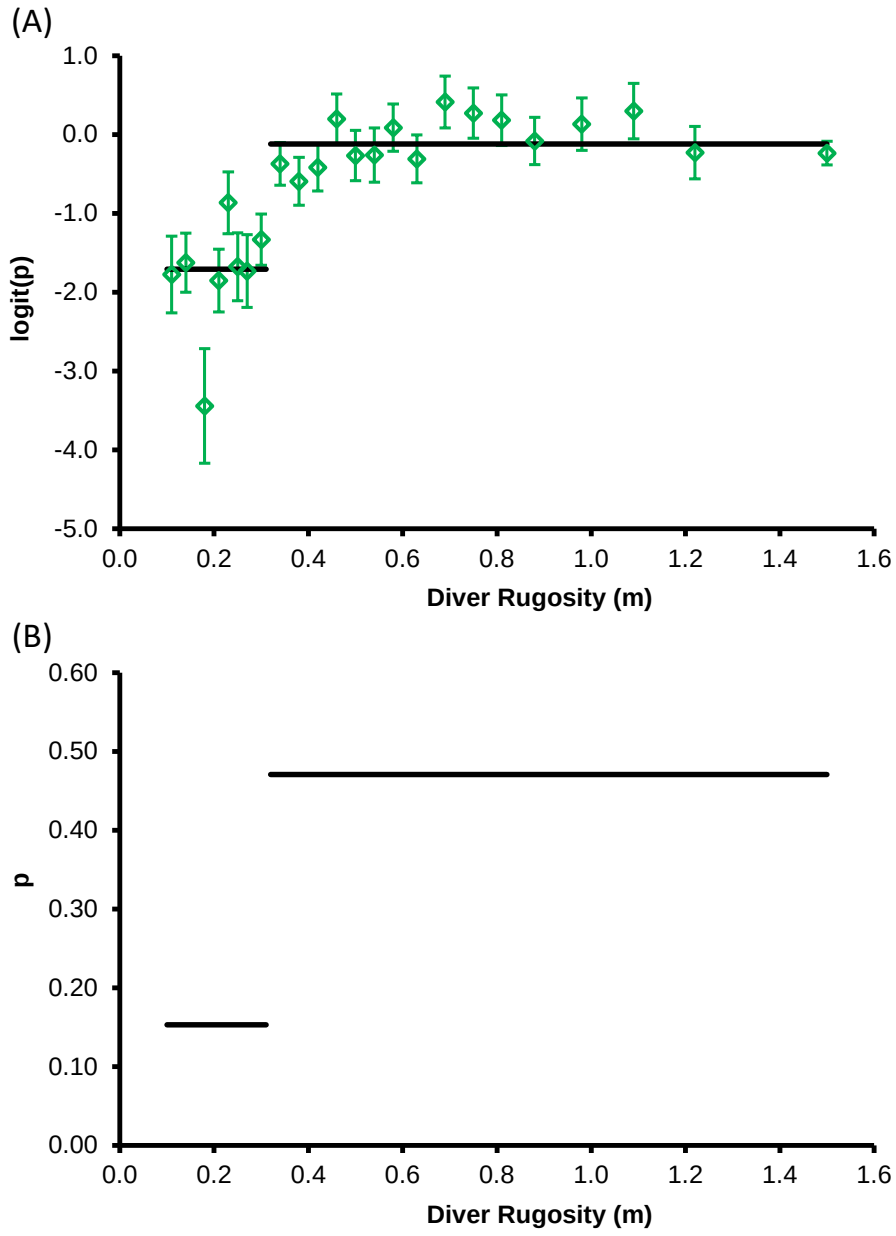

Figure 7.12. Logistic regression modeling for juvenile Red Grouper (A) logit(p) and (B) occurrence p as a function of diver rugosity (average vertical relief; see Fig. 7.1). Data were from 2011-2014 surveys in Dry Tortugas National Park. Each point estimate (A) for rugosity was based on 30 or more observations. Regression functions are shown for rugosity strata models.

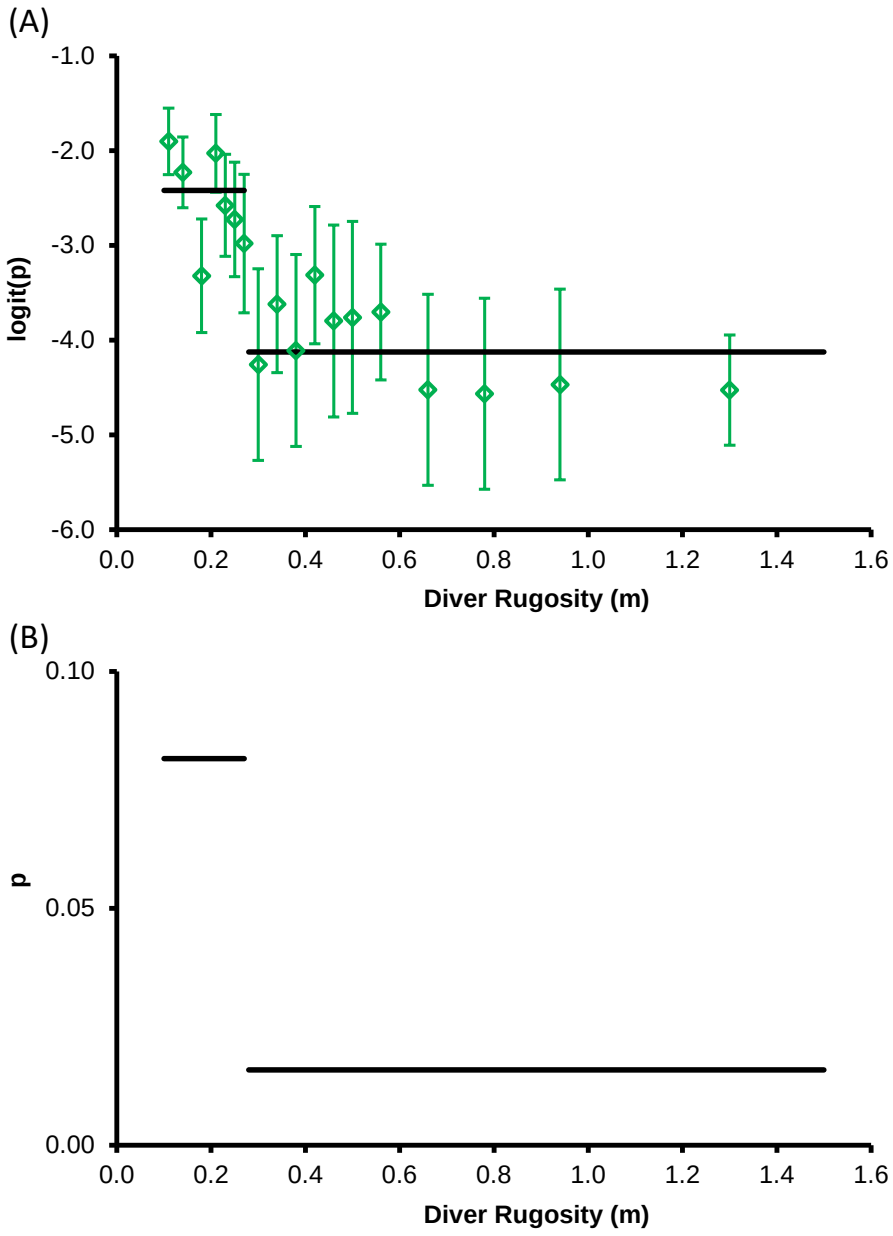

Table 7.1. Composite strata variables for depth and diver rugosity (average vertical relief) for southern Florida design species (see Table 5.1).

	Composite Strata Variables	
Variable	**Code**	**Description**
Depth	D1	< 12 m
	D2	≥ 12 m to < 22 m
	D3	≥ 22 m to ≤ 33 m
Diver Rugosity	R1	≥ 0 to < 0.15 m
	R2	≥ 0.15 to < 0.26 m
	R3	≥ 26.0 to < 0.4 m
	R4	≥ 0.4 m

Figure 7.13. Relative frequencies of diver recorded vertical relief categories (see Fig. 7.1) by rugosity strata (see Table 7.1 for definitions).

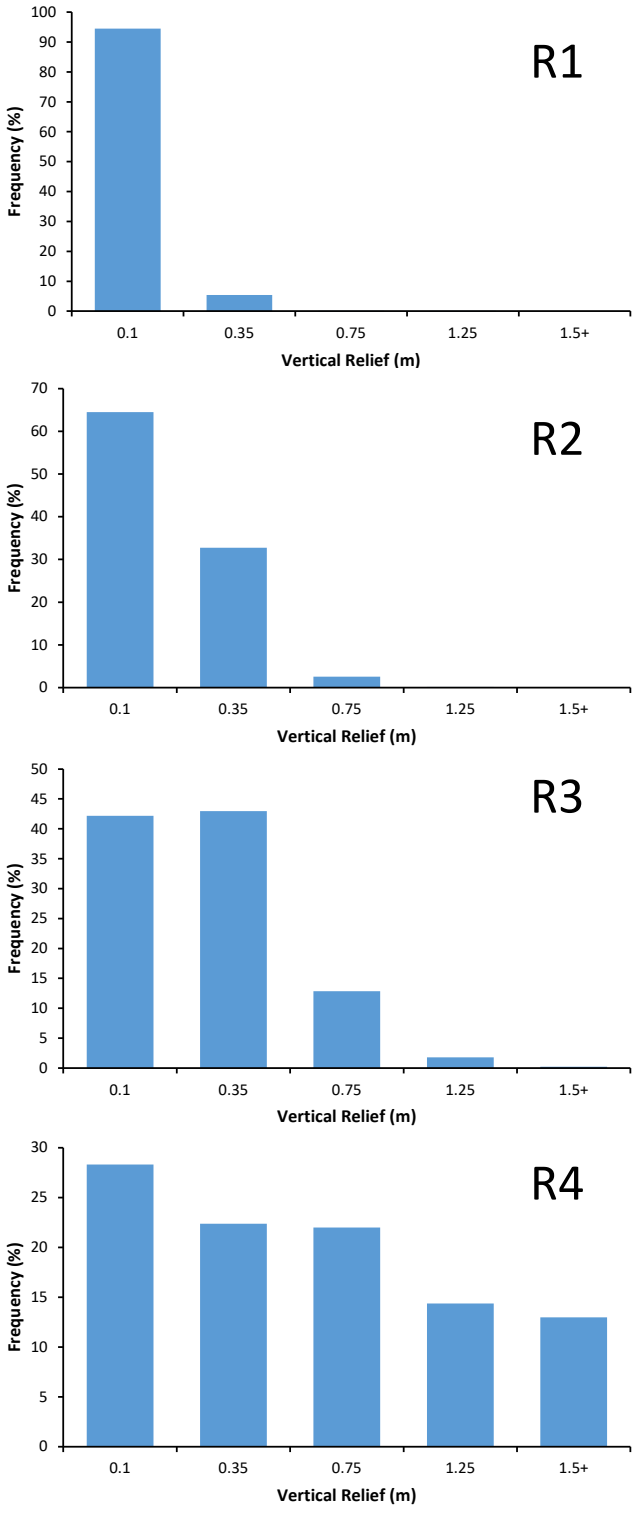

8.0 Relationships between Diver and Map Rugosity

The refinement of life stage designations (section 5.0), depth stratification (section 6.0), and rugosity stratification (7.0) will serve to improve the efficiency of the statistical sampling design for RVC in southern Florida. While depth and rugosity have been an integral part of the RVC stratification for the past 20 years, a key problem has been the accurate classification of primary sample units (i.e., map grid cells) in terms of depth and rugosity strata for the complete spatial sampling frame. Especially for rugosity, incorrect classification of strata in the spatial frame due to the current qualitative benthic maps impacts the accuracy of the RVC survey via uncertainty in stratum weighting factors (i.e., the proportion of area assigned to a specific stratum), as well as survey precision via misallocation of sample units to strata due to map inaccuracies (e.g., divers sample locations thought to be high rugosity but in fact are low rugosity). A key objective of this study was to utilize newly-acquired high-resolution bathymetry mapping data (section 3.0) for quantitative characterization of benthic habitat for each survey sample unit (i.e., map grid cell, section 4.0).

Research was conducted to identify potential map substrate variables, in addition to depth, for delineating the RVC survey frame in terms of substrate complexity/rugosity for the 9 design species and associated life stages. Substrate complexity variables were derived from the synthesized high-resolution bathymetry data described in section 3.0. Research on fishery-independent sampling of reef fishes in Hawaii (Richards et al. 2019) has identified the following potential substrate complexity variables: slope, vector ruggedness measure (VRM; Sappington et al. 2005), and arc chord ratio (ACR; Du Preez 2015). The three variables for substrate rugosity—slope, VRM, ACR—were derived from bathymetry data. Computational code for the substrate metrics ACR and VRM is provided in **Appendix A**. As a rugosity measure, slope combines substrate "roughness" and the overall incline of the seafloor, whereas VRM and ACR were designed to isolate the roughness component of complexity. Diagnostic checks for these substrate variables in the Tortugas study region showed that VRM and ACR were mostly independent from slope (e.g., **Fig. 8.1**).

Initial regression analyses to evaluate relationships between reef fish abundance metrics and map substrate complexity variables showed little to no meaningful relationships for target species life stages. This was in stark contrast to the well-defined relationships observed between species occurrence and diver-measured rugosity (section 7.0). Consequently, our analysis approach shifted to evaluating relationships between diver-measured rugosity and map-derived rugosity. The objectives were to develop statistical functions to predict diver rugosity from map rugosity, and then characterize the spatial sampling frame in terms of diver rugosity.

Figure 8.1. Rugosity variable Arc Chord Ratio (ACR) as a function of bathymetric slope estimated from multi-beam sonar data from Tortugas Bank.

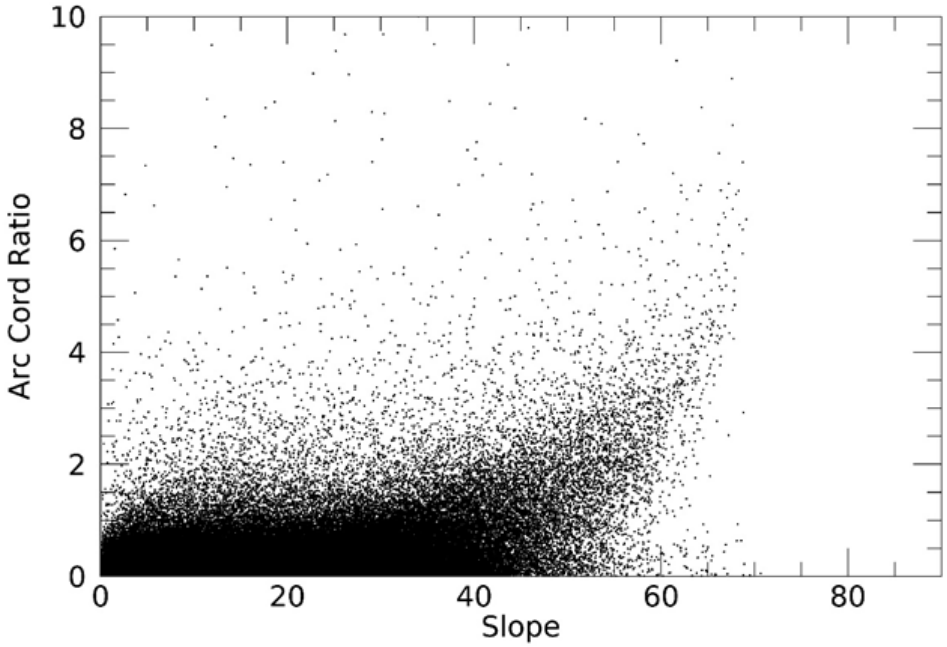

Our investigations uncovered several key computational aspects for calculating rugosity metrics at both the pixel scale (horizontal resolution of underlying multibeam or lidar bathymetry data) and map grid scale (50 x 50 m) (**Table 8.1A**). At the pixel scale, gridding resolution and spatial averaging were key considerations. The gridding resolution, or pixel size, stems from the horizontal resolution of the original bathymetry data. For the mapping data acquired for southern Florida, the minimum horizontal resolution was around 1-2 m. The choice of pixel size impacts the number of observations for calculating a rugosity metric at the sample unit (i.e., map grid cell) scale, e.g., a gridding resolution of 1 m yields 2500 pixels per 50 x 50 m grid cell. Spatial averaging is a common technique for minimizing potential artifacts in remote-sensed bathymetry data, such as visible track lines from multibeam sonar transects. The procedure obtains the average depth for a small neighborhood of pixels around a given target pixel, e.g., a 3x3 'smoother' would obtain the average depth for the center pixel in a small matrix of 3 rows and 3 columns. The procedure is applied to every pixel in a given map grid before computing pixel-level rugosity metrics. Two sample unit (50 x 50 m map grid cell) estimation procedures were evaluated for computing rugosity metrics from the underlying pixel values: (1) the median value, and (2) a weighted average analogous to the procedure used for computing diver rugosity (e.g., **Figs. 7.1** and **7.13**). The suite of pixel-scale and map grid-scale options tested for computing rugosity metrics is provided in **Table 8.1A**.

Table 8.1. (A) Options tested for defining the most appropriate map rugosity variable for relating to diver-measured rugosity. (B) Selected specifications for computing a map rugosity variable by region.

(A) Options Tested

Pixel Observations			
Rugosity Metric	**Gridding Resolution**	**Spatial Averaging Filter**	**Sample Unit (50 x 50 m) Variable**
slope, ACR, VRM	1m, 2m, 3m	none, 3x3, 5x5, 7x7	median, weighted average

(B) Selected Specifications

Region	Bathymetry Sensor	Rugosity Metric	Gridding Resolution	Spatial Avg. Filter	Sample Unit Variable
Florida Keys	Airborne LiDAR	VRM	2 m	none	Weighted Average
Dry Tortugas NP	Airborne LiDAR	VRM	2 m	none	Weighted Average
Tortugas Bank	Multibeam Sonar	ACR	2 m	none	Weighted Average

Due to differences in map sensor technologies and specifications, analyses of diver-map rugosity relationships were conducted for three separate regions: Florida Keys, Dry Tortugas National Park, and Tortugas Bank. Buddy-pair latitude-longitude points from 2010-2014 RVC surveys were used as center points for constructing corresponding 50 x 50 m map grid cells for the analyses. Analysis steps were: (i) select gridding resolution; (ii) compute pixel-level bathymetry; (iii) apply spatial averaging filter; (iv) compute pixel-level rugosity (slope, ACR, VRM); (v) apply computational method (median or weighted average) to obtain grid cell-level rugosity; (vi) develop a regression function of diver rugosity dependent upon map rugosity; (vii) use the regression function to obtain predicted diver rugosity from map rugosity; and (viii) compute the percentage of grid cells in which diver rugosity was accurately predicted. This analysis procedure was carried out for the suite of specification options listed in **Table 8.1A**.

In general, applying a gridding resolution of 2 m and no spatial averaging filter at the pixel level in conjunction with a weighted average procedure at the map grid level yielded the highest prediction accuracy irrespective of region, bathymetry sensor, and rugosity metric (**Table 8.1B**). For the Florida Keys, weighted average VRM outperformed other map rugosity metrics; the underlying frequency distributions of VRM by diver rugosity strata, the basis for computing the weighted average, are shown in **Fig. 8.2**. Fitting procedures for the diver-map rugosity relationship followed the approach applied above in sections 6.0 and 7.0. Initial point estimates of diver rugosity (y-variable) for intervals of map rugosity (x-variable) along the

range of x were carried out to facilitate (i) identification of an appropriate error pdf, and (ii) description of the mathematical form of the diver-map rugosity relationship (e.g., linear, quadratic, etc.) (**Fig. 8.3**). Log-transformation of diver rugosity yielded normally-distributed error residuals. The relationship between log diver rugosity and map weighted average VRM was described by a quadratic polynomial. The main objective of the regression model was to assign map grid cells to the appropriate diver rugosity stratum (**Table 7.1**). Keeping this objective in mind, data in the upper right quadrant of the point estimate graph (**Fig. 8.3**, top panel) would be assigned to the highest rugosity stratum R4. Consequently, the regression model was restricted to the range of x mostly encompassing lower rugosity strata R1-R3, which provided a better fitting relationship in this portion of the graph (**Fig. 8.3**, lower panel) compared to using the full x range. In application, map VRM values above 134 (**Fig. 8.3**, lower panel, vertical dashed line) were assigned to stratum R4, and the regression model was used to assign rugosity strata R1-R3 for map VRM values below 134. For the matched set of diver and map rugosity observations (n=1,332), the overall prediction accuracy for strata R1-R4 was very low, 47.2%; however, when rugosity strata were pooled into two basic categories, very low-low (R1-R2) and moderate-high (R3-R4), prediction accuracy improved to 76.1%.

For Dry Tortugas National Park, weighted average VRM outperformed other map rugosity metrics; the underlying frequency distributions of VRM by diver rugosity strata, the basis for computing the weighted average, are shown in **Fig. 8.4**. Log-transformation of diver rugosity yielded normally-distributed error residuals. The relationship between log diver rugosity and map weighted average VRM was described by a linear function (**Fig. 8.5**). For the matched set of diver and map rugosity observations (n=289), the overall prediction accuracy for strata groupings R1-R2 and R3-R4 was 68.5%. Prediction accuracy was better for higher rugosity strata (R3-R4, 77.8%) compared to lower rugosity strata (R1-R2, 58.1%).

For Tortugas Bank, weighted average ACR outperformed other map rugosity metrics; the underlying frequency distributions of ACR by diver rugosity strata, the basis for computing the weighted average, are shown in **Fig. 8.6**. The relationship between log diver rugosity and map weighted average ACR for the R1-R3 x-range was described by a linear function (**Fig. 8.7**). For the matched set of diver and map rugosity observations (n=671), the overall prediction accuracy for strata groupings R1-R2 and R3-R4 was 80.9%. Prediction accuracy was better for higher rugosity strata (R3-R4, 92.7%) compared to lower rugosity strata (R1-R2, 52.1%).

Figure 8.2. Relative frequencies of map VRM categories by diver rugosity strata (see Table 7.1 for definitions) for the Florida Keys region.

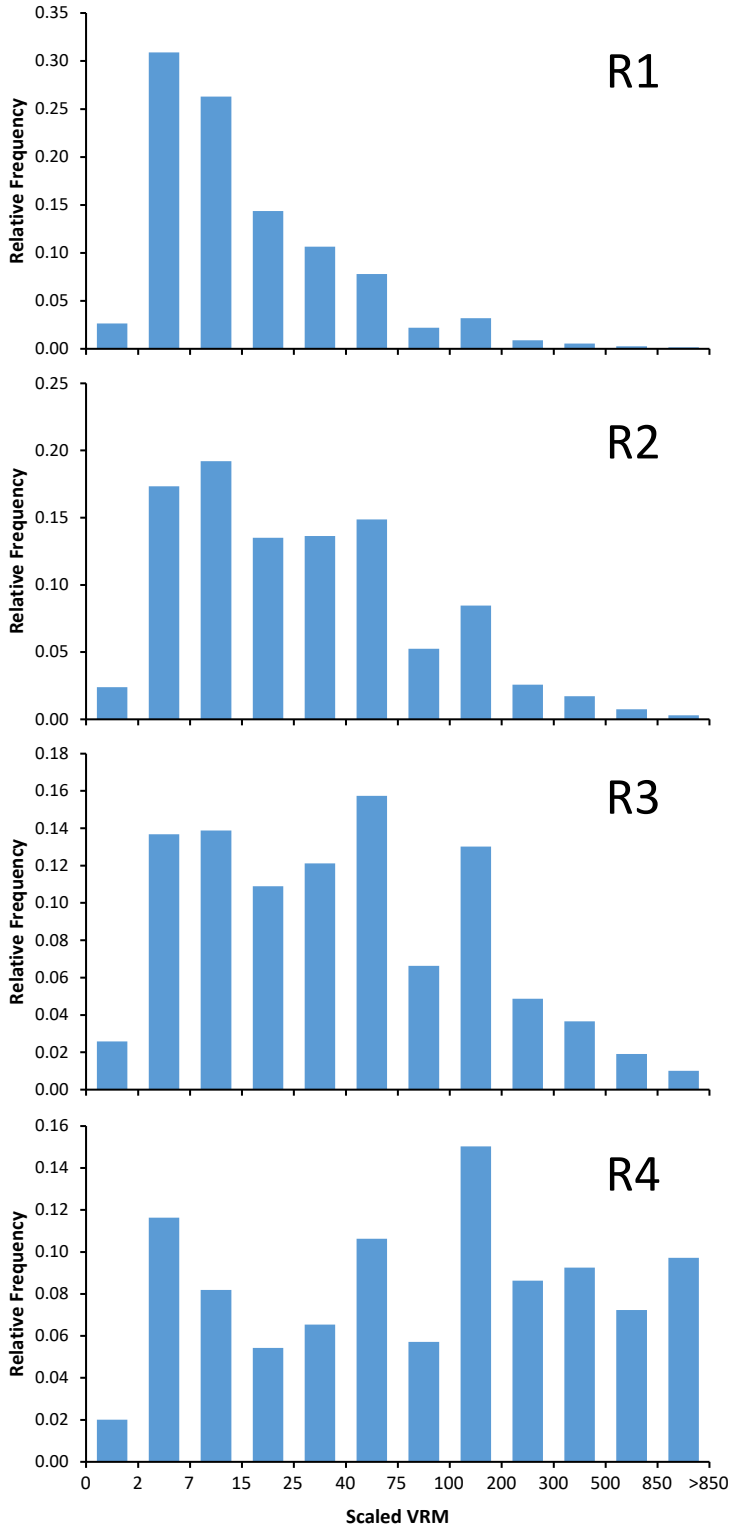

Figure 8.3. Relationship between diver and map rugosity for the Florida Keys region. Top panel: least-squares regression point estimates of log diver rugosity by intervals of map rugosity (weighted average VRM); the horizontal dashed line demarcates the highest diver rugosity level (R4) from lower levels (R1-R3). Bottom panel: inset from top panel (red box) showing the fitted regression relationship for log diver rugosity dependent on map rugosity; the vertical dashed line demarcates the weighted average VRM for predicting the highest rugosity level (R4) vs. lower levels (R1-R3).

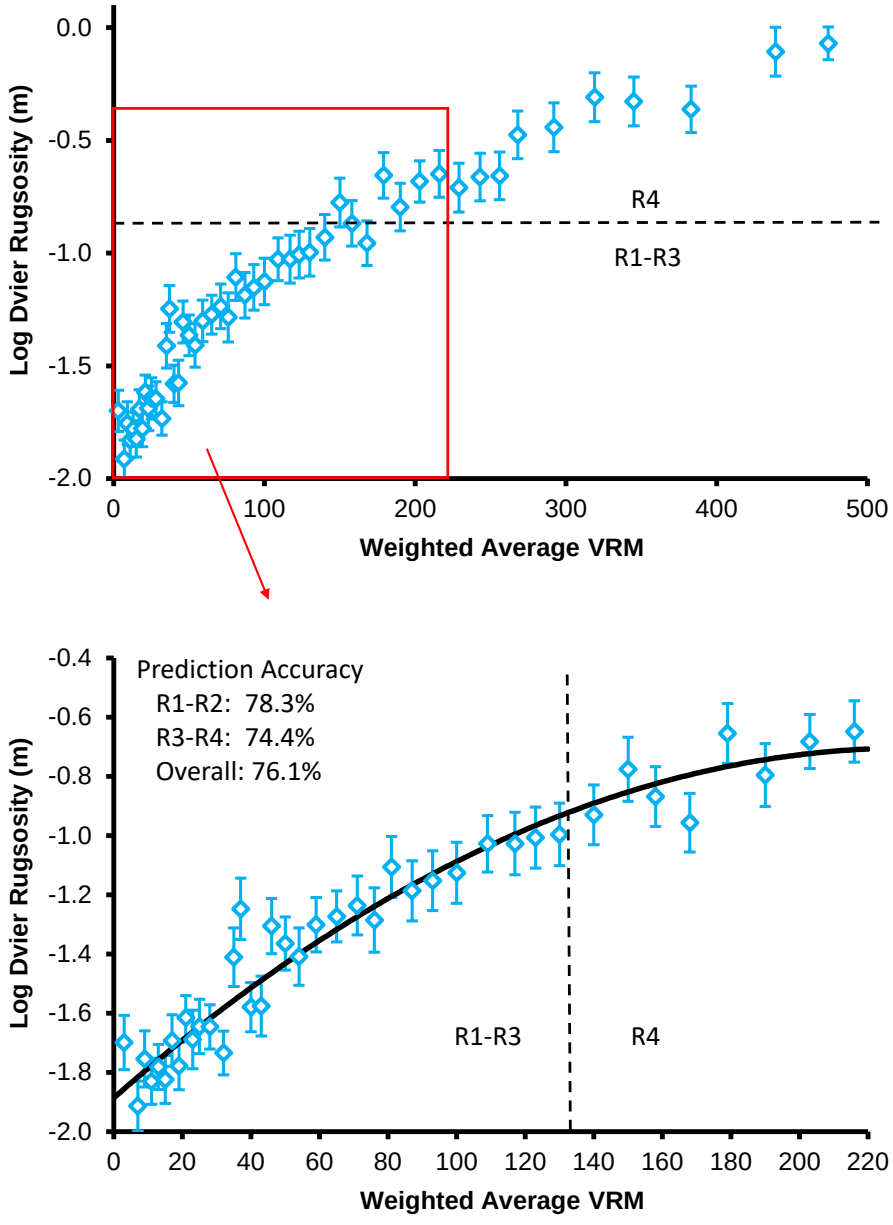

Figure 8.4. Relative frequencies of map VRM categories by diver rugosity strata (see Table 7.1 for definitions) for Dry Tortugas National Park.

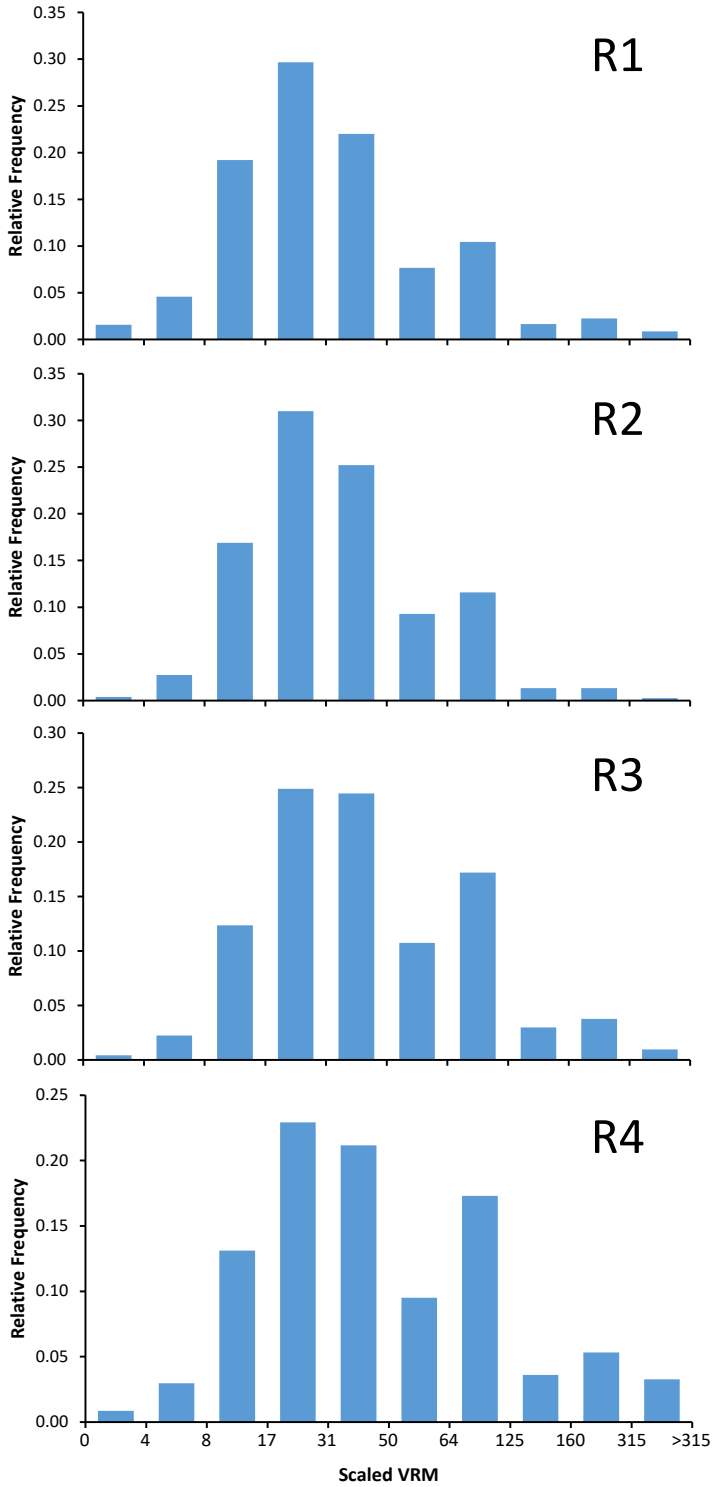

Figure 8.5. Relationship between diver and map rugosity for Dry Tortugas National Park, showing least-squares regression point estimates of log diver rugosity by intervals of map rugosity (weighted average VRM) and the corresponding fitted regression relationship. The horizontal dashed line demarcates the highest diver rugosity level (R4) from lower levels (R1-R3); the vertical dashed line demarcates the weighted average VRM for predicting the highest rugosity level (R4) vs. lower levels (R1-R3).

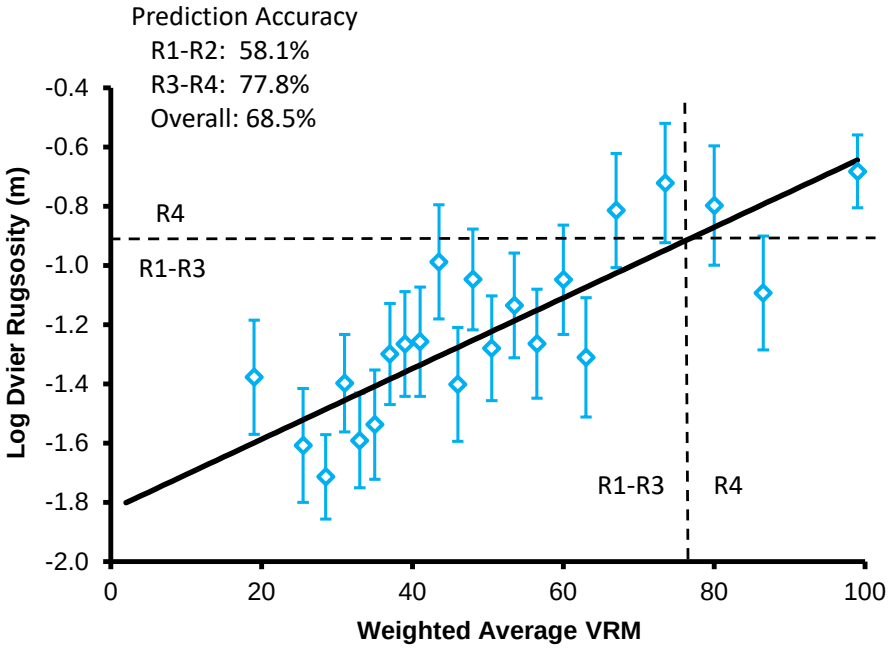

Figure 8.6. Relative frequencies of map ACR categories by diver rugosity strata (see Table 7.1 for definitions) for Tortugas Bank.

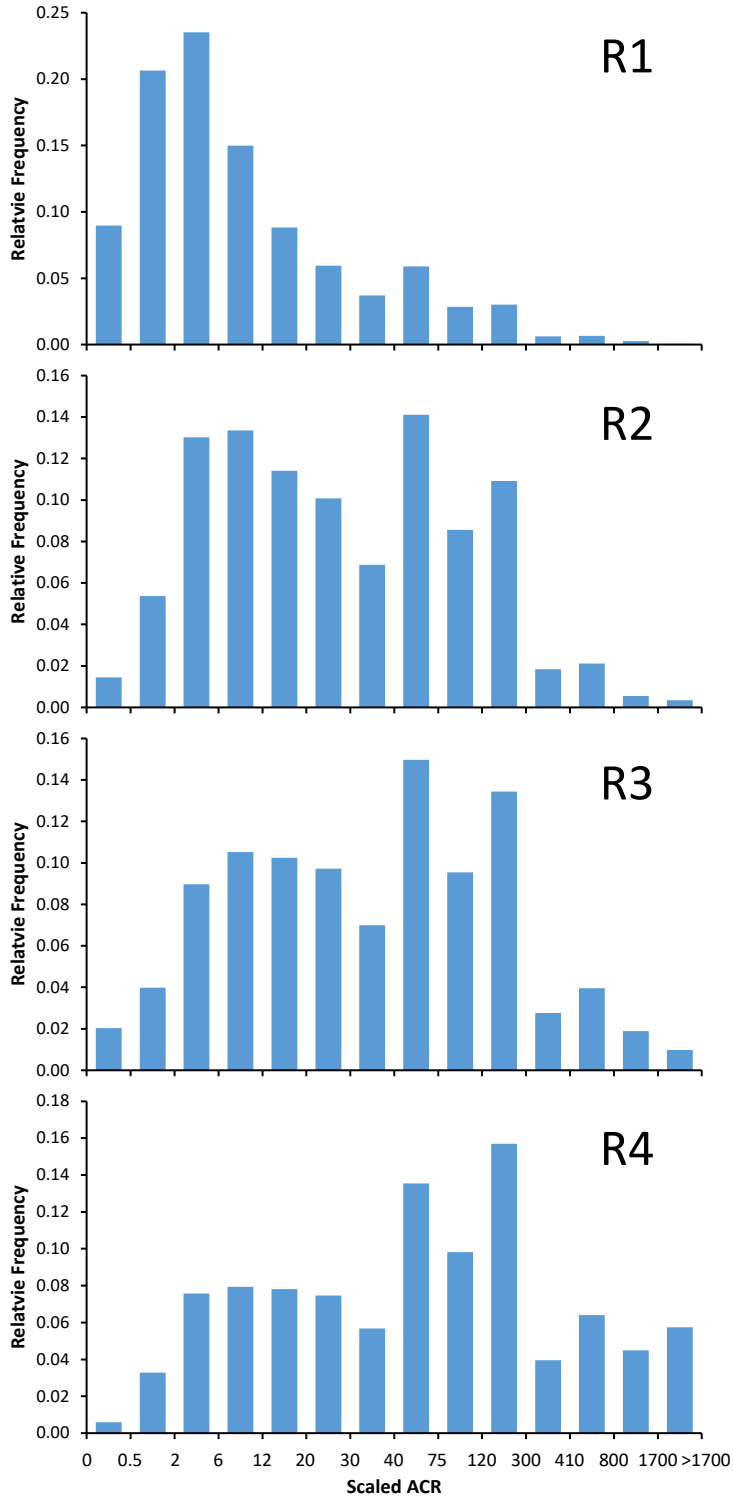

Figure 8.7. Relationship between diver and map rugosity for Tortugas Bank. Top panel: least-squares regression point estimates of log diver rugosity by intervals of map rugosity (weighted average ACR); the horizontal dashed line demarcates the highest diver rugosity level (R4) from lower levels (R1-R3). Bottom panel: inset from top panel (red box) showing the fitted regression relationship for log diver rugosity dependent on map rugosity; the vertical dashed line demarcates the weighted average ACR for predicting the highest rugosity level (R4) vs. lower levels (R1-R3).

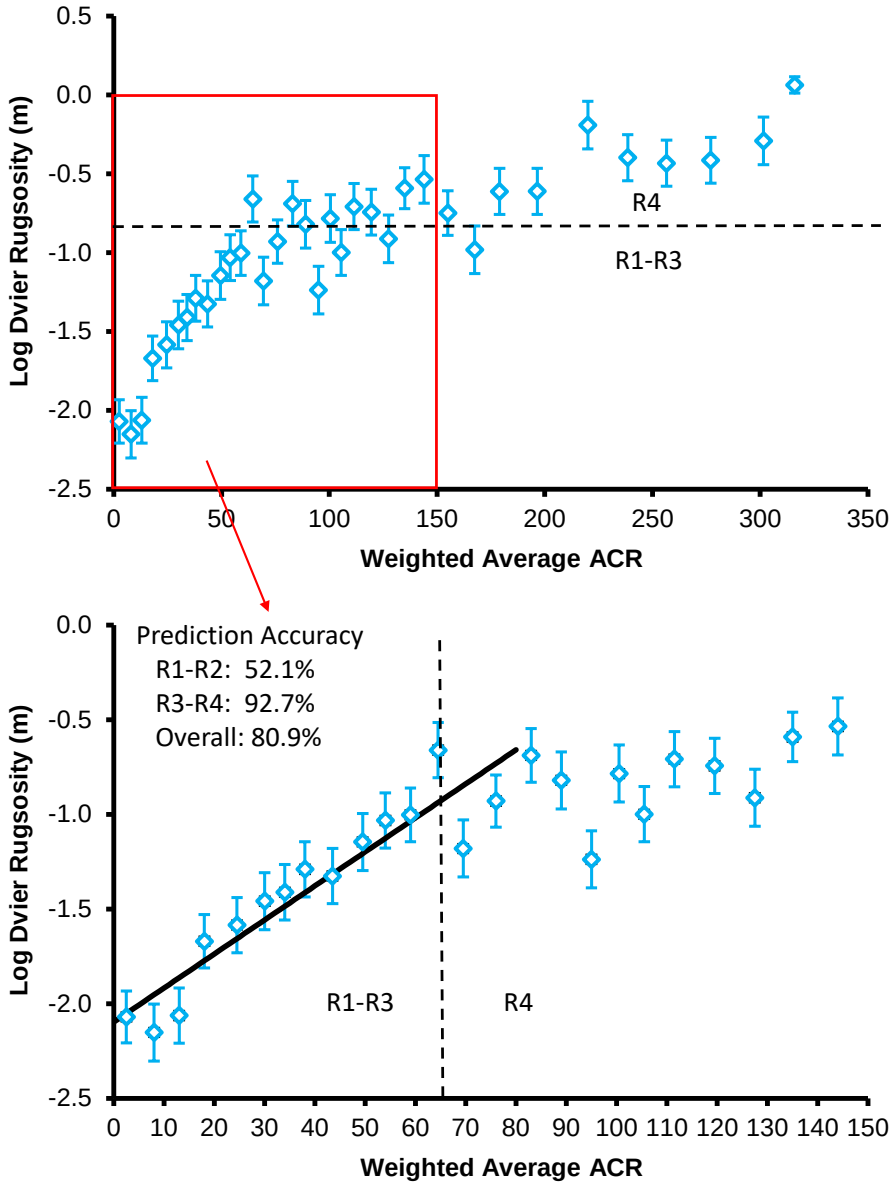

9.0 Creation of New 50x50 m Sampling Survey Grid

A new 50x50 m sampling survey map grid was developed using data and analyses from the previous sections (**Fig. 9.1**). The new map grid incorporated habitat rugosity measured by divers during RVC surveys from 2003-2018. The number of unique 50 x 50 m grid cells sampled by RVC divers was 6,096 in the Florida Keys, 2,363 in Dry Tortugas National Park, and 1,079 in Tortugas Bank. For sample units (50x50 m grid cells) that have not been sampled by RVC divers, habitat rugosity was estimated using high-resolution bathymetry data and diver-map rugosity regression functions described above (section 8.0). New and updated variables in the sampling grid are provided in **Table 9.1**. New variables include a map quality indicator (**Table 9.2**), and variables for newly defined depth strata (**Table 9.3**) and rugosity strata (**Table 9.4**). Key variables that were not updated in the new sampling grid were cross-shelf reef zone (**Table 9.5**), which is relevant for stratification in the Florida Keys region, and benthic habitat codes distinguishing between reef and non-reef (e.g., sand, seagrass) habitats. Unfortunately, the majority of high-resolution mapping data was based on LiDAR technology, which does not provide any useful information on substrate hardness, in contrast to multibeam sonar in which hardness can be derived from backscatter information. It is thus not possible to discern whether low rugosity substrate is hardbottom or softbottom.

The new 50x50 m map grid for the Florida Keys was used to develop the RVC stratified random survey sampling grid, which can then be used for allocation analysis and subsequent randomization of sampling locations for upcoming field surveys (**Fig. 9.1**). Ecological strata were defined as a combination of cross-shelf zone, depth, and rugosity (**Table 9.6**). The sampling design incorporated management zones (inside or outside MPAs) along with ecological strata for allocation and randomization (**Table 9.7**). The newly-acquired high-resolution bathymetry data mostly comprised the shallow forereef in the Florida Keys, resulting in portions of the sampling frame that are still unmapped with respect to substrate complexity. These unmapped areas were designated as an unknown rugosity stratum (RU) in cross-shelf zones and depths with partial coverage of high-resolution mapping data (**Table 9.6**). In addition, there were two zone-depths with no new mapping data, inshore reefs (**Table 9.6**, strata2020=S1) and deep forereef (**Table 9.6**, strata2020=S11), in which rugosity was not used in the strata definitions. Taken together, these unmapped strata (S01, S04, S07, S10, S11) account for 39% of the Florida Keys RVC sampling grid (**Table 9.7**). The Florida Keys ArcGIS shapefiles for the 50x50 m map grid, as well as the associated computational code and files for the RVC sampling grid, were provided to Dr. Jay Grove and her design analysis team.

Figure 9.1. Conceptual diagram of data inputs for creating new 50 m benthic maps for the Florida Keys and Dry Tortugas regions.

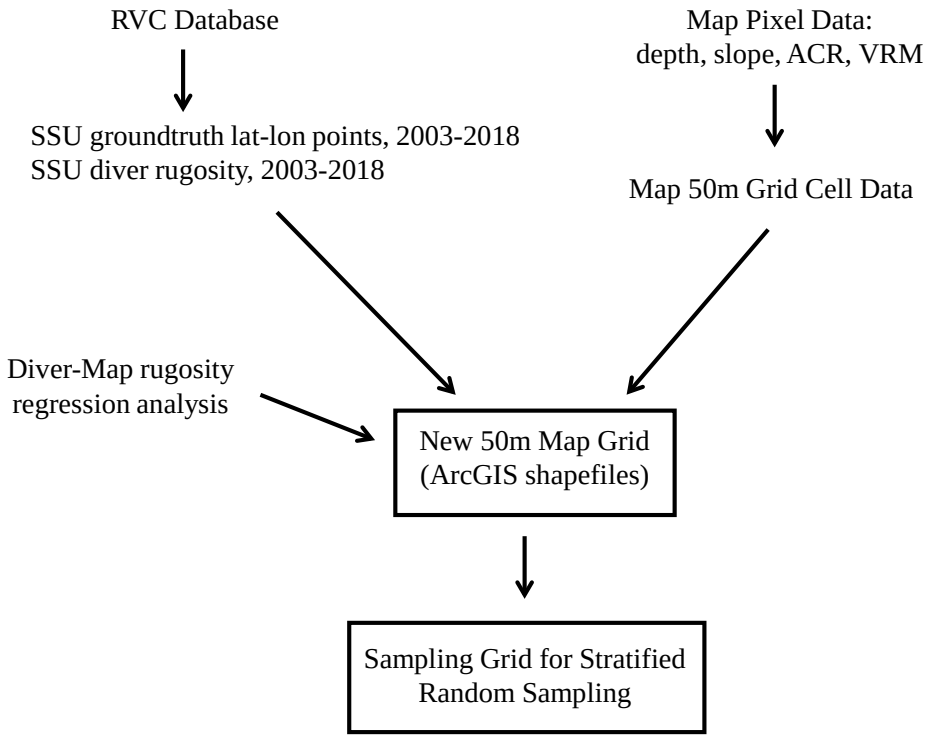

Table 9.1. Description of variables in the new 50x50 m map grid.

Variable	Description
grid_id_50	unique map id number for 50x50 m grid cell
lat_deg	latitude, decimal degrees
lon_deg	longitude, decimal degrees
depth_m	depth of the 50 x 50 m grid cell, meters
prot	prot 1=inside mpa; prot=0 outside mpa
strata2020	new 50 m map grid habitat-depth stratification variable
subregion_nr	id number for subregion of Dry Tortugas
mpa_nr	id number for specific marine protected area
depstrat	new 50 m map grid depth stratification variable, component of strata2020
rugstrat	new 50 m map grid rugosity stratification variable, component of strata2020
habitat_cd	reef habitat code (from previous 100 m grid map)
map_qual	indicator variable for map quality in terms of depth and rugosity

Table 9.2. Definition of map quality codes for 50x50 m grid cells.

map_qual	Description
0	no high-resolution bathymetry mapping
1	high-resolution bathymetry mapping of 50 m grid cell
2	50 m grid cell previously sampled by RVC divers

Table 9.3. Definition of depth strata codes for 50x50 m grid cells.

depstrat	Description
D0	all depths
D1	depth<12m
D2	12m<=depth<22m
D3	22m<=depth<33m

Table 9.4. Definition of rugosity strata codes for 50x50 m grid cells.

rugstrat	description
R1	substrate average vertical relief<0.15 m
R2	0.15m<=vertical relief<0.26m
R3	0.26m<=vertical relief<0.4m
R4	vertical relief>=0.4 m
RU	vertical relief unknown

Table 9.5. Definition of cross-shelf zone codes for 50x50 m grid cells; relevant for Florida Keys region

zone_nr	cross-shelf zone
1	inshore reefs
2	mid-channel patch reefs
3	offshore patch reefs
4	forereef

Table 9.6. Definition of ecological strata (strata2020) for the Florida Keys sampling grid.

strata2020	zone_nr	depstrat	rugstrat
S01	1	D0	
S02	2	D0	R1 & R2
S03	2	D0	R3 & R4
S04	2	D0	RU
S05	3 & 4	D1	R1 & R2
S06	3 & 4	D1	R3 & R4
S07	3 & 4	D1	RU
S08	3 & 4	D2	R1 & R2
S09	3 & 4	D2	R3 & R4
S10	3 & 4	D2	RU
S11	4	D3	

Table 9.7. Number of 50x50 m map grid cells for Florida Keys sampling strata. Sampling strata are a combination of management zones (prot) and ecological strata (strata2020, see Table 9.6 for definitions). Management zone strata definitions: prot=0, outside MPAs; prot=1, inside MPAs.

prot	strata2020	Grid Cells (N_h)
0	S01	6,183
0	S02	25,033
0	S03	4,740
0	S04	29,796
0	S05	93,747
0	S06	18,292
0	S07	10,194
0	S08	9,390
0	S09	5,885
0	S10	32,481
0	S11	23,747
1	S01	556
1	S02	208
1	S03	89
1	S04	1,047
1	S05	4,386
1	S06	2,263
1	S07	815
1	S08	451
1	S09	319
1	S10	923
	total	**270,545**

The new 50x50 m map grids for Dry Tortugas National Park and Tortugas Bank were used to develop the RVC stratified random survey sampling grid for the Tortugas region. Ecological strata were defined as a combination of depth and rugosity (**Table 9.8**). The sampling design incorporated three management zones—Tortugas Bank open, Tortugas Bank Ecological Reserve, Dry Tortugas National Park—along with ecological strata for allocation and randomization (**Table 9.9**). The high-resolution bathymetry data for Dry Tortugas National Park was from LiDAR surveys conducted in 2004, which was limited by depth. Deeper portions of the sampling frame are thus unmapped with respect to substrate complexity, accounting for about 26% of the Park RVC sampling grid (**Table 9.9**; prot=2; strata2020=T03, T06, T09). In contrast, Tortugas Bank was mapped with multibeam sonar which is not depth-limited. Unmapped areas occurred in deeper reefs (**Table 9.9**; prot=0, 1; strata2020=T09), accounting for about 6% of the Tortugas Bank RVC sampling grid. The Tortugas region ArcGIS shapefiles for the 50x50 m map grid, as well as the associated computational code and files for the RVC sampling grid, were provided to Dr. Jay Grove and her design analysis team.

Table 9.8. Definition of ecological strata (strata2020) for the Tortugas region sampling grid.

strata2020	depstrat	rugstrat
T01	D1	R1 & R2
T02	D1	R3 & R4
T03	D1	RU
T04	D2	R1 & R2
T05	D2	R3 & R4
T06	D2	RU
T07	D3	R1 & R2
T08	D3	R3 & R4
T09	D3	RU

Table 9.9. Number of 50x50 m map grid cells for Tortugas region sampling strata. Sampling strata are a combination of management zones (prot) and ecological strata (strata2020, see Table 9.8 for definitions). Management zone strata definitions: prot=0, Tortugas Bank open; prot=1, Tortugas Bank MPA (Tortugas North Ecological Reserve; prot=2, Dry Tortugas National Park.

prot	strata2020	Grid Cells (N_h)
0	T04	7,001
0	T05	6,214
0	T07	8,323
0	T08	1,449
0	T09	157
1	T04	5,441
1	T05	7,727
1	T07	5,740
1	T08	8,633
1	T09	3,292
2	T01	14,032
2	T02	11,797
2	T03	2,264
2	T04	19,406
2	T05	7,168
2	T06	10,550
2	T09	5,192
	sum	**124,386**

10.0 Conclusions and Future Mapping Recommendations

This study analyzed biological and environmental sampling data from RVC surveys in southern Florida in conjunction with remote-sensed, high-resolution mapping data to take significant strides in moving from qualitative to quantitative habitat characterization of the RVC coral reef sampling frame. The main result—the production of a survey sampling grid with habitat-depths quantitatively characterized to a 50 x 50 m resolution—represents a landmark event in the evolution of the RVC. Improvements to the accuracy, precision, and cost-effectiveness of RVC surveys in the Florida Keys and Tortugas regions are expected due to: (1) refinements to several integral components of the statistical design, namely life stage designations of target species (section 5.0), depth stratification (section 6.0), and rugosity stratification (section 7.0); (2) quantitative habitat characterization of the spatial sampling frame that will provide accurate computations of stratum areas and associated weighting factors, which will in turn improve the accuracy of frame-wide population metrics and minimize misallocation impacts on survey precision; and (3) improvements in the efficiency of field logistics by transitioning from a two-stage design with 100x100 m sample units to a single-stage design with 50x50 m sample units. The net result of these design changes on the actual

efficiency of RVC will be understood once a survey is completed using the new maps and statistical design.

The employment of a variety of innovative analysis techniques was key to the study's success. Important advancements for analyzing RVC survey data were the PCA technique for identifying the length at habitat shift, and generalized linear modeling to refine depth and rugosity stratification schemes. Perhaps the most important advancements were the development and application of a system of data processing and analysis procedures for assimilating ecological sampling data and remote-sensed mapping data to compute substrate rugosity metrics and integrate them into the RVC spatial sampling frame. These innovations will undoubtedly facilitate future improvements to the RVC sampling grids for other regions, e.g., Marquesas, Puerto Rico, US Virgin Islands, etc.

While the study produced the first quantitative benthic habitat maps for the Florida Keys and Tortugas regions, some key limitations to the current high-resolution mapping data were uncovered. The first, and most obvious, limitation was that the mapping data did not cover the entire RVC spatial sampling domain. The majority of the unmapped areas were due to the depth limitation of LiDAR, the mapping technology employed for the Florida Keys and Dry Tortugas National Park. As a result, reef habitats deeper than 14-15 m were not mapped in these regions. A second limitation was that LiDAR data provide no information on substrate hardness; consequently, it is not possible to use these data to distinguish between reef and non-reef habitats, a critical feature of the RVC sampling frame since it delineates map grid cells that should be included (reef) or excluded (non-reef) from the sampling grid. In contrast, multibeam sonar mapping data include backscatter information that are a direct measure of substrate hardness. Backscatter can thus be used to distinguish reef from non-reef habitats (c.f., Richards et al. 2019).

A third limitation was that mapping rugosity data could only discriminate between broad categories of rugosity (R1-R2 and R3-R4) in contrast to diver-measured rugosity data that was able to discriminate to a much finer degree (R1, R2, R3, R4). Some insight to this limitation can be gained by comparing the underlying frequency distributions of diver rugosity measurements (**Fig. 7.13**) with the corresponding frequency distributions of map rugosity (**Figs. 8.2, 8.4, 8.6**). Focusing on the very low rugosity stratum R1, 95% of the diver observations were in the lowest frequency category of 0 to 0.2 m vertical relief (**Fig. 7.13**). The frequency distributions of map rugosity for R1 also show a high frequency of observations at lower rugosity values, but the distributions are less skewed and also contain a secondary mode at moderate to high rugosity values (**Figs. 8.2, 8.4, 8.6**). Thus, while the divers are recording a very flat terrain for R1 sample units, the map data show a persistent frequency of pixels with high rugosity in R1 grid cells. This suggests some inherent 'noise' in the mapping data that produces spurious high rugosity pixels, likely contributing to the diminished ability to discern fine-scale rugosity categories.

The study findings suggest some clear mapping priorities for fully characterizing the RVC sampling grid for the Florida Keys and Tortugas regions:

Mapping Technology:- Multibeam sonar is the clear choice of mapping technology for future endeavors**.** While there are some logistical obstacles to overcome with respect to sampling

in shallow depths, multibeam can provide high-resolution bathymetry as well as backscatter data. LiDAR should not be deployed in any future mapping.

Noise Filtering:- While we identified data processing procedures that effectively reduced noise in the underlying bathymetry observations and subsequent rugosity metrics, such as gridding to a 2-m resolution, more sophisticated procedures for noise filtering are sorely needed. This needs to be communicated to the mapping teams and persons responsible for producing the mapping datasets for use by RVC and other researchers.

Priority Areas for Future Mapping:- The following areas for future mapping efforts are listed in order of priority.

(1) *Dry Tortugas National Park.* The highest priority is to re-map Dry Tortugas National Park in its entirety with multibeam sonar. The 2004 LiDAR data analyzed in this study provided the least accurate classification of rugosity strata of the regions analyzed, and more recent LiDAR data for the Park were depth-limited to the extent that they were non-usable. The Park is the key region in southern Florida and the US Caribbean for understanding ecological fish-habitat relationships given that it has lower human impacts on reef fish populations (low fishing pressure) and their habitats (low anthropogenic environmental disturbance). In this study, RVC sampling data from the Park were instrumental for refining life history designations for target design species and refining depth and rugosity stratification schemes. These ecological data will be critical for interpreting multibeam backscatter data for substrate hardness that can then be used to delineate reef from non-reef habitats in the spatial sampling frame for the Park and other regions (Tortugas Bank, Florida Keys, etc.).

(2) *Florida Keys, Cross-Shelf Zones 1-3.* The second priority is to map the inshore and Hawk's Channel cross-shelf reef zones in the Florida Keys, including Biscayne National Park. Multibeam backscatter data will help to finally understand where all the patch reef habitats are located in this extensive area of the RVC spatial frame.

(3) *Florida Keys, Forereef Zone 4, Mid-depth and Deep Strata (D2-D3).* The third priority is to map the Florida Keys forereef zone for depths deeper than 12 m. The location and extent of reef habitat in this area is perhaps almost as uncertain as the patch reefs described in priority 2. Mapping data for rugosity and substrate hardness are entirely missing for this area. As a practical matter, mapping the forereef zone at 12-35 m depths could be combined with planned mapping of reefs to 50 m in depth to support extension of the RVC survey frame to 'mesophotic' reefs.

(4) *Florida Keys, Forereef Zone 4, Shallow Depths (D1), Low Rugosity (R1-R2).* The fourth priority is to re-map the shallow (<12 m) forereef zone targeting low rugosity strata (R1-R2) using multibeam. This will enable discrimination of reef vs. non-reef low rugosity habitats. The current LiDAR data are likely sufficient for classifying higher rugosity habitat (R3-R4) as reef.

11.0 Literature Cited

Du Preez, C. 2015. A new arc-chord ratio (ACR) rugosity index for quantifying three-dimensional landscape structural complexity. Landscape Ecol. 30: 181-192.

Richards, B. L., J. R. Smith, S.G. Smith, J.S. Ault, C. D. Kelley, V. N. Moriwake. 2019. Development and Use of a Novel Main Hawaiian Islands Bathymetric and Backscatter Synthesis in a Stratified Fishery-Independent Bottomfish Survey. U.S. Dep. Commer., NOAA Tech. Memo. NMFS-PIFSC-87. doi:10.25923/bh8v-0184

Sappington, J.M., Longshore, K., and Thompson, D.B. 2005. Quantifying landscape ruggedness for animal habitat analysis: a case study using bighorn sheep in the Mojave Desert. J. Wildlife Mgmt. 71: 1419-1426.

Appendix A -- IDL Computational Code

A1. IDL code for computing ACR

```
Function Get_Arc_chord_ratio,grid,bin
  ;#grid is the input grid of 3x3 dimension,
  ;#bin is grid bin size in meter
  ;#output is ACR values of the center cell.
  ;#Reference: Burrough, P. A. and McDonell, R.A., 1998. Principles of Geographical
 ;# Information Systems (Oxford University Press, New York), p. 190.

;# grid cell label
  ;  a|b|c
  ;  d|e|f
  ;  g|h|i
  bin=float(bin)
  a=grid(0,2)
  b=grid(1,2)
  c=grid(2,2)
  d=grid(0,1)
  e=grid(1,1)
  f=grid(2,1)
  g=grid(0,0)
  h=grid(1,0)
  i=grid(2,0)

  dzdx=float((c+2.*f+i)-(a+2.*d+g))/float(8.*bin)
  dzdy=float((g+2.*h+i)-(a+2.*b+c))/float(8.*bin)
  slope=atan(sqrt(dzdx^2.+dzdy^2.))
  dzx=(d+f)/2.-e
  dzy=(b+h)/2.-e
  dzxx=(a+i)/2.-e
  dzyy=(c+g)/2.-e
  dzsq=(dzx^2.+dzy^2.+dzxx^2.+dzyy^2.)/((bin)^2./cos(slope))
  acr=1+dzsq
  return, acr

end
```

A2. IDL code for computing VRM

```
pro Get_VRM_binsize,grid,vrm,slope,aspect,rug,bin
;#grid is the input bathymetric data gridded at resolution of bin size
;#bin is the size of grid in meters
;#vrm is output grid of “vector ruggedness measure”, Sappington et al 2007.
;# Quantifying Landscape Ruggedness for Animal Habitat Analysis: A Case Study Using Bighorn Sheep in the
;# Mojave Desert.  J of Wildlife Management, 71(5):1419-1426. https://doi.org/10.2193/2005-723
;# slope is the output grid of slope of the same size of input grid
;# aspect is the output grid of aspect of the same size of input grid
;# rug is the output grid of rugosity of the same size of input grid

sz=size(grid)
nc=sz[1]
nr=sz[2]
slope=fltarr(nc,nr)
aspect=fltarr(nc,nr)
vrm=fltarr(nc,nr)
x=fltarr(nc,nr)
y=fltarr(nc,nr)
z=fltarr(nc,nr)
rug=fltarr(nc,nr)
 for j=1,nr-2 do begin
  for i=1,nc-2 do begin
  grid1=grid[i-1:i+1,j-1:j+1]
  slope_aspect1=get_slope_aspect(grid1,bin)
  rug[i,j]=get_surf_area(grid1)/(bin*2)^2.
  slope[i,j]=slope_aspect1[0]
  aspect[i,j]=slope_aspect1[1]
  z(i,j)=bin*cos(slope[i,j]*!dtor)
  xy=bin*sin(slope[i,j]*!dtor)
  x(i,j)=xy*sin(aspect[i,j]*!dtor)
  y(i,j)=xy*cos(aspect[i,j]*!dtor)
  endfor
 endfor
 ;set the boundary values
 slope(0,*)=slope(1,*)
 slope(nc-1,*)=slope(nc-2,*)
 slope(*,0)=slope(*,1)
 slope(*,nr-1)=slope(*,nr-2)

 aspect(0,*)=aspect(1,*)
 aspect(nc-1,*)=aspect(nc-2,*)
 aspect(*,0)=aspect(*,1)
 aspect(*,nr-1)=aspect(*,nr-2)

 x(0,*)=x(1,*)
 x(nc-1,*)=x(nc-2,*)
 x(*,0)=x(*,1)
 x(*,nr-1)=x(*,nr-2)

 y(0,*)=y(1,*)
 y(nc-1,*)=y(nc-2,*)
 y(*,0)=y(*,1)
 y(*,nr-1)=y(*,nr-2)
```

```
 z(0,*)=z(1,*)
 z(nc-1,*)=z(nc-2,*)
 z(*,0)=z(*,1)
 z(*,nr-1)=z(*,nr-2)

 for j=1L,nr-2 do begin
  for i=1L,nc-2 do begin
   r=sqrt((total(x[i-1:i+1,j-1:j+1]))^2.+(total(y[i-1:i+1,j-1:j+1]))^2.+(total(z[i-1:i+1,j-1:j+1]))^2.)
   vrm(i,j)=1.-r/(9.*bin)

  endfor
 endfor

;# the following lines set the edge of the vrm grid to the next cell value.
 vrm(0,*)=vrm(1,*)
 vrm(nc-1,*)=vrm(nc-2,*)
 vrm(*,0)=vrm(*,1)
 vrm(*,nr-1)=vrm(*,nr-2)

end
```